REPORT DOCUMENTATION PAGE

Public reporting burden for this collection of information is estimated to average 1 hour per response, including the time for reviewing instructions, searching existing data sources, gathering and maintaining the data needed, and completing and reviewing the collection of information. Send comments regarding this burden estimate or any other aspect of this collection of information, including suggestions for reducing this burden, to Washington Headquarters Services, Directorate for Information Operations and Reports, 1215 Jefferson Davis Highway, Suite 1204, Arlington, VA 22202-4302, and to the Office of Management and Budget, Paperwork Reduction Project (0704-0188), Washington, DC 20503.

1. AGENCY USE ONLY (Leave blank)	2. REPORT DATE 28 May 96	3. REPORT TYPE AND DATES COVERED

4. TITLE AND SUBTITLE
Winter Extratropical Cyclogenesis Over The Northern Gulf of Mexico

5. FUNDING NUMBERS

6. AUTHOR(S)

Daniel Anthony Peters

7. PERFORMING ORGANIZATION NAME(S) AND ADDRESS(ES)

AFIT Student Attending:

Florida State University

8. PERFORMING ORGANIZATION REPORT NUMBER

96-057

9. SPONSORING / MONITORING AGENCY NAME(S) AND ADDRESS(ES)

DEPARTMENT OF THE AIR FORCE
AFIT/CI
2950 P STREET, BLDG 125
WRIGHT-PATTERSON AFB OH 45433-7765

10. SPONSORING / MONITORING AGENCY REPORT NUMBER

11. SUPPLEMENTARY NOTES

12a. DISTRIBUTION / AVAILABILITY STATEMENT

Approved for Public Release IAW AFR 190-1
Distribution Unlimited
BRIAN D. GAUTHIER, MSgt, USAF
Chief Administration

12b. DISTRIBUTION CODE

13. ABSTRACT (Maximum 200 words)

19960809 119

14. SUBJECT TERMS			15. NUMBER OF PAGES 137
			16. PRICE CODE

17. SECURITY CLASSIFICATION OF REPORT	18. SECURITY CLASSIFICATION OF THIS PAGE	19. SECURITY CLASSIFICATION OF ABSTRACT	20. LIMITATION OF ABSTRACT

NSN 7540-01-280-5500

DTIC QUALITY INSPECTED 1

GENERAL INSTRUCTIONS FOR COMPLETING SF 298

The Report Documentation Page (RDP) is used in announcing and cataloging reports. It is important that this information be consistent with the rest of the report, particularly the cover and title page. Instructions for filling in each block of the form follow. It is important to *stay within the lines* to meet *optical scanning requirements*.

Block 1. Agency Use Only *(Leave blank)*.

Block 2. Report Date. Full publication date including day, month, and year, if available (e.g. 1 Jan 88). Must cite at least the year.

Block 3. Type of Report and Dates Covered. State whether report is interim, final, etc. If applicable, enter inclusive report dates (e.g. 10 Jun 87 - 30 Jun 88).

Block 4. Title and Subtitle. A title is taken from the part of the report that provides the most meaningful and complete information. When a report is prepared in more than one volume, repeat the primary title, add volume number, and include subtitle for the specific volume. On classified documents enter the title classification in parentheses.

Block 5. Funding Numbers. To include contract and grant numbers; may include program element number(s), project number(s), task number(s), and work unit number(s). Use the following labels:

C	-	Contract	**PR**	- Project
G	-	Grant	**TA**	- Task
PE	-	Program Element	**WU**	- Work Unit Accession No.

Block 6. Author(s). Name(s) of person(s) responsible for writing the report, performing the research, or credited with the content of the report. If editor or compiler, this should follow the name(s).

Block 7. Performing Organization Name(s) and Address(es). Self-explanatory.

Block 8. Performing Organization Report Number. Enter the unique alphanumeric report number(s) assigned by the organization performing the report.

Block 9. Sponsoring/Monitoring Agency Name(s) and Address(es). Self-explanatory.

Block 10. Sponsoring/Monitoring Agency Report Number. *(If known)*

Block 11. Supplementary Notes. Enter information not included elsewhere such as: Prepared in cooperation with...; Trans. of...; To be published in.... When a report is revised, include a statement whether the new report supersedes or supplements the older report.

Block 12a. Distribution/Availability Statement. Denotes public availability or limitations. Cite any availability to the public. Enter additional limitations or special markings in all capitals (e.g. NOFORN, REL, ITAR).

DOD	-	See DoDD 5230.24, "Distribution Statements on Technical Documents."
DOE	-	See authorities.
NASA	-	See Handbook NHB 2200.2.
NTIS	-	Leave blank.

Block 12b. Distribution Code.

DOD	-	Leave blank.
DOE	-	Enter DOE distribution categories from the Standard Distribution for Unclassified Scientific and Technical Reports.
NASA	-	Leave blank.
NTIS	-	Leave blank.

Block 13. Abstract. Include a brief *(Maximum 200 words)* factual summary of the most significant information contained in the report.

**Block 14.** Subject Terms. Keywords or phrases identifying major subjects in the report.

Block 15. Number of Pages. Enter the total number of pages.

Block 16. Price Code. Enter appropriate price code *(NTIS only)*.

Blocks 17. - 19. Security Classifications. Self-explanatory. Enter U.S. Security Classification in accordance with U.S. Security Regulations (i.e., UNCLASSIFIED). If form contains classified information, stamp classification on the top and bottom of the page.

Block 20. Limitation of Abstract. This block must be completed to assign a limitation to the abstract. Enter either UL (unlimited) or SAR (same as report). An entry in this block is necessary if the abstract is to be limited. If blank, the abstract is assumed to be unlimited.
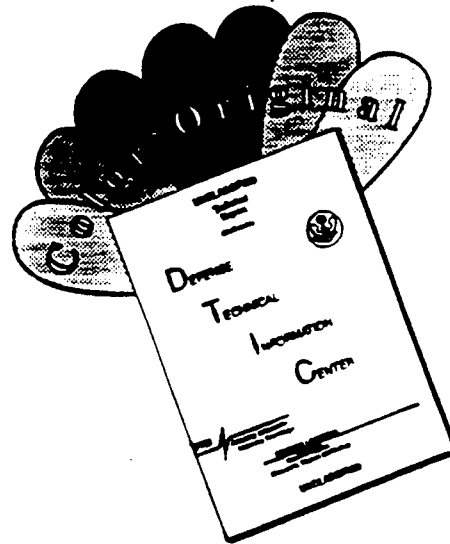
DISCLAIMER NOTICE

THE FLORIDA STATE UNIVERSITY

COLLEGE OF ARTS AND SCIENCES

WINTER EXTRATROPICAL CYCLOGENESIS
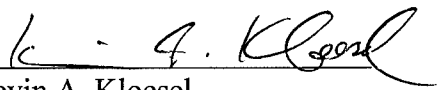
OVER THE NORTHERN GULF OF MEXICO

By

DANIEL ANTHONY PETERS

A Thesis submitted to the
Department of Meteorology
in partial fulfillment of the
requirements for the degree of
Master of Science

Degree Awarded:
Summer Semester, 1996

The members of the Committee approve the thesis of Daniel Anthony Peters defended on 28 May 1996.

Kevin A. Kloesel
Professor Directing Thesis

Jon E. Ahlquist
Committee Member

Paul H. Ruscher
Committee Member

ACKNOWLEDGMENTS

Many thanks go to my major professor, Dr. Kevin Kloesel, whose instruction in synoptic and mesoscale meteorology has provided me the necessary tools for understanding the complexities of the atmosphere. Dr. Kloesel is second to none in his dedication to teaching meteorology, and I will certainly strive to emulate him in my upcoming position as an instructor at the USAF Weather School.

I would also like to thank my committee members, Dr. Jon Ahlquist and Dr. Paul Ruscher, for their helpful comments. Dr. Chris Herbster (who was placed by God at the desk next to mine for the past year) demonstrated his tremendous capacity for patience by fielding my endless barrage of questions about Unix, DOS, and yes, meteorology, and making my life easier in ways I would have never have thought possible (for example, the C-shell script!). Darin Meyer saved me a great deal of time by providing me an electronic copy of his thesis, so that I could simply "cut" out his work and "paste" in mine. Jeff Stein provided statistical guidance through the University's Statistical Consulting Center.

Thanks also to all of my friends here at FSU, for making graduate school a very worthwhile experience, despite the academics! And thanks, of course, to the United States Air Force for providing me with such an incredible opportunity.

TABLE OF CONTENTS

v

LIST OF FIGURES

viii

xii

xiv

LIST OF TABLES

ABSTRACT

Winter extratropical cyclogenesis over the northern Gulf of Mexico is examined by assigning a synoptic classification to each winter cyclone which developed during the 41-season period 1950-51 to 1990-91. The classifications of "frontal" and "nonfrontal" cyclogenesis are used to differentiate between those cyclones which were analyzed to have formed along pre-existing, airmass-type frontal boundaries, and those which developed in the absence of such boundaries.

Spatial distributions of cyclogenesis events indicate that the open water of the northwest Gulf tends to be a preferred region for cyclone initiation, for both the frontal and the nonfrontal cases. This is particularly evident during the coldest months, when sea surface temperatures exhibit a strong gradient along the continental shelf break.

Case studies reveal that after a cold air outbreak, air which resides for an extended period of time over the continental shelf of the northwest Gulf becomes differentially modified by spatially varying fluxes of heat and moisture from the sea surface, resulting in the formation of an atmospheric baroclinic zone which lies well to the north of the polar front. A solenoidal circulation develops within the boundary layer, increasing convergence and cyclonic vorticity, and inducing a horizontal discontinuity in atmospheric stability. Thus, this region is a favored location for

further cyclonic intensification, provided that the upper-level pattern is also favorable. Although a lack of surface data makes the processes which induce cyclogenesis in this region difficult to resolve, visible satellite imagery is suggested to be beneficial.

CHAPTER 1

INTRODUCTION

Extratropical cyclones which develop over the Gulf of Mexico (Gulf) during the winter months often have a significant impact on the weather of the eastern United States. The majority of winter storms which produce significant widespread precipitation over the eastern half of the United States develop over the Gulf (Businger et al. 1990, see Table 2.1). In addition, extratropical cyclones which develop over the Gulf west of 85W longitude can cause significant damage along the entire east coast of the U.S. (Mather et al. 1964). Indeed, Gulf cyclones have considerable implications in terms of human suffering (Lewis 1992).

Historically, studies of cyclogenesis over North America have indicated a wintertime maximum in the frequency of cyclogenesis over the Gulf. Despite these many investigations, however, cyclogenesis over the Gulf remains a poorly understood process, with few works providing accurate and complete descriptions as to *why* that maximum exists. The purpose of this study is to provide an explanation.

A review of past investigations of North American and Gulf of Mexico cyclogenesis will be presented in Chapter 2. Chapter 3 will introduce the results of a

1

climatology of Gulf cyclones which has been performed by the author. A new storm

classification scheme will be offered here, and will yield information regarding the

factors contributing to Gulf cyclogenesis. In Chapter 4, evidence will be presented that

a semi-permanent baroclinic zone exists over the northwest Gulf during the winter

months, which makes the region favorable for cyclone development. Three case

studies which support these ideas will be examined in Chapter 4. Chapter 5 will

present conclusions.

CHAPTER 2

HISTORICAL REVIEW

Several cyclone climatologies have documented the existence of a maximum in the frequency of wintertime extratropical cyclogenesis (from here on referred to as simply "cyclogenesis") over the Gulf of Mexico and adjacent coastal regions. Saucier (1949) studied 388 cyclones originating in the Texas-West Gulf region during a 40-year period. He determined that during the colder months such as January and February, a high frequency of cyclogenesis events occurs over the coastal waters off Texas and Louisiana due to the "reactivation of the polar front" in the region of "natural land-sea temperature contrast." During the autumn and spring months, however, no definite grouping is evident (see Figure 2.1). Though Saucier's conceptual model of Gulf cyclogenesis was particularly insightful at the time of its inception, it does have a significant flaw. A goal of the current investigation will be to revisit Saucier's conclusions, placing a greater emphasis on the low-level, mesoscale preconditions for Gulf cyclogenesis.

Hosler and Gamage (1956) tabulated the number of cyclones per month passing through each 5-degree latitude-longitude grid in the United States during the years
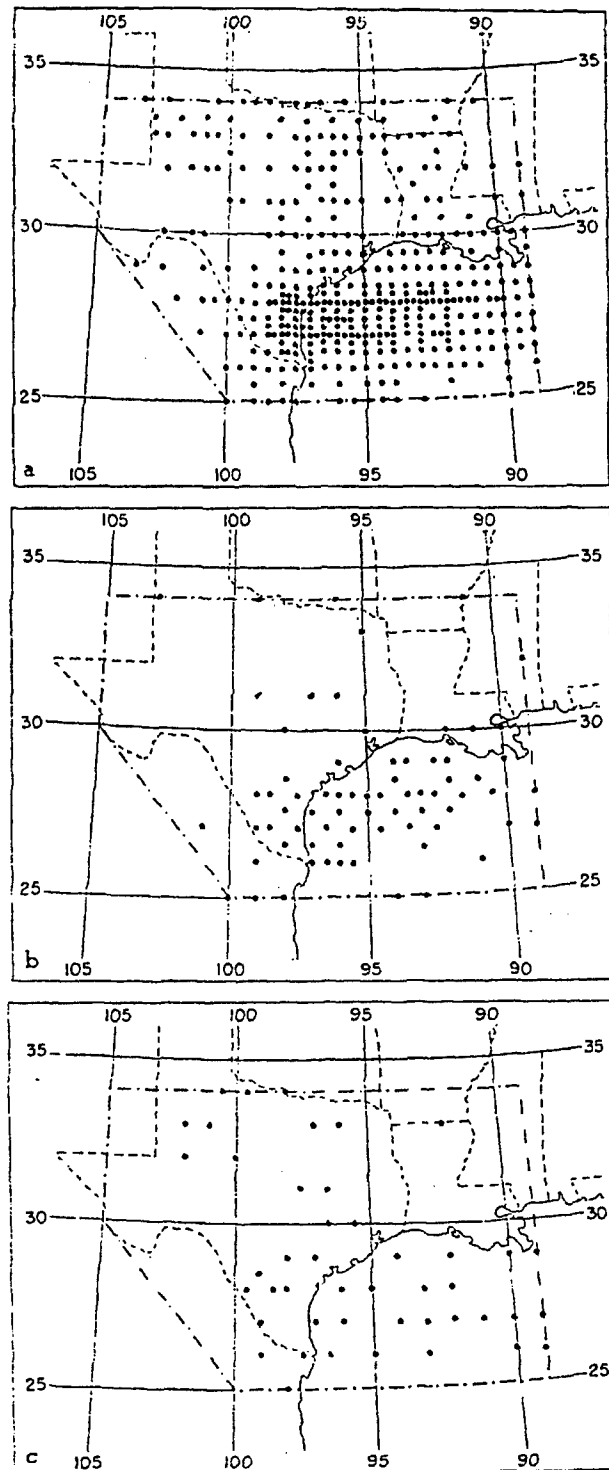
Figure 2.1. Locations of cyclone formation for (a) the seven months October through April, (b) February, and (c) November (from Saucier 1949).

4

1905 through 1954, and found a maximum of cyclone frequency extending southward into the northwest Gulf during the winter months (Figure 2.2). Petterssen (1956) showed that a significant percentage of winter cyclogenesis in the Northern Hemisphere from 1899 to 1939 occurred over the northwest Gulf (Figure 2.3), and that there was a high rate of alternation between cyclones and anticyclones over the same region during winter (not shown). In a study of cyclones which were analyzed during the period 1951 to 1970, Reitan (1974) found a maximum of January events (Figure 2.4) to occur over the *northeast* Gulf and the southeastern United States, and attributed such a pattern to the fact that "the cold air from the continent would find the ocean surface to be an excellent source of heat and moisture, factors which contribute to the development of cyclonic systems."

Using 1-degree latitude-longitude quadrangles, Colucci (1976) developed a detailed distribution of winter cyclone frequencies for the years 1964 through 1973 (Figure 2.5), which showed a local minimum of cyclone passage over the Florida peninsula, calling into question Reitan's lower-resolution results. Colucci justified this minimum by stating that there is an observed tendency for surface lows in the northeast Gulf to reform along the Carolina coast as opposed to moving directly across the peninsula. In fact, the net deepening rate for all storms in his data sample was negligible over the northeast Gulf (Figure 2.6). Of the approximately 1 out of every 2 northeastern Gulf storms which *were* observed to deepen on successive 3-hourly surface charts (corrections for diurnal pressure changes were not made),

5
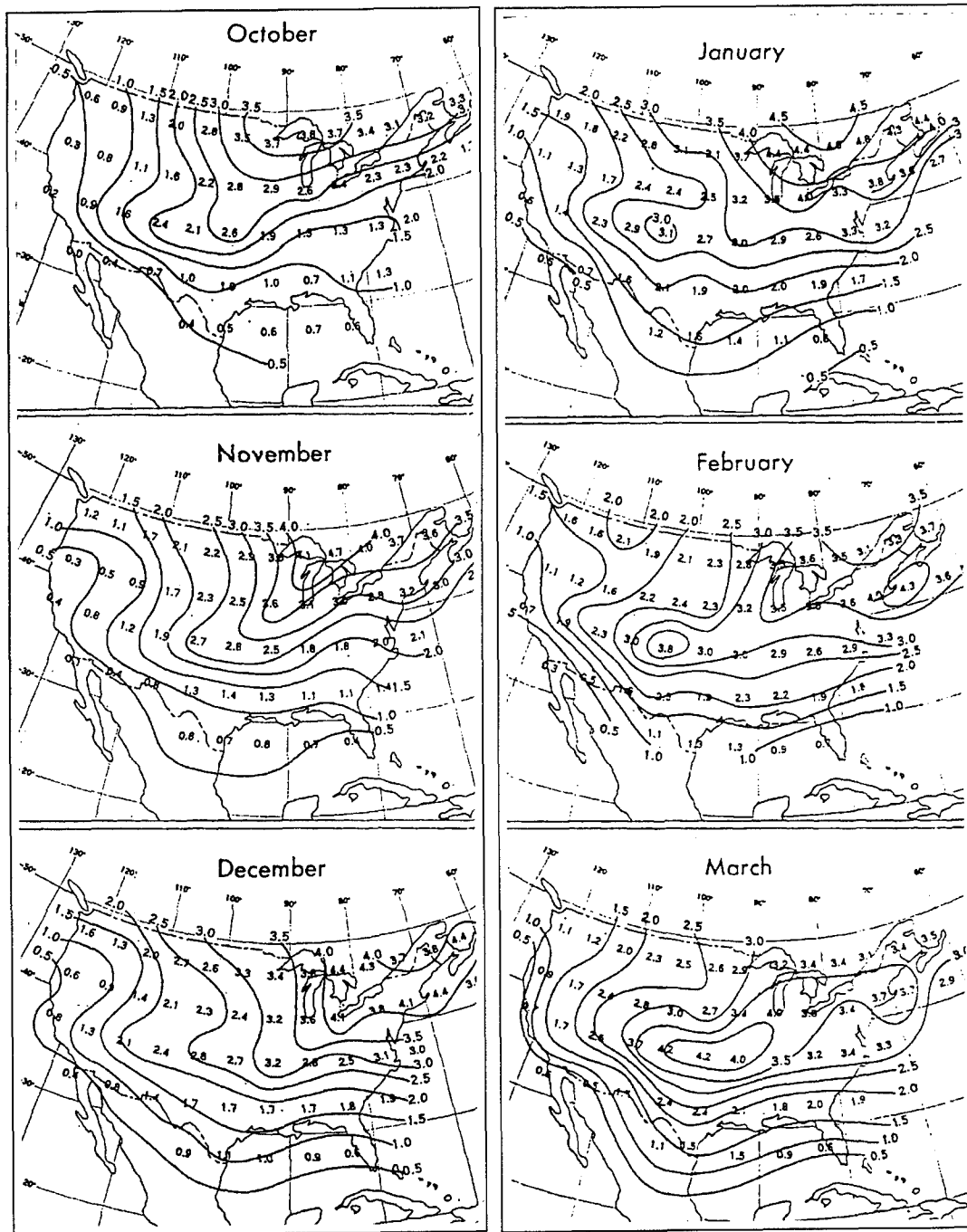
Figure 2.2. Number of cyclones passing through each 5-degree latitude-longitude grid in the United States, by months, 1905 through 1954 (from Hosler and Gamage 1956).

6
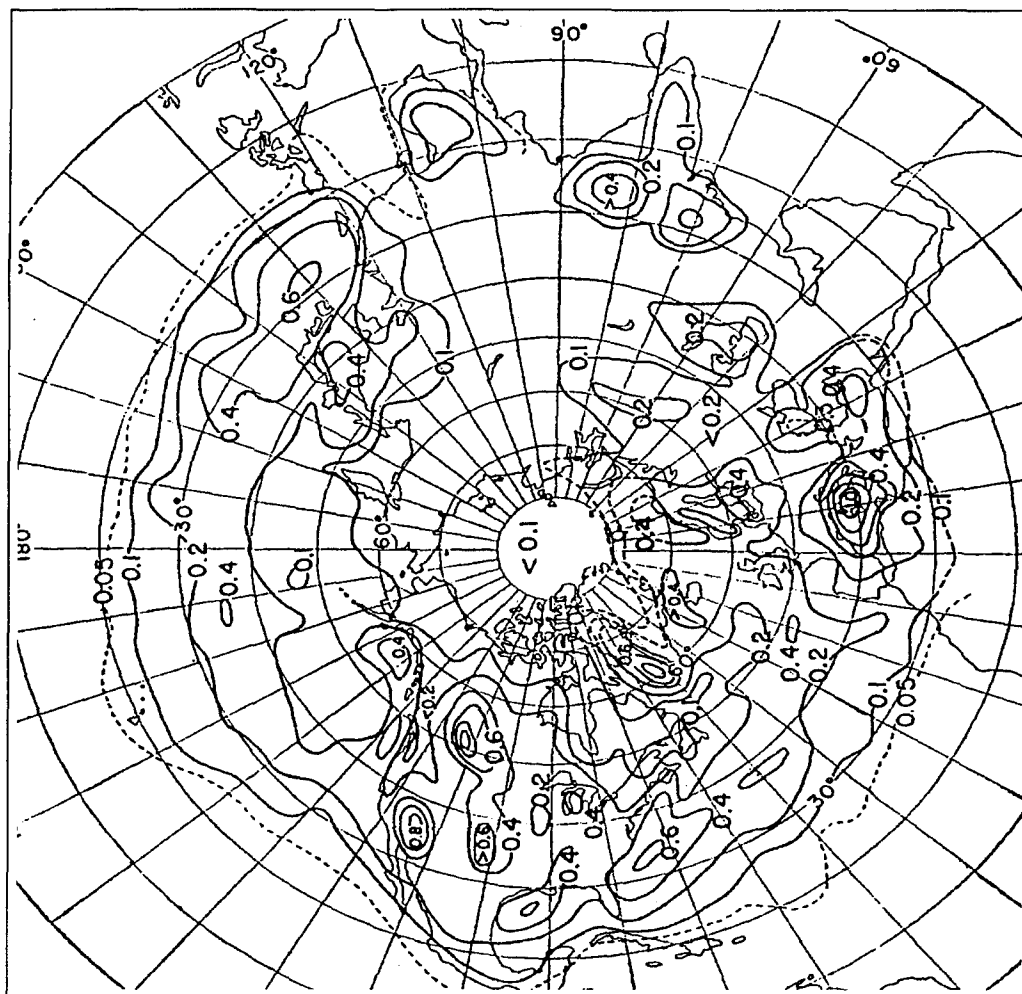
Figure 2.3. Percentage frequency of occurrence of cyclogenesis in squares of 100,000 km^2 in winter, 1899 to 1939 (from Petterssen 1956).

deepening rates were limited to about 2 millibars (mb) per 3 hours (Figure 2.7). This deepening rate is about half that which occurs off the Carolina coast and along the northwestern boundary of the Gulf Stream.

Using a 2-degree latitude-longitude grid spanning North America and the surrounding oceans, Zishka and Smith (1980) determined areal distributions of cyclone

7
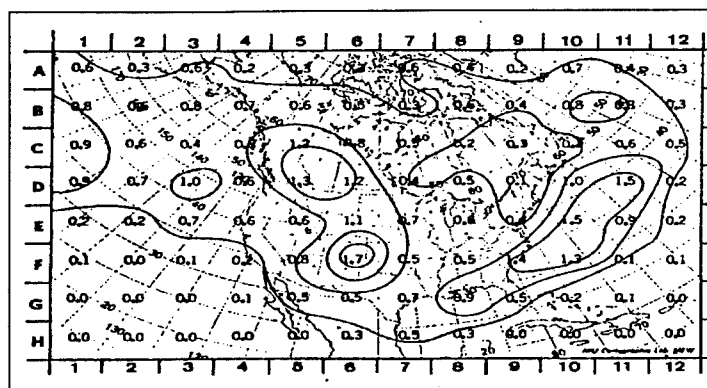
Figure 2.4. The average number of cases of cyclogenesis during the 20-year period 1951-1970, in January (from Reitan 1974).
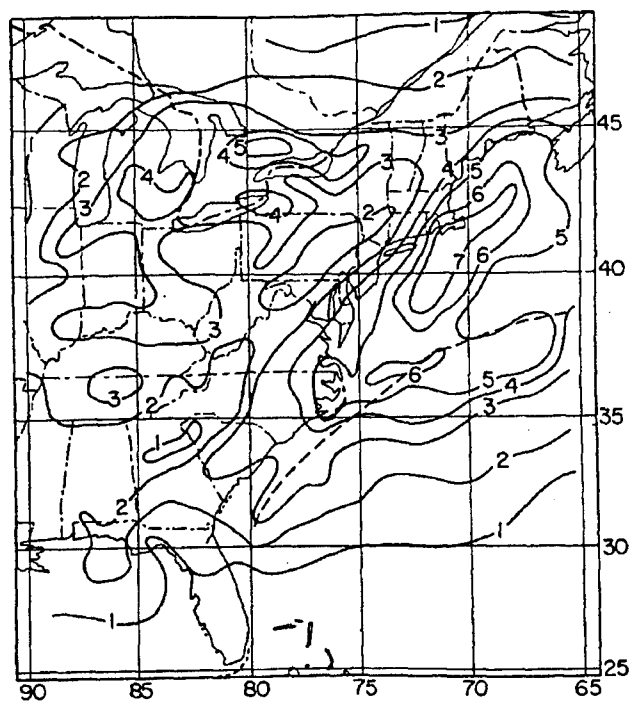
Figure 2.5. Winter cyclone frequencies by 1-degree latitude-longitude quadrangles, January 1964 to December 1973. Contour values should be multiplied by 10. Mean position of the northern and western boundary of the Gulf Stream, 1966-1973, is shown by dashed line (from Colucci 1976).

8
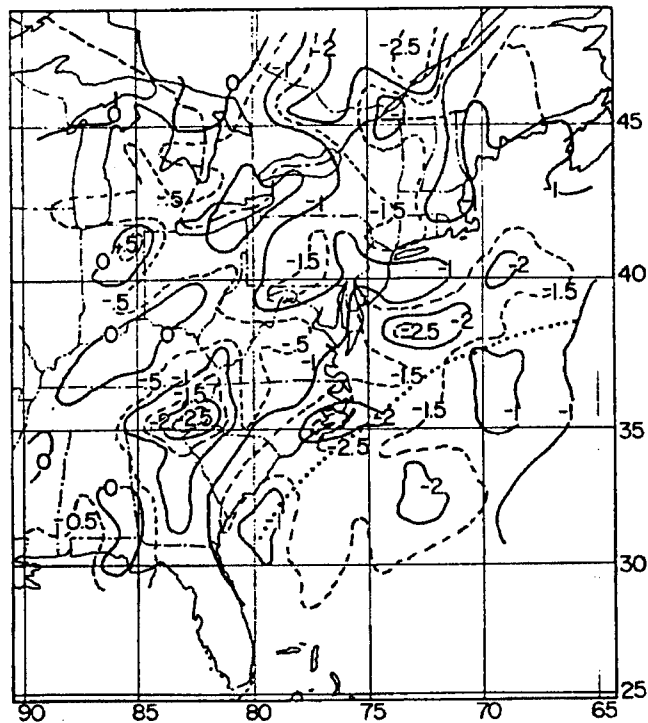
Figure 2.6. Net 3-hour pressure change (millibars) for all storms for the data sample in Figure 2.5. Dotted line is the same as the dashed line in Figure 2.5 (from Colucci 1976).

and anticyclone events for January and July of 1950 through 1977, including genesis, decay, and propagation tracks. They found that a distinct January maximum of genesis events exists over the northwest Gulf (Figure 2.8), while Gulf cyclone activity is almost completely absent in July (Figure 2.9). They also found that although the northwest Gulf tends not to be a genesis region for January *anti*cyclones (Figure 2.10), high pressure centers do migrate into the northwest Gulf with relatively high frequency during January (Figure 2.11).

9
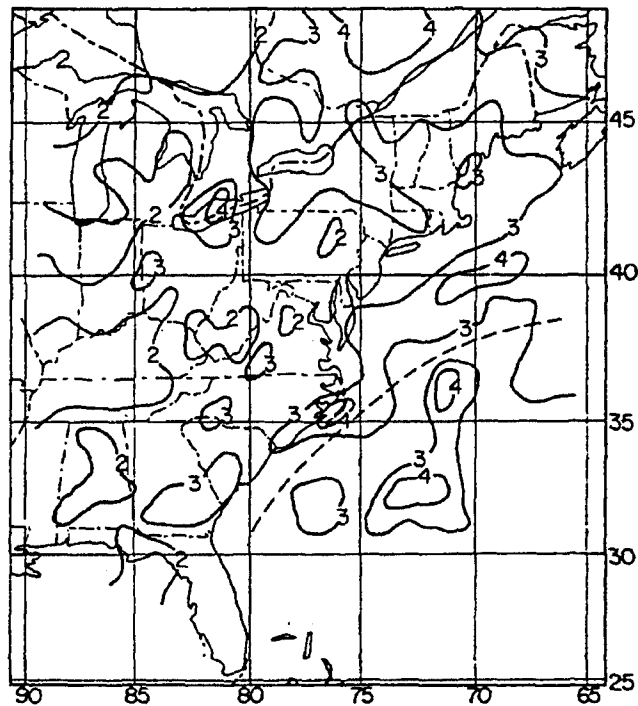
Figure 2.7. Net 3-hour pressure change (millibars) for all storms that deepened for the data sample in Figure 2.5. Dashed line is the same as in Figure 2.5 (from Colucci 1976).
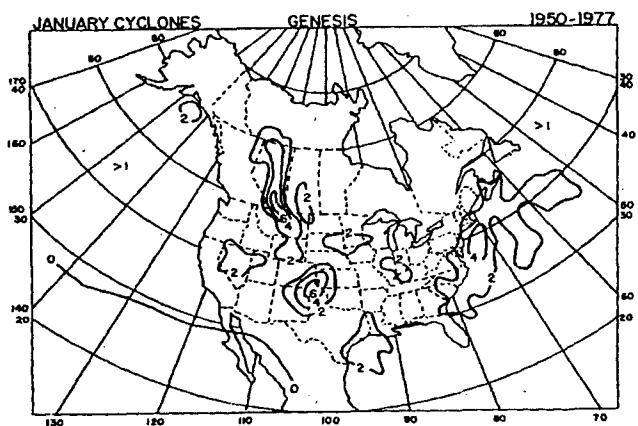
Figure 2.8. 1950-1977 areal distributions of genesis for January cyclones. Values represent 28-year totals (from Zishka and Smith 1979).

10
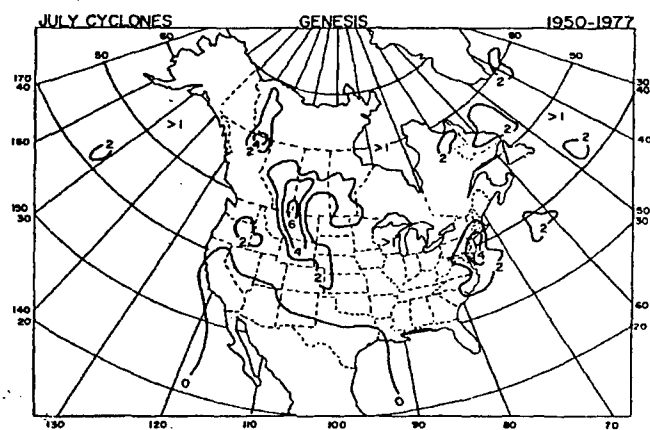
Figure 2.9. As in Figure 2.8 but for July cyclones (from Zishka and Smith 1979).
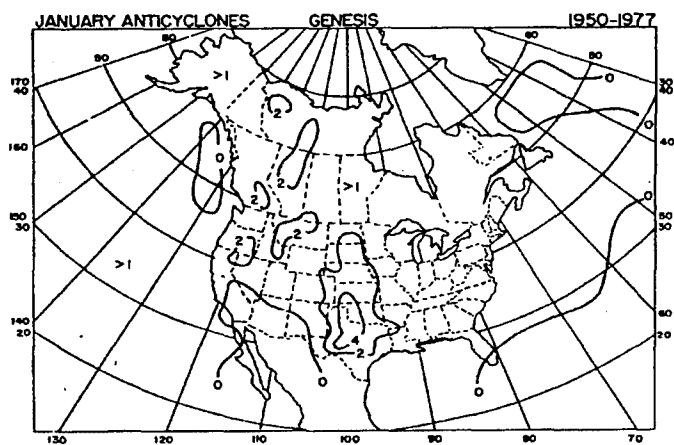
Figure 2.10. As in Figure 2.8 but for January anticyclones (from Zishka and Smith 1979).

11
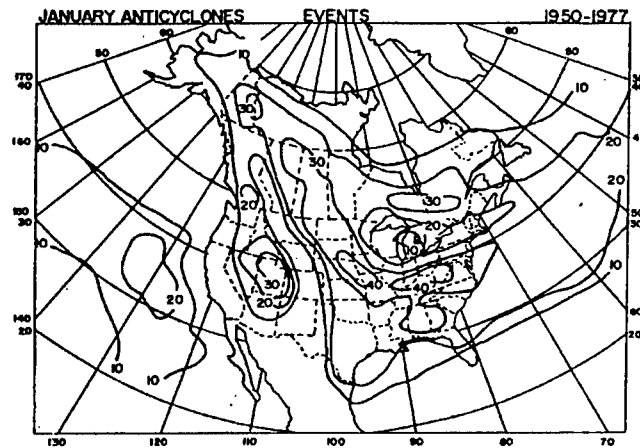
Figure 2.11. 1950-1977 areal distributions of events for January anticyclones. Values represent 28-year totals (from Zishka and Smith 1979).

In a study of the geographical and seasonal distribution of North American cyclogenesis for the years 1958 through 1977, Whittaker and Horn (1981) identified three major areas of cyclogenetic activity (Figure 2.12): 1) East Coast (E) combined with western Gulf of Mexico (G), 2) Colorado (C) combined with Great Basin (B) and 3) Alberta (A) combined with Northwest Territories (N). Similar to the results of Zishka and Smith (1989) was Whittaker and Horn's finding that cyclogenesis in the Gulf is quite rare in the summer months, although the East Coast remains active throughout the year (an observation which "may reflect some tendency for leeside development to the east of the Appalachians throughout much of the year"). They also noted a marked decline in the frequency of North American cyclogenesis during the 1958-1977 period, in agreement with the results of Reitan (1979) and Zishka and Smith (1980).

12
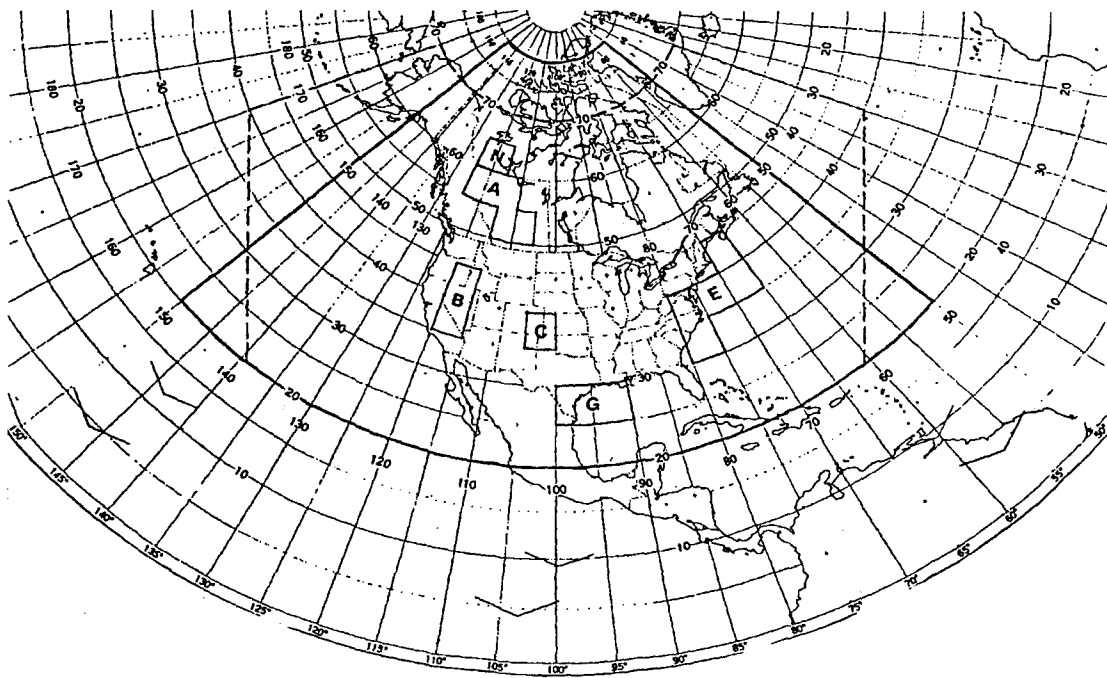
Figure 2.12. North American sector. Solid line encloses study area of Zishka and Smith (1980) and Reitan (1974, 1979). Enclosed 5-degree latitude-longitude boxes are areas of frequent cyclogenesis: (A) Alberta, (B) Great Basin, (C) Colorado, (E) East Coast, (G) Gulf of Mexico, and (N) Northwest Territories (from Whittaker and Horn 1981).

Johnson et al. (1984) studied winter cyclogenesis in the Gulf for the period 1977 through 1983 and found that of 70 total events, 80% developed between 23N and 30N latitude, from 90W to 99W longitude, and found that more than half were initiated over the northwest Gulf between 25N and 28N, from 94W to 98W (Figure 2.13). This work also related an abnormally high frequency and intensity of Gulf cyclones during the winter of 1982-83 to the southward displacement of the polar jet stream by a strong ENSO event, topographic influences of the Sierra Madre Oriental mountains, and sea surface temperature gradients of the northwest Gulf.
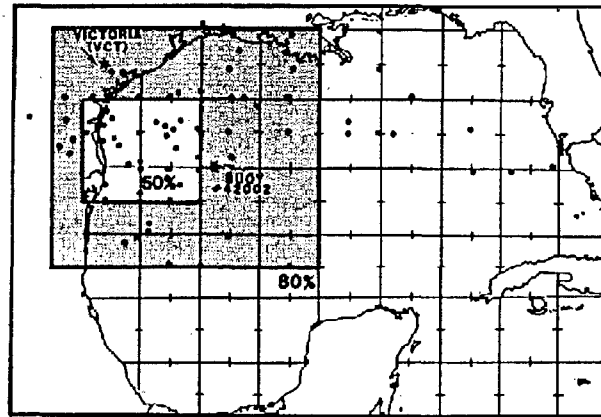
Figure 2.13. Distribution of points of initial cyclogenesis during the winter season, 1977 to 1983. The outer box encloses 80% of the points, whereas the inner box encompasses 50% of the points (from Johnson et al. 1984).

Businger et al. (1990) compiled a storm-following climatology for the precipitation distributions associated with winter cyclones that originated over the Gulf of Mexico and adjacent coastal region during January through March, 1960-1983. The climatology included only those storms producing at least 25 millimeters (mm) of precipitation per 24 hours at a minimum of three reporting stations, and covering roughly a two-state area along the storm's track. Of 453 identified cyclones, 130 met the above criteria (genesis locations plotted in Figure 2.14), 51% of which originated over the Gulf Coast Region (Table 2.1). Consistent with Colucci's (1976) findings was the determination that the northeast Gulf of Mexico is not a region which is conducive to cyclogenesis. Businger et al. also identified 3 primary tracks of the Gulf storms

14
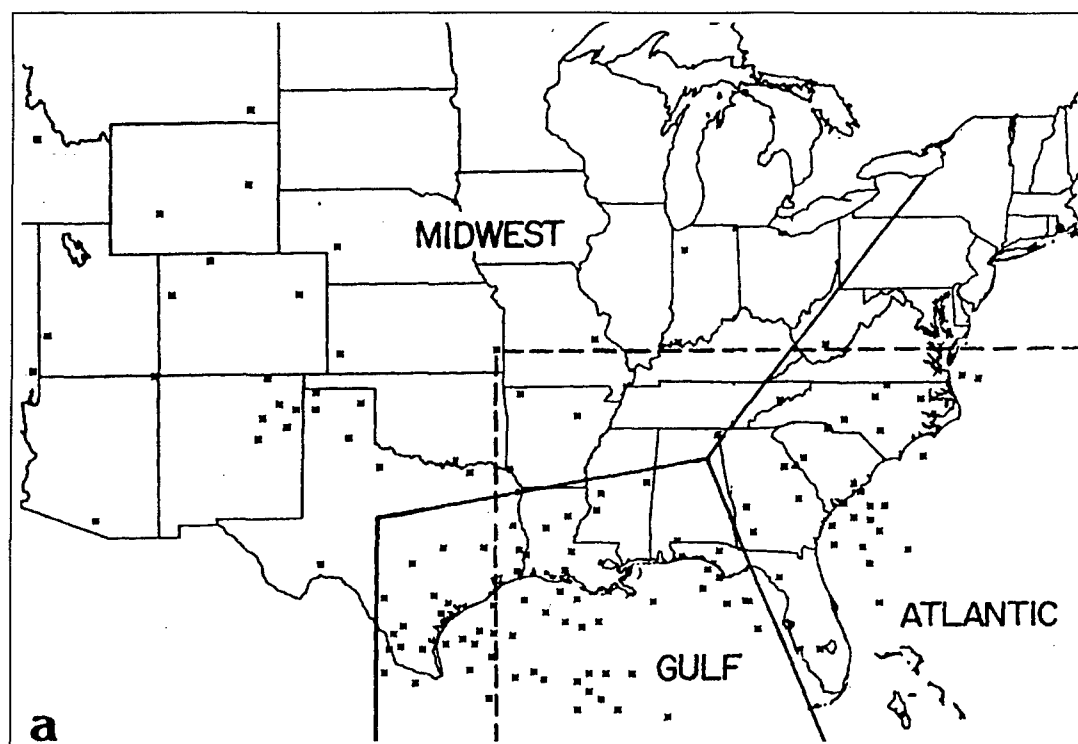
Figure 2.14. Geographic areas of cyclogenesis; asterisks indicate locations of low centers when closed isobars were first analyzed on surface charts for significant precipitation producing cyclones. Dashed line indicates boundary across which cyclones must traverse to be included in the climatology (from Businger et al. 1990).

Table 2.1. Significant precipitation producing cyclones, January-March, 1960-1983 (from Businger et al. 1990).

Origin of low	Number with precipitation ≥ 25 mm	Percent of all lows with precipitation ≥ 25 mm	Percent of total lows
Midwest	33	25	7
Gulf Coast	66	51	15
Atlantic	31	24	7
Total	130		

15

(Figure 2.15). Track A corresponds to cyclones which migrated primarily along the

United States east coast, east of the Appalachians, and represented ~58% of the sample.

Track B passes inland to the west of the Appalachians (~27%), and Track C delineates

cyclones which passed due east across northern Florida and southern Georgia (~15%).

Composite tracks (Figure 2.16) represent the mean axes of the individual tracks shown

in Figure 2.15. Various statistics were tabulated for each of the tracks over multiple

legs, including propagation speed, central pressure tendency, and geostrophic relative

vorticity changes following the storms (Table 2.2). The region of greatest

intensification occurs along Leg 3 of Track A, a region well-known for cyclogenesis.

Storms tend to weaken, however, along Tracks A and C as they move across the

northeast Gulf to the Florida peninsula, confirming previous studies.

Table 2.2. Track statistics. Speed is given in km hr^{-1}. $\delta p/\delta t$ = change in pressure (mb hr^{-1}) following the storm. $\delta\zeta/\delta t$ = change in surface geostrophic relative vorticity ($\times$ 10^{-5} s^{-1} hr^{-1}), where $\zeta = \rho^{-1}f^{-1}\nabla^2 p$ (from Businger et al. 1990).

		Leg 1	Leg 2	Leg 3
A	Speed	48	76	55
	$\delta p/\delta t$	-0.3	-0.3	-0.4
	$\delta\zeta/\delta t$	-0.4	-0.2	1
B	Speed	23	58	
	$\delta\zeta/\delta t$	-0.6	-0.3	
	$\delta p/\delta t$	-0.01	0.2	
C	Speed	45	52	
	$\delta p/\delta t$	-0.2	-0.3	
	$\delta\zeta/\delta t$	0.2	-0.3	
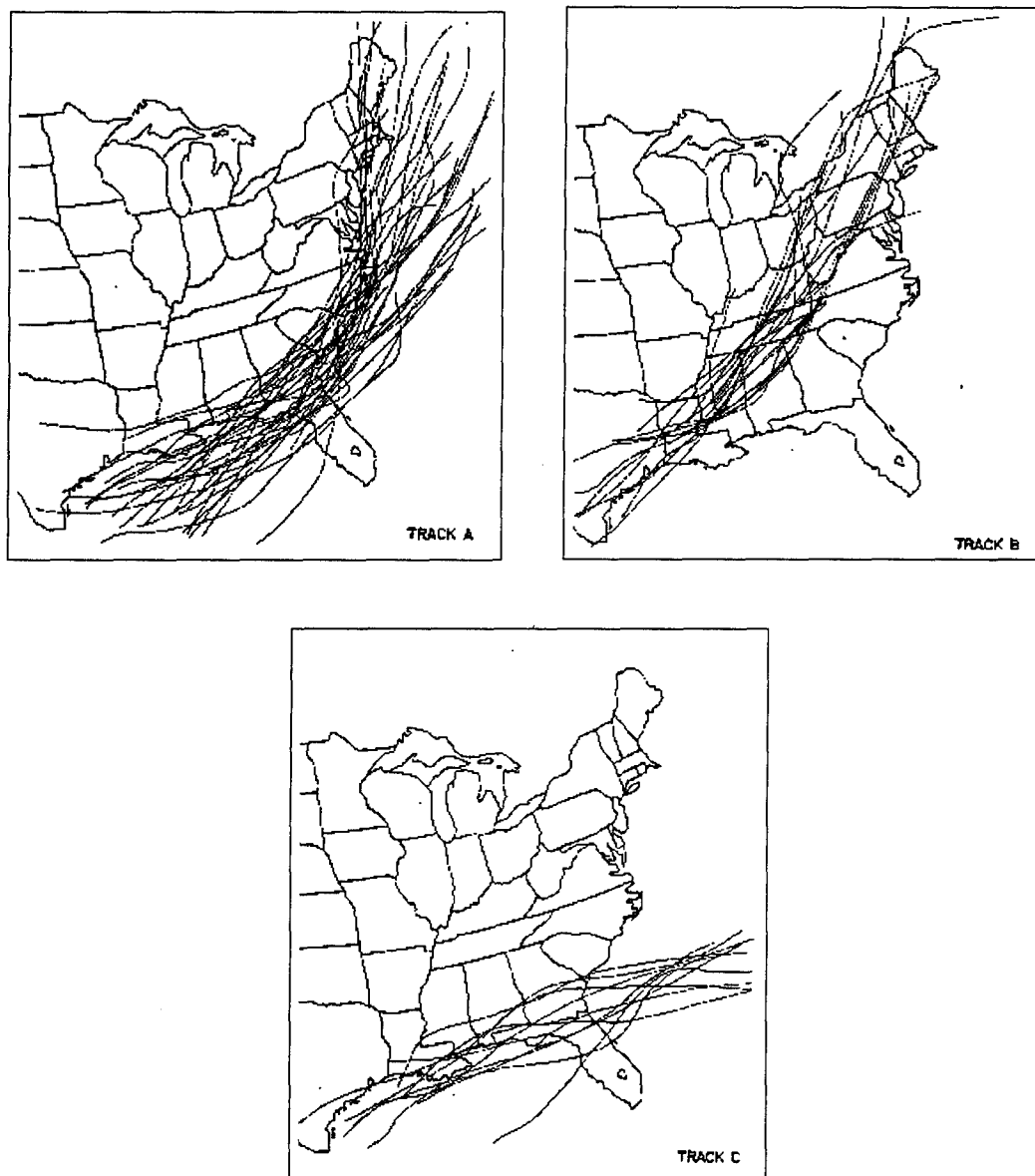
Figure 2.15. Storm tracks of the 66 cyclones that originated over the Gulf of Mexico and its coastal region (area labeled "Gulf" in Figure 2.14). a) Tracks of lows that comprise composite Track A. b) Tracks of lows that comprise composite Track B. c) Tracks of lows that comprise composite Track C (from Businger et al. 1990).

17
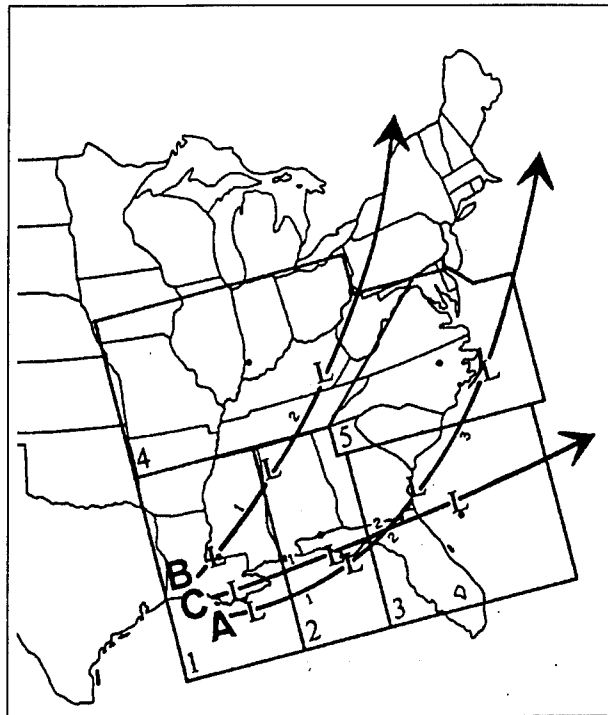
Figure 2.16. Composite storm Tracks A, B, and C, and geographic regions numbered 1 through 5. The "L"s indicate the locations along each composite track closest to the centers of geographic regions (indicated by solid dots). Regional legs along Tracks A, B, and C are indicated by the small numbers (from Businger et al. 1990).

In a study of extratropical cyclones which produced waves which were at least

1.6 meters deep at Cape Hatteras, North Carolina from 1943 to 1984, Davis et al.

(1993) identified eight distinct storm types, based on the storm's origin, track, and

intensification rate. Their classification of "Gulf Low" included cyclones which

typically form

> over the Gulf of Mexico along a stationary front but can occur anywhere over the
> south-eastern USA west of Florida ... A surface disturbance develops downstream of
> either a short-wave upper air trough or a closed low embedded in a fairly zonal
> long-wave pattern. The typical track brings them north-east over southern Georgia
> then over the Atlantic where they often reintensify along the coastal baroclinic zone
> and north of the Gulf Stream (Colucci 1976). These cyclones are not blocked by an

18

anticyclone to the north and therefore move much more rapidly than the Bahamas or Florida lows, but their north-easterly track and rapid intensification over the Atlantic Ocean can produce a long fetch and substantial wave heights. [The Gulf Lows have a] February maximum in cyclone frequency.

Davis et al. placed Gulf lows third in the ranking of northwestern Atlantic Ocean damaging extratropical storms, based on storm duration and average significant wave height.

Summary

Many researchers who have investigated cyclogenesis over North America have documented the existence of a wintertime maximum in the frequency of cyclogenesis in the Gulf of Mexico region. Cyclone classifications have been made based on either identifiable synoptic patterns during genesis and subsequent evolution or on the amount of damage which ultimately results from these storms. Saucier's (1949) synoptic classifications of Gulf cyclones will be revisited in Chapter 3 and will be used to introduce the results of a new Gulf cyclone climatology. In addition, a unique classification scheme will be presented. Cyclones which develop along analyzed, pre-existing, airmass-type frontal boundaries will be distinguished from those which do not, in order to determine the role of the polar front in Gulf cyclogenesis.

CHAPTER 3

SPATIAL DISTRIBUTIONS, TEMPORAL VARIABILITY, AND SYNOPTIC

CLASSIFICATIONS OF GULF OF MEXICO CYCLOGENESIS

<u>A Climatological Study of Gulf Cyclogenesis</u>

<u>Methodology</u>

A study involving manual map classification was performed by the author to

determine the characteristics of cyclogenesis over the Gulf of Mexico. Manual map

classification is commonly used in synoptic climatological research to identify

preferred regions of cyclogenesis and circulation regimes (see, e.g., Muller 1977; Crisp

and Lewis 1992), and, despite its limitations, has been demonstrated to be as

advantageous as some automated approaches in identifying variations in environmental

parameters (Davis et al. 1993).

In this study, a cyclogenesis event was defined as the initial formation of a

surface cyclone which subsequently persisted for at least 24 hours. Each surface

cyclone was identified by the appearance of an "L" (i.e., a center of low pressure) on a

surface synoptic chart, within a region between 25N and 31N latitude and 82W and

98W longitude (see Figure 3.1). Unlike in other climatologies (see, i.e., Norris 1992;
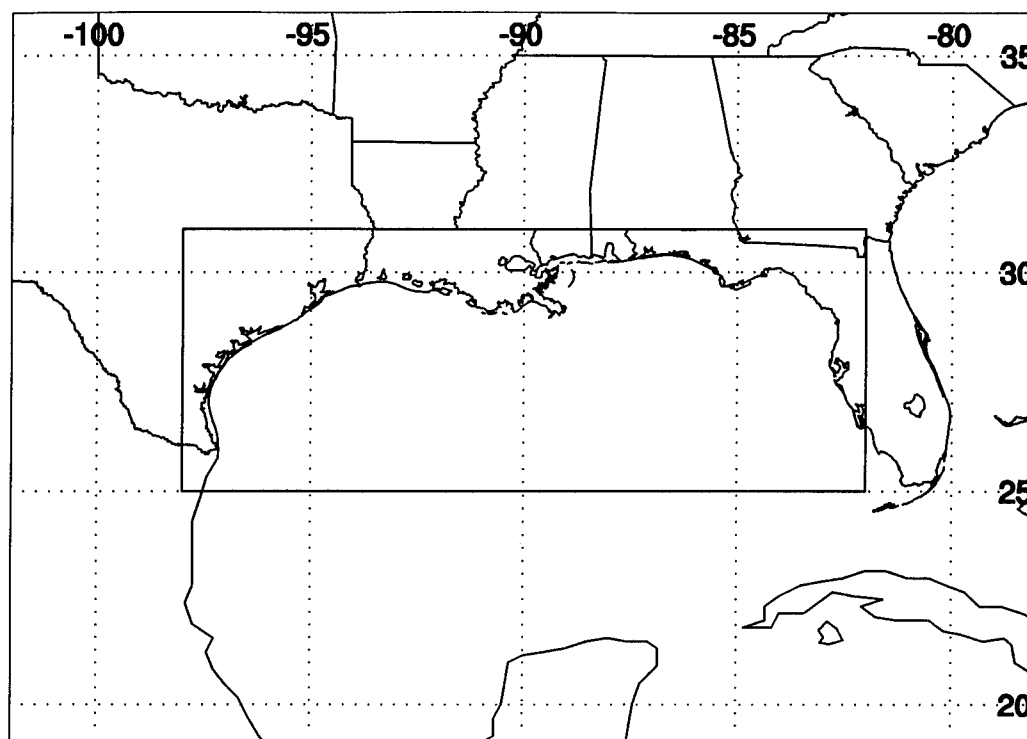
Figure 3.1. Domain of author's study.

Whittaker and Horn 1981; Zishka and Smith 1980), a closed isobar was not used as a criterion. (Such a restriction is unnecessary since any analyzed center of low pressure *would* have a closed isobar surrounding it, given a sufficient contour interval). Cyclone centers which migrated into the domain were not included in this study; only those surface systems which were analyzed to form within the domain were identified. In order to restrict the study to that of winter extratropical cyclogenesis, only the months of September through April were included, and systems which were clearly tropical in nature were disregarded. Forty-one "seasons" (1950-1951 through 1990-1991) were investigated by an inspection of the *Daily Series Synoptic Weather*

Maps, which has been in existence in one form or another for the past 120 years (Kocin et al. 1991), produced by the United States National Oceanographic and Atmospheric Administration. The *Daily Series Synoptic Weather Maps* and *Daily Weather Maps -- Weekly Series* were generated once per day to depict surface and upper-air data. The 1200 UTC observations were normally used in the author's study, but the time of daily analysis was not consistent for all years.

The locations of cyclogenesis were determined by carefully aligning a 1-degree by 1-degree latitude-longitude grid over each surface map. If a low pressure center which had not been analyzed on the previous chart (24 hours earlier) appeared in the domain on the current chart and was determined not to have migrated into the domain but rather to have first appeared within the domain at the current time, then the next synoptic chart (24 hours later) was investigated. If the same low was (subjectively) present on the next chart, even if no longer in the domain, then the date and time of the current chart were noted as the date and time of cyclogenesis, and the location of cyclogenesis was estimated to the nearest one-tenth of a degree. Examples of typical sequences of events will be provided later in Figures 3.19 and 3.23.

Tracks of well-defined cyclones were plotted explicitly on the synoptic charts. A typical example of this is provided in Figure 3.2. In such instances, the time and location of cyclogenesis were taken directly from the surface chart, and the above methodology was not employed.
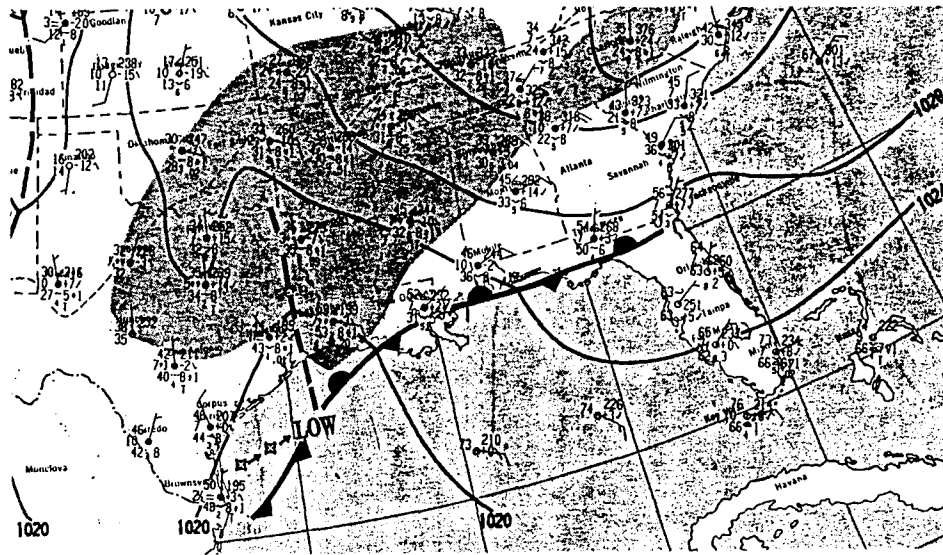
Figure 3.2. Example of an explicitly-tracked low. Surface analysis for 1200 UTC
27 December 1990 (from *Daily Weather Maps, Weekly Series*).

Spatial Distributions and Sources of Error

The resulting spatial distribution of all 313 Gulf cyclogenesis events for the years

1950-1951 through 1990-1991 is plotted in Figure 3.3. Errors in this distribution may

be attributed to position and timing discrepancies on the surface analyses themselves.

Such errors are likely to be most serious over the open water far from shore, and in

regions of few cyclogenesis events (Colucci, 1976). In addition, the analyses

themselves cannot be considered invariable representations of the data, since subjective

and automated analysis techniques have changed considerably through the years

(Kocin, *et. al.*, 1991).

23
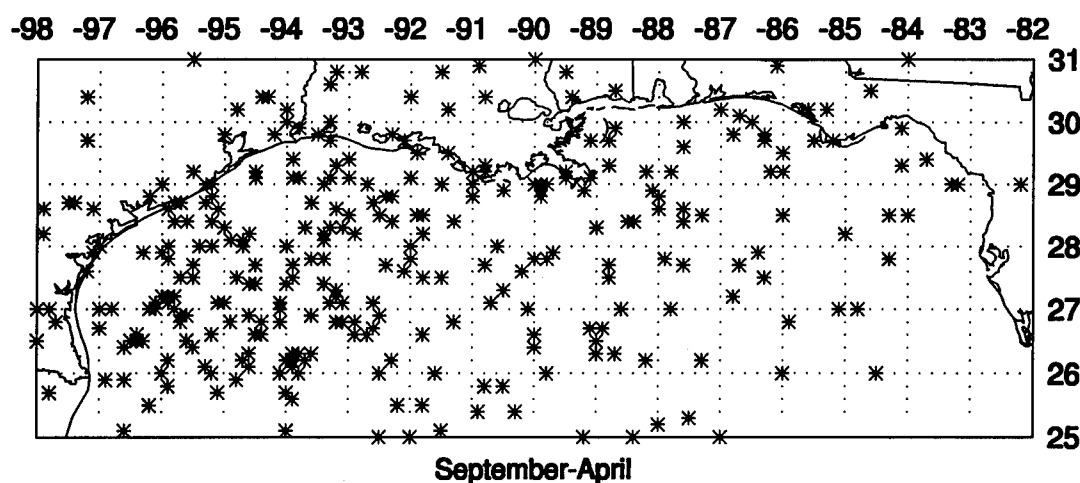
Figure 3.3. Locations of cyclogenesis, as defined in the text, during the months of September-April, 1950-1991.

Even if the data had been sufficient for accurate, consistent analyses of cyclogenesis events, errors are also introduced due to the once per day sampling methodology. Since cyclones which form in this region generally move to the east-northeast at speeds of up to 25 miles per hour on average (Saucier 1949), discretely sampling these events at 24-hour intervals created some ambiguity in determining the exact locations of cyclone initiation. For example, if a cyclone had actually been initiated outside the domain, but the site of first detection was within the domain, then this event would have been erroneously included as a Gulf cyclogenesis event, and the location of genesis would have been inaccurate. Similarly, if a cyclone were to have developed within the domain, but migrated out of the domain before its first appearance on an inspected surface chart, this Gulf cyclogenesis event would have been missed. Such errors were minimized, though, since the tracks of well-defined

24

cyclones are plotted explicitly in the *Daily Weather Maps* series.

From a cursory inspection of Figure 3.3, it is evident that cyclogenesis in the northern Gulf occurred with highest frequency over the open water southeast of the Texas coastline, and not at the land-sea boundary. Cyclogenesis was less frequent over the eastern, and particularly the southeastern, region of the domain to the west of the Florida peninsula. The benchmark works of Saucier (1949) and Petterssen (1956) referred to in Chapter 2 showed similar distributions of Gulf cyclogenesis frequency, with highest concentrations offshore the Texas/Louisiana coast and lesser values to the east. Their data were independent from those used in the current study. In addition, the research of Zishka and Smith (1979) encompassed a larger domain and also showed similar results. The author is therefore confident that the pattern noted in Figure 3.3 is representative of the process under consideration.

Temporal Variability

A time series of the number of cyclogenesis events per winter season is presented in Figure 3.4. The number of events ranged from 3 to 20 over the 41-season period, with an average of 7.6 per season. Although no other research has investigated cyclogenesis frequencies over exactly the same location and for the same time period, the maxima in frequency for the seasons 1982-83 and 1986-87 are consistent, for example, with the findings of Johnson et al. (1984) and Norris (1992). The overall upward trend in the seasonal frequency of events, however, is not in agreement with Norris (1992), who detected a downward trend in 10-year running means from the
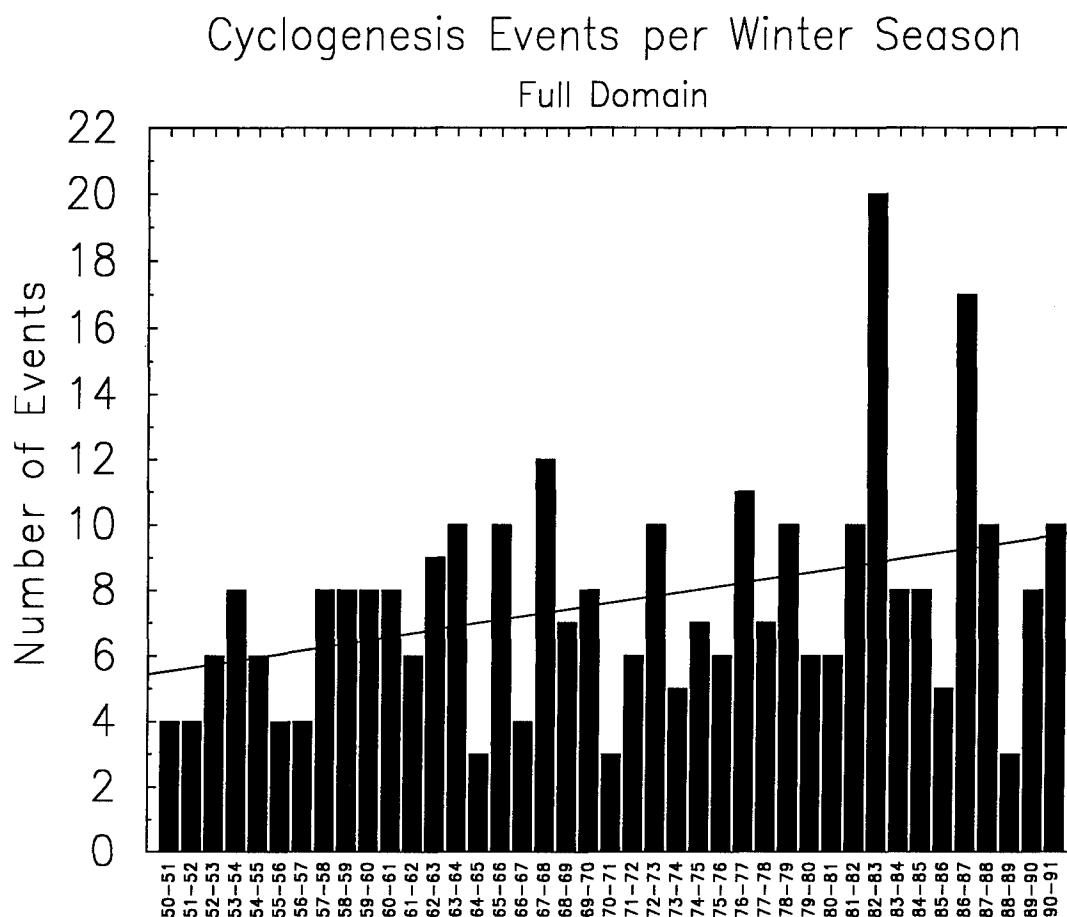
Figure 3.4. Time series of cyclogenesis events per winter season, with linear regression (solid line).

winter season of 1961-61 to that of 1984-85, with an upward trend thereafter.

Analysis of Trends. Differences between these data sets may be explained in part by the differing study domains chosen by each author. Norris' study domain extended to 35N latitude and included much of eastern Texas. The area of the current study lies completely within Norris' study domain, but about three-fifths of the region is located over the open water of the Gulf, where data sources have been more variable over the period of study.
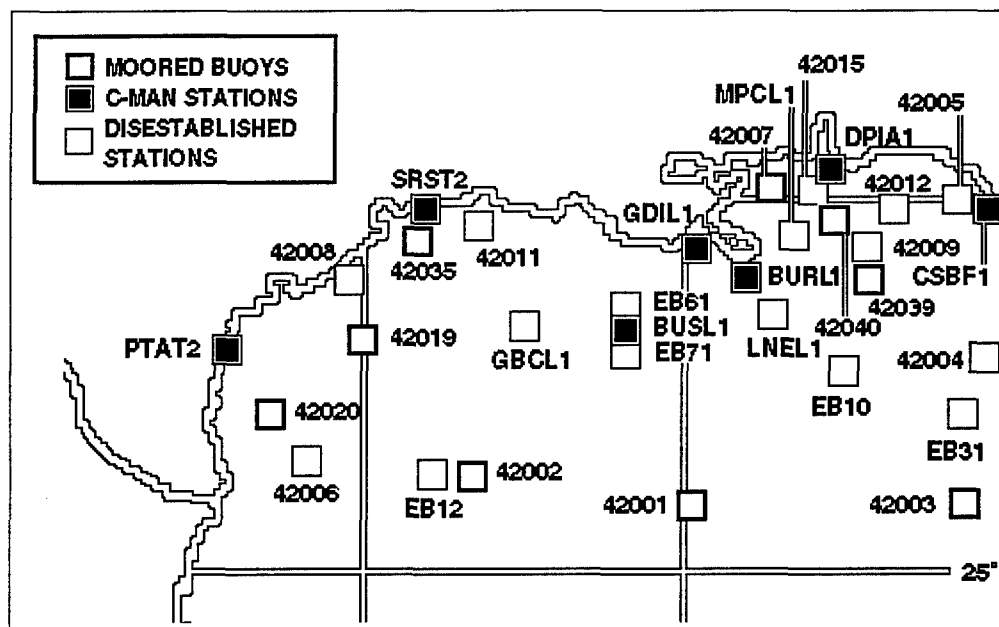
Figure 3.5. Locations of surface data sources over the northwest Gulf as of August 1995 (obtained via the internet from National Data Buoy Center, cited 1996: http://seaboard.ndbc.noaa.gov/).

Prior to the early 1970s, data buoys had not yet been deployed into the Gulf. See

Figure 3.5 for locations of both operational and disestablished moored buoys and

coastal marine automated stations (CMANs) in the northwest and north-central Gulf.

Although an explanation of observed trends in cyclogenesis frequency is beyond the

scope of this paper, it *is* necessary to understand how data availability might have

affected the results of the study.

In order to determine whether the addition of buoys and CMAN stations into the

Gulf affected trends in the analyses of cyclogenesis events, the study domain was

divided into three regions (Figure 3.6). The Coast region was the first to be defined. It
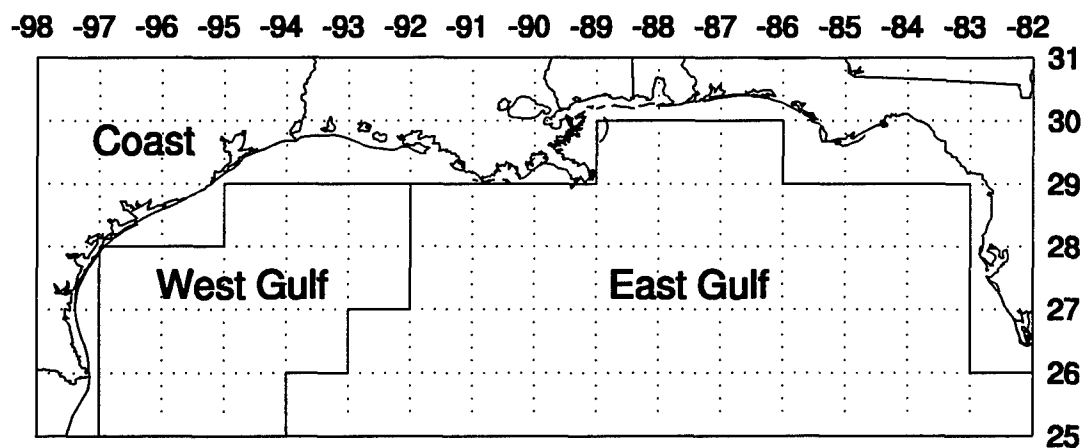
Figure 3.6. Regions used for statistical analysis.

includes all 1-degree by 1-degree latitude-longitude grid boxes which contain land, and covers about 40 percent of the total study domain. It is assumed that there has been little variability in the concentration of surface data sources in this region throughout the period of study. The total number of observed cyclogenesis cases in this region was 106.

The offshore area was divided into two regions which each contain approximately the same number of observations as the Coast region. The West Gulf region, which covers only about 16 percent of the study domain's total area, contained 107 observations of cyclogenesis, while the East Gulf region (about 45 percent of the total area) contained 100 observations. Although the boundary between these two offshore areas was chosen somewhat arbitrarily, it will be found useful in upcoming discussion.

Plots of cyclogenesis frequency for each of the three regions (Figures 3.7, 3.8,

28
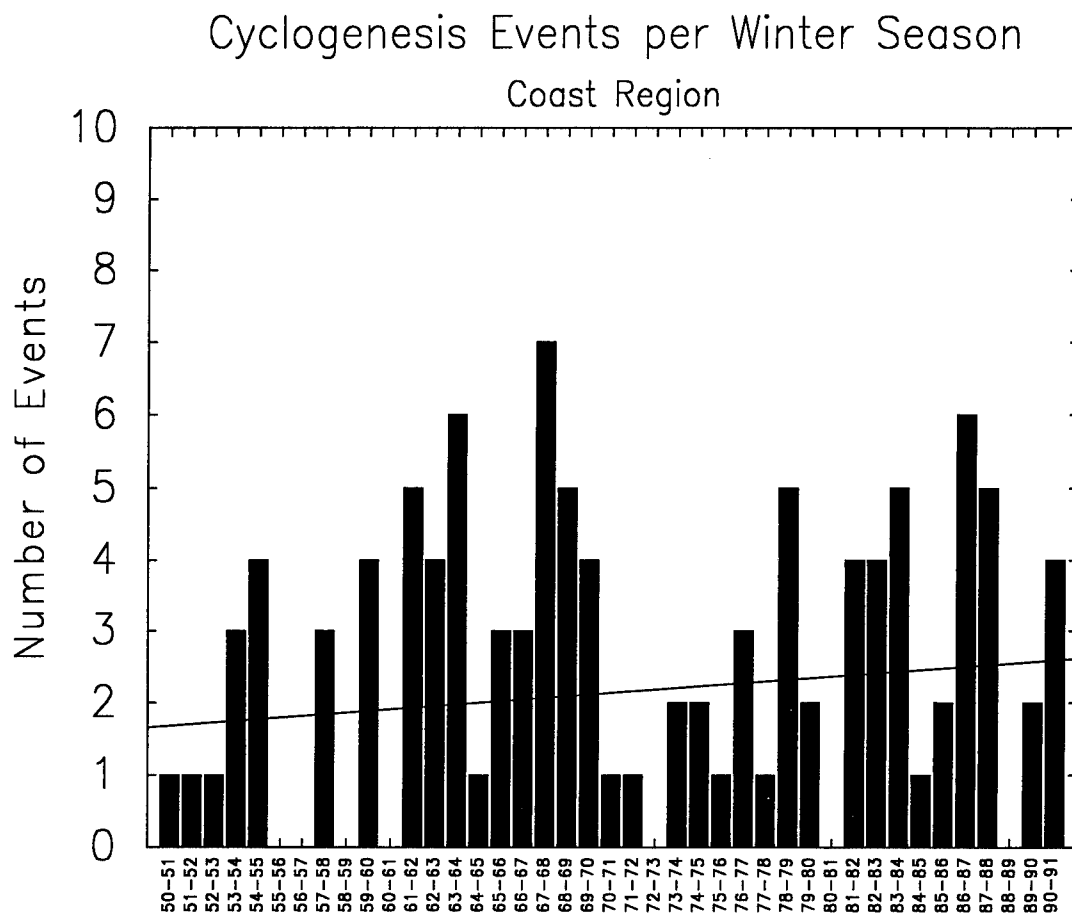
Figure 3.7. Time series of cyclogenesis events per winter season within the Coast region, with linear regression (solid line).

and 3.9) show upward trends which appear similar in magnitude. An equality of slopes hypothesis test was performed (Draper and Smith 1981) in order to determine whether there is statistically significant evidence to reject the hypothesis that all three linear regressions have the same slope.

The objective of the test was to model the number of cyclogenesis events over time where three subsets of data were available. A test of homogeneity of regression

29
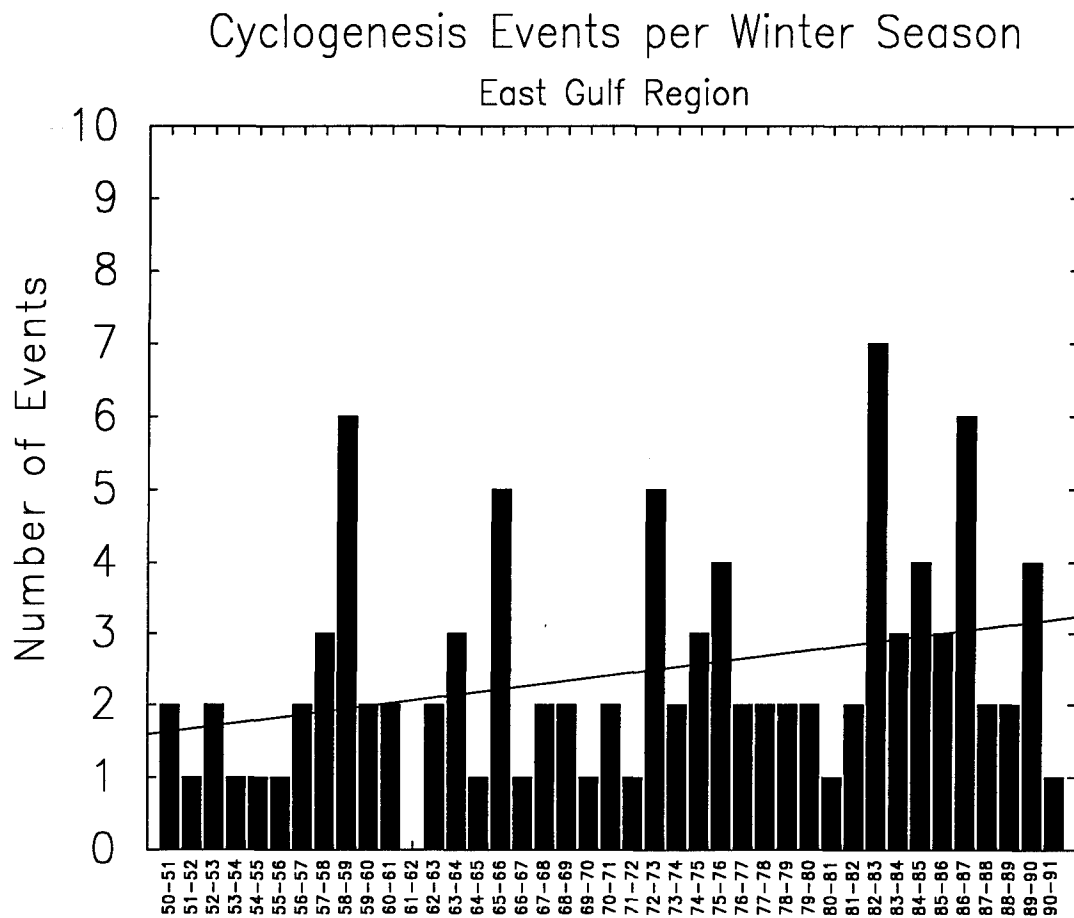
Figure 3.8. Time series of cyclogenesis events per winter season within the East Gulf region , with linear regression (solid line).

slopes (allowing for separate intercepts) was performed to determine if a single

regression equation would adequately describe the relationship (between number of

events and time) for all three regions, or if different regression slopes would be

required for each of the three regions.

One method of reporting the results of a hypothesis test is to report the p-value,

which is data-dependent. A p-value indicates the amount of sample evidence in favor

30

Cyclogenesis Events per Winter Season
West Gulf Region
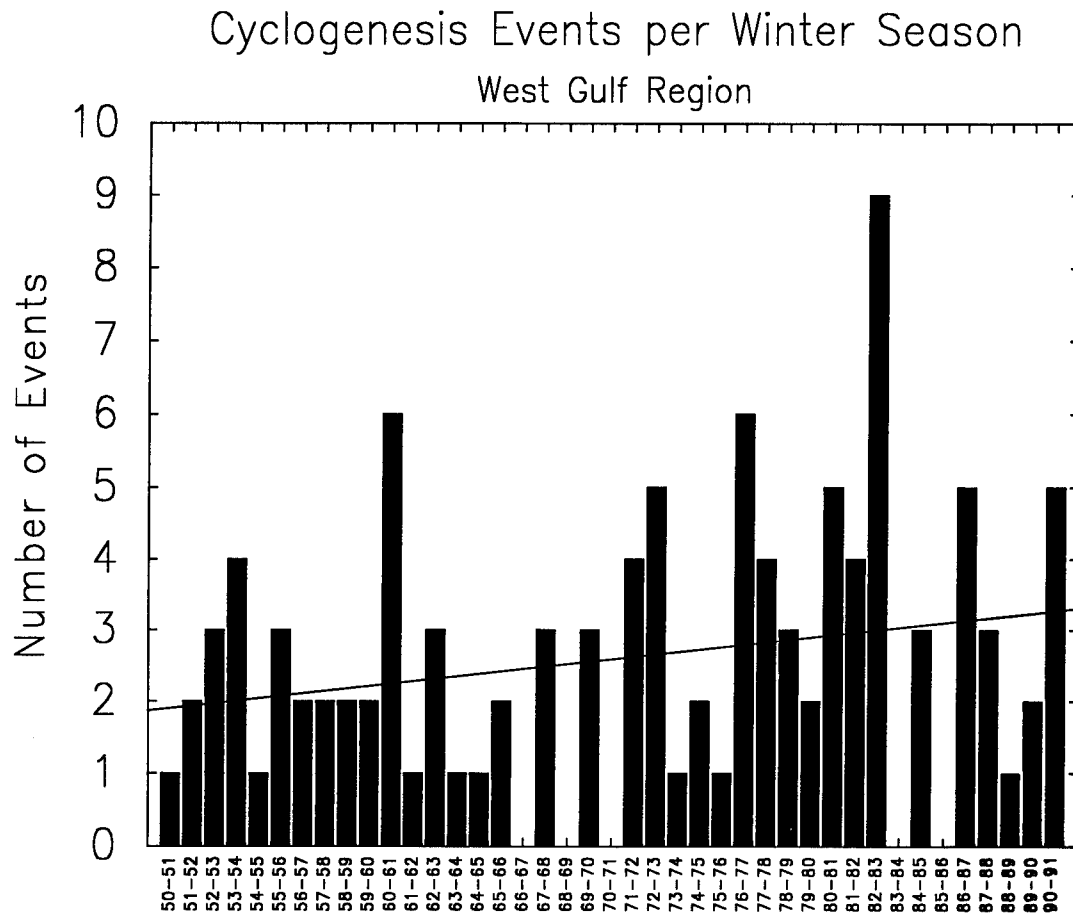
Figure 3.9. Time series of cyclogenesis events per winter season within the West Gulf region, with linear regression (solid line).

of the null hypothesis. If a pre-specified level of significance of alpha = 0.05 is chosen, then the null hypothesis would be rejected if a p-value less than 0.05 is found. The smaller the p-value, the stronger the sample evidence that the alternative hypothesis is true. If the p-value is large, then the sample does not indicate enough evidence to reject the null hypothesis. In this case, a p-value of p=0.86 was obtained, indicating that a single regression equation is appropriate to model the number of events

31
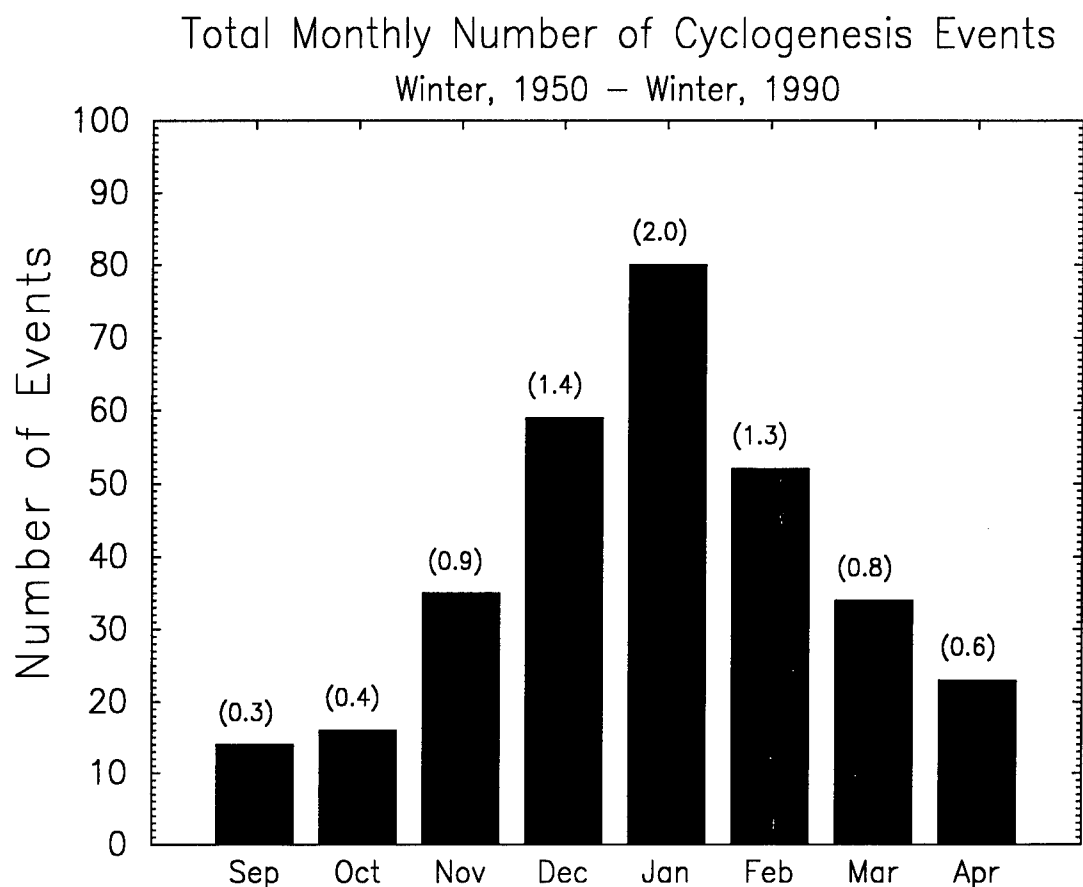
Figure 3.10. Monthly totals of cyclogenesis events for all 41 seasons studied, with average number of events per month in parentheses.

occurring in all three regions, and that the null hypothesis (that all three slopes were equal) could not be rejected.

Although this test does not by any means prove that data coverage is not a factor in the analysis of cyclogenesis events, it does suggest that the increase of data sources in the Gulf has not affected overall trends, since similar trends were observed where data sources are assumed to have remained constant and plentiful over time.

Interseasonal variability. As seen from Figure 3.10 most cyclones developed in January, and just under two-thirds of all events occurred in the combined months of December through February. The number of events per month varied from 0 (even in January) to 6. The distribution of minimum pressures attained by each cyclone while within the study domain is plotted in Figure 3.11. In agreement with Norris (1992), the extrema in minimum pressure were 984 and 1024 mb. The average minimum pressure was 1011.1 mb, but about two-thirds of all cyclones deepened no lower than 1012 mb, and 85 percent had minimum pressures of 1004 mb and higher.

Plots of bimonthly spatial distributions of cyclogenesis yield information regarding the evolution of the pattern of cyclone initiation during the winter months. Figure 3.12 shows the spatial distribution of observed cyclogenesis for the bimonthly periods October-November, December-January, and February-March. September and April have been considered transition months, and are disregarded here due to the low number of events during those months. In these and upcoming plots of spatial distributions of cyclogenesis, limited numbers of observations can make interpretation less conclusive. Samples which have a high number of observations , though, may be most representative of the processes which contribute to Gulf cyclogenesis. To this end, pattern comparisons are determined to be useful.

During October-November, it appears that cyclogenesis is preferred over the open water of the Gulf, particularly east of Texas and south of Louisiana, but has also been observed at scattered locations over the central and eastern Gulf and near the coast of

Minimum Analyzed Pressures
of All Gulf Cyclones, While Remaining in Domain
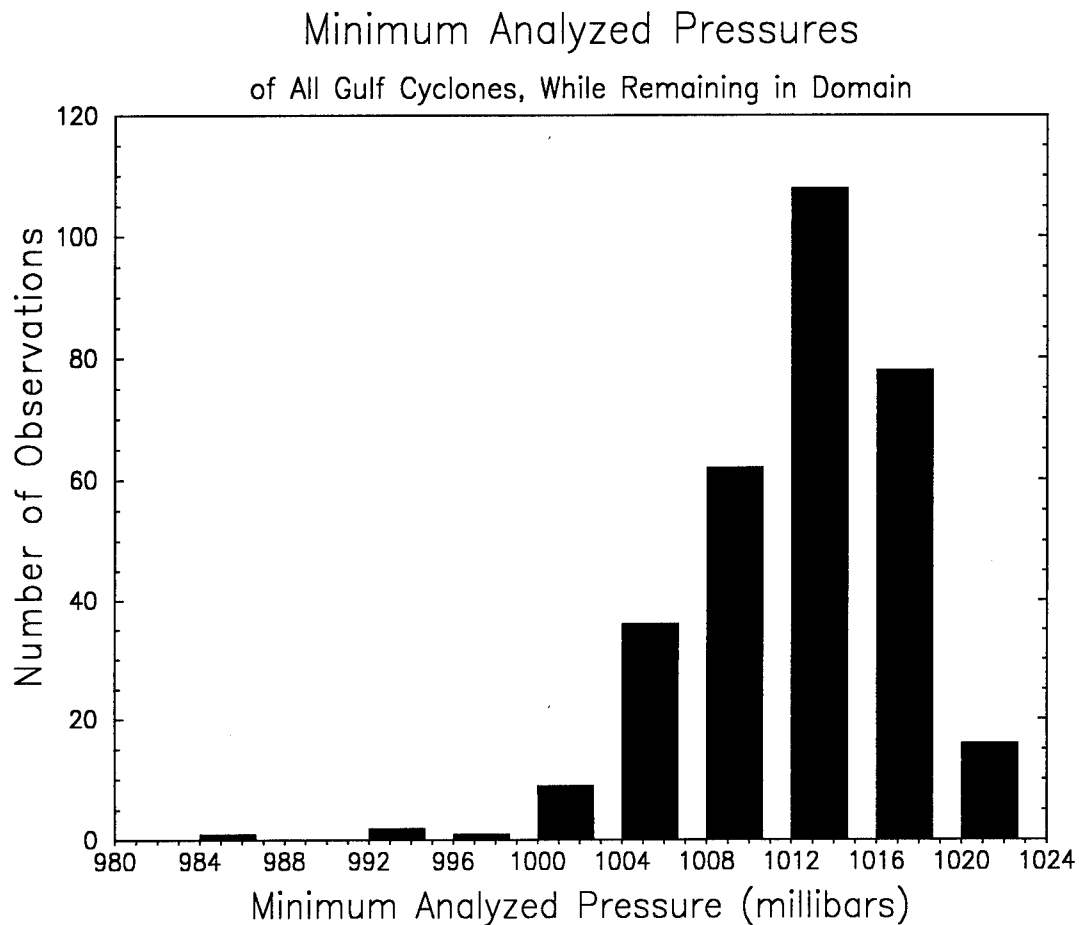
Figure 3.11. Minimum analyzed pressures (while remaining in the domain) of all extratropical cyclones which developed over the Gulf of Mexico, September-April, 1950-1991.

northern Florida. The months of December-January show a marked increase in the frequency of cyclogenesis, and a slight pattern shift which still favors the open water of the northwest Gulf, but indicates less activity (in a domain-relative sense) over the northeast Gulf. During February-March the northwest Gulf remains fairly active, but cyclogenesis is common throughout most of the domain.
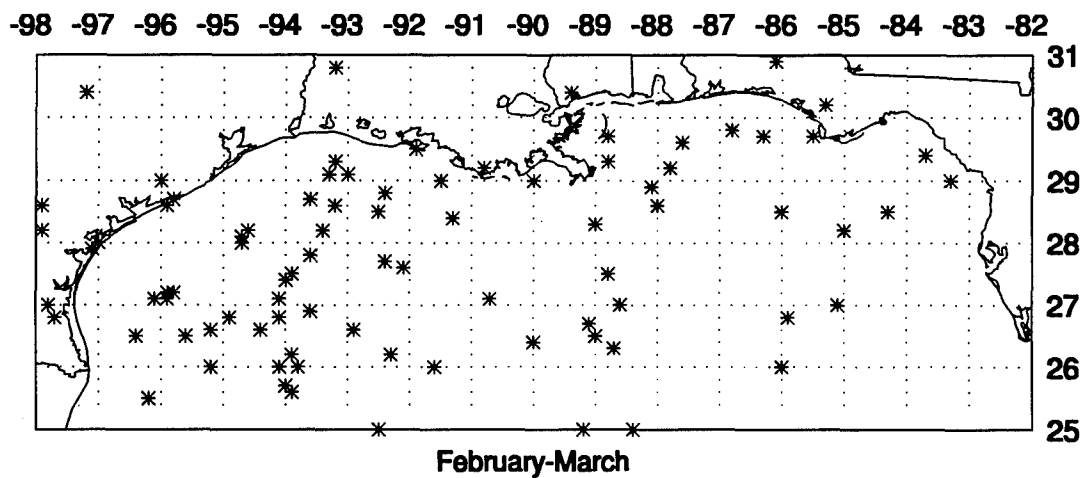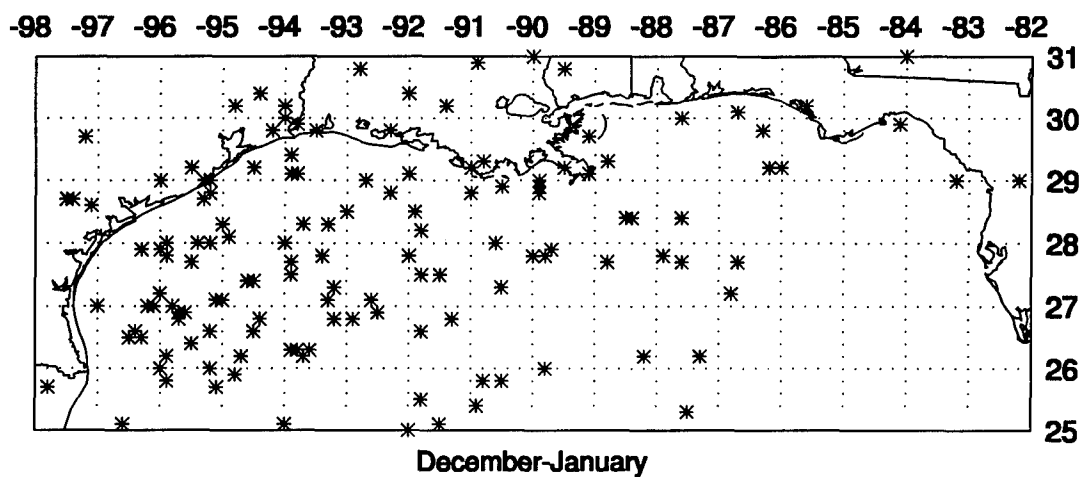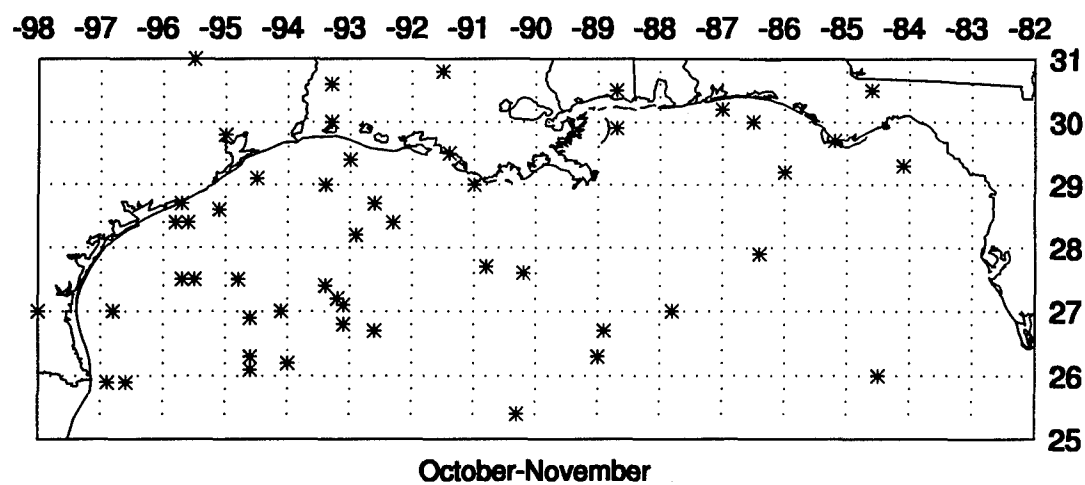
Figure 3.12. Locations of cyclogenesis, for all cyclones: October-November, 51 observations (top); December-January, 139 observations (center); and February-March, 86 observations (bottom).

Synoptic Classifications

As mentioned in Chapter 2, Saucier (1949) studied 388 cyclones which developed in the Texas-West Gulf region, and classified each of these cyclones according to the synoptic (upper-air) pattern present during its inception. Although the domain of his study was to the north and west of the current investigation (including, for example, all of Louisiana and much of Texas), a region which *is* common to both studies is the northwest Gulf, offshore Texas and Louisiana. For this reason it is felt that a similar synoptic classification would be useful.

Saucier found that the Texas-West Gulf cyclones formed when there was polar or arctic air at the surface north of the latitude of the impending cyclone, with almost any degree of modification. He further observed that cyclones tended to form under two distinct flow regimes: 1) eastward motion of an upper cyclonic center (cold-core low) from the southwest United States or from the Baja California region, and 2) the retrogression, development, or persistence of a large-amplitude upper-level trough over the United States Great Plains. He also made distinctions within these classes, creating a total of five synoptic groups which are evident during surface cyclone initiation. Each of these groups are briefly described below (for more complete descriptions see Saucier 1949), and spatial distributions of events from the present study which correspond to each of the synoptic patterns are provided.

Southwest Cold-Core Low

(Group 1) Low latitude of the westerlies east of the Rockies. Most frequent

Group 1, September-April
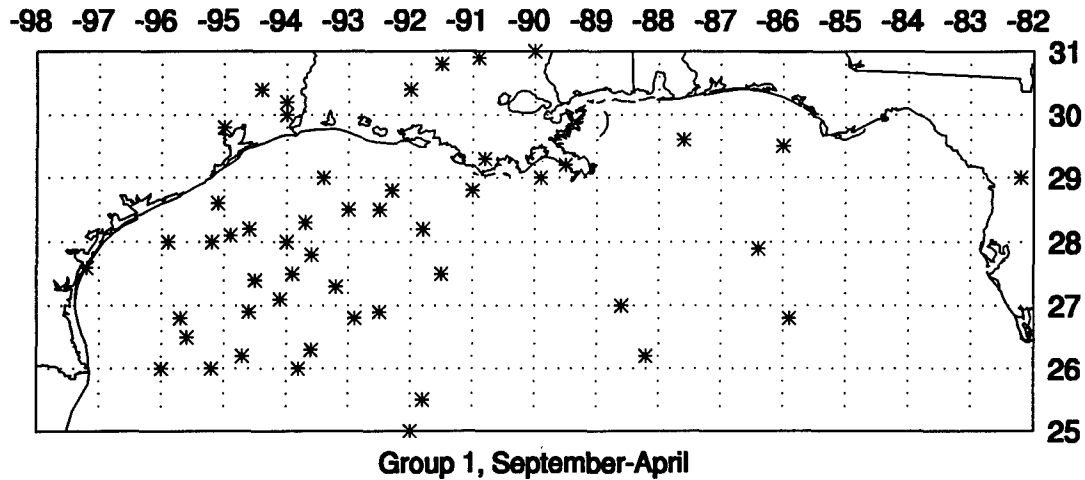
Figure 3.13. Locations of cyclogenesis for Group 1 cyclones, 50 observations.

during the winter months, the cyclones in this group usually form along a persistent

and quasi-stationary front oriented along the northern Gulf Coast when an upper

cyclonic center (cold-core low) migrates eastward from the southwest United States.

In this case, the upper-level westerlies are strongest at low latitudes (relative to the

United States Rocky Mountains), and a broad, cold, north-south ridge dominates the

surface pattern east of the Rockies. In the present study, 50 of the 313 cyclones

identified fell into this group, making this group the second largest of five

classifications. Figure 3.13 shows the spatial distribution for this type of development,

and indicates a strong preference for offshore development over the northwest Gulf.

(Group 2) High latitude of the westerlies east of the Rockies. Most frequent

during autumn, cyclones in this group form when the strongest upper-level westerlies

lie closer to the Canadian border. Although the surface of the eastern United States

37
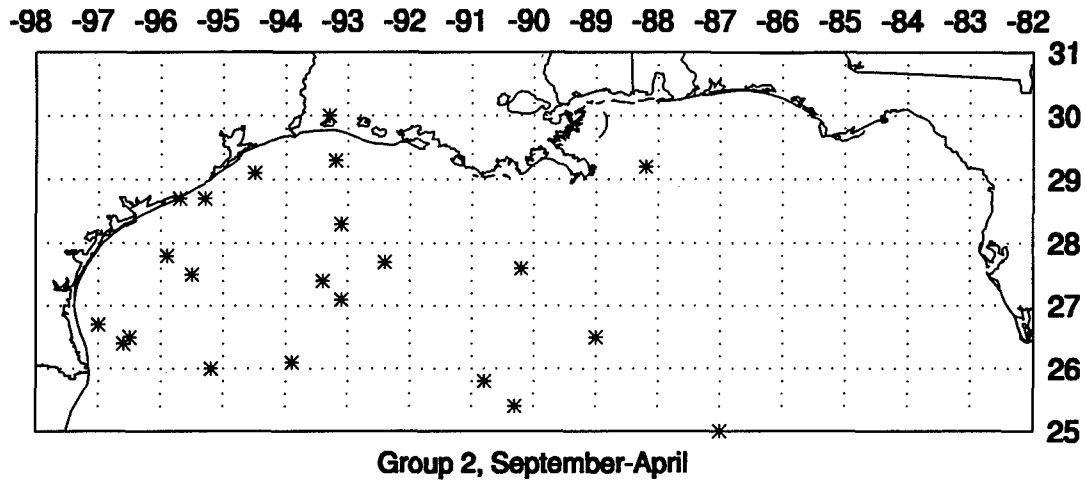
Figure 3.14. Locations of cyclogenesis for Group 2 cyclones, 22 observations.

remains dominated by a ridge, the source region of this high pressure cell was likely

the Pacific Ocean, so that the cool air has had sufficient time to undergo modification

during its eastward migration. As with Group 1, the southwest cold-core low migrates

eastward and initiates Gulf cyclogenesis, but in this case along a weaker polar front. In

the current study, 22 cyclones were classified by these conditions (Figure 3.14).

Again, it appears that the northwest Gulf is preferred for this type of genesis, though

fewer observations yield less confident results.

Great Plains Trough

(Group 3) Retrogressive upper trough. In Saucier's investigation, Group 3

comprised the largest single group of cyclones, and as such, "represents most clearly

the principle of the processes leading to cyclogenesis in the Texas-West Gulf region."

In the current study, 154 of the 313 cyclones were classified as Group 3. The synoptic

38

Group 3, September-April
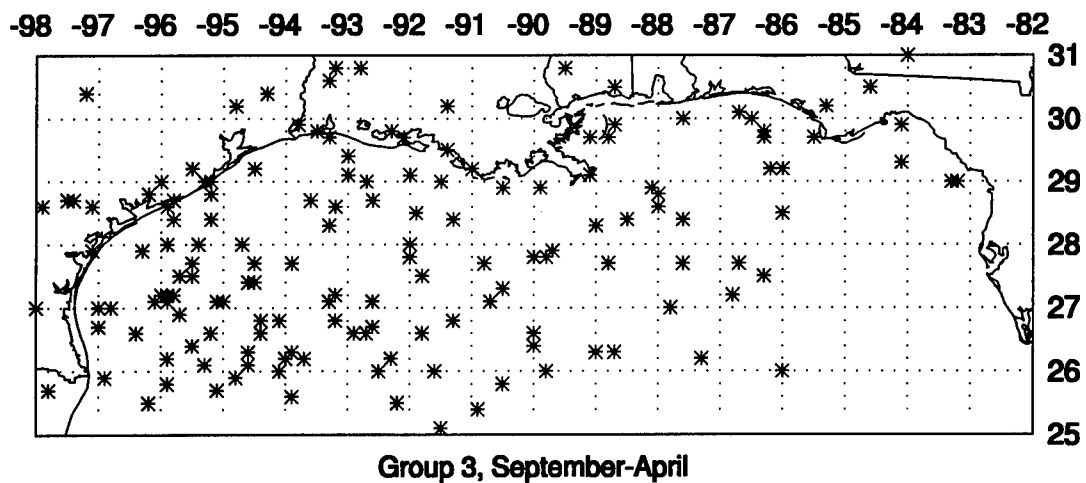
Figure 3.15. Locations of cyclogenesis for Group 3 cyclones, 154 observations.

situation during their inception consists of the apparent slow eastward motion of a high-amplitude trough or closed low at upper levels originally near Colorado, which gives rise to small Gulf cyclones which usually lose their identity within about two days. Saucier described the initiation of a typical cyclone within this classification as a "frontal wave with weather," appearing on the Gulf Coast along the "reactivated polar front," in a region "where the front was previously undergoing dissolution."

The spatial distribution of Group 3 cyclogenesis events (Figure 3.15) shows a high concentration of events southeast of the Texas coast. Cyclogenesis associated with the retrogressive upper trough is somewhat less common over the eastern half of the domain.

Considering the data sources used in his research, Saucier's description of the low-level preconditions for Group 3 cyclogenesis was as complete as possible.

39

Group 4, September-April
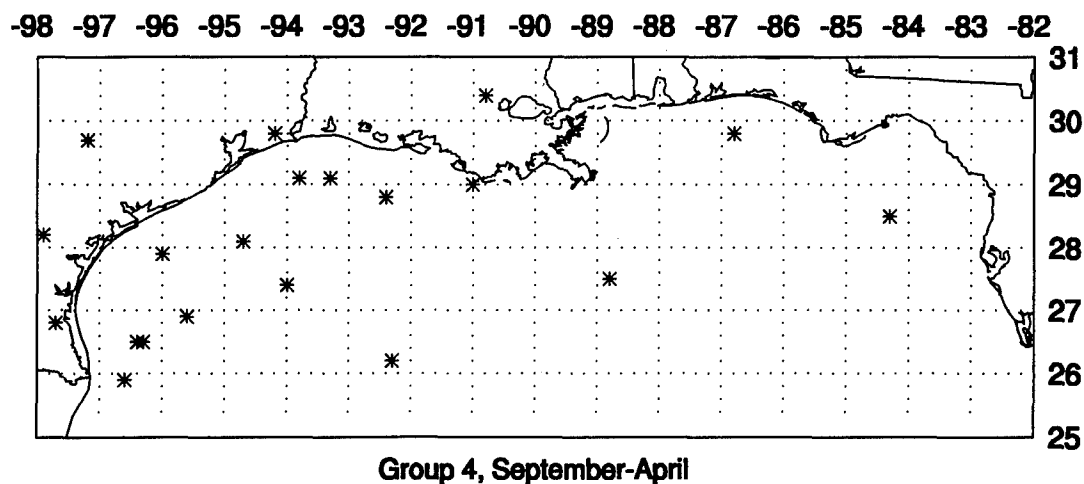
Figure 3.16. Locations of cyclogenesis for Group 4 cyclones, 20 observations.

Evidence will be presented, though, which indicates that a significant number of Group 3 cyclones *do not* form along a polar front which has undergone dissolution, and then become "reactivated," as Saucier suggested.

(Group 4) Discontinuous redevelopment of the upper trough. During the later stages of a cold air outbreak in the eastern United States, the strongest upper-level westerlies may shift northward coinciding with a relaxation of meridional flow, allowing weak upper-level short waves from the Pacific to advance over the continent. Concurrently, intensification of a large-scale trough between longitudes 180W and 140W (the central Pacific Ocean) causes general pressure rises over the United States, but the approaching short wave diminishes this trend over the Plains. Surface pressure falls are concentrated over Texas, and surface and upper-level cold advection occurs rapidly east of the Rockies, contributing to the formation of a sharp upper-level trough.

40

The surface cold front becomes oriented north-south from the Gulf to the lower

Mississippi Valley and southeastern States, and cyclogenesis occurs along it.

As expected, the restrictive nature of this synoptic pattern caused it to be present

during only 20 of the 313 cyclogenesis events. Even for this small group of events,

though, the northwest Gulf appears to be a favored region of cyclogenesis (see Figure

3.16).

(Group 5) Persistent upper trough. Cyclones which fall into this category form

during the primary cold air outbreak, when a high-amplitude trough persists at upper

levels over the Plains. During this scenario, a quasi-stationary front remains in place

along or near the Gulf coast, and waves of low pressure can develop and move along it

with high frequency, even in cyclone "families." Saucier contended that the rapid

migration of these weak cyclones creates difficulty in tracking them from only daily

charts, so that the number of cyclones classified as Group 5 has been minimized. This

author agrees, noting that only 34 cyclones from the present study fell into this

category. Saucier also states that there is a "tendency for these small waves to

originate along various sections of the front without preference for the Texas-West

Gulf region." Indeed, the pattern noted in Figure 3.17 shows a fairly continuous region

of preferred development from well offshore the Texas coast, northeastward to the

western Florida panhandle, with more scattered occurrences to the southeast. One

might envision an analyzed stationary front which lies on average within this region.

Unclassifiable. 33 Gulf cyclones were determined to be unclassifiable according

41
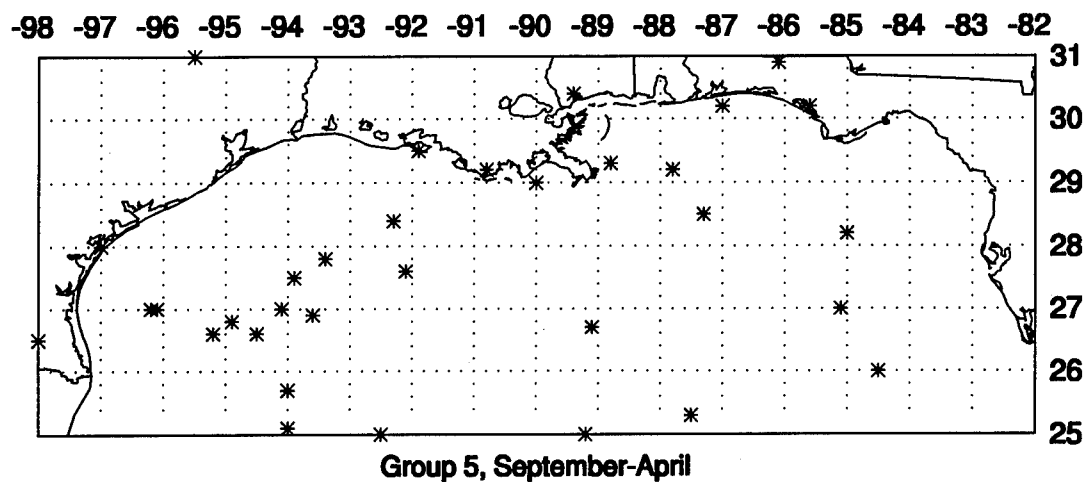
Figure 3.17. Locations of cyclogenesis for Group 5 cyclones, 34 observations.

to Saucier's synoptic scheme. Such cyclogenesis events may have been unclassifiable

due to the fact that a significant number of them occurred east of 89W longitude, an

area which was not within Saucier's domain. Nonetheless, the pattern (Figure 3.18)

appears independent of longitude, with event occurrences almost exclusively offshore,

stretching west to east across the northern Gulf. Such a pattern may be indicative of a

particular process which has not been identified. Johnson et al. (1984) suggested that a

significant number of Gulf lows developed during the winter of 1982-83 under the

influence of upper-level anticylonic shear, such as that which might be found to the

south of an west-east oriented polar jet. Such a scenario *would* be considered

"unclassifiable" in the present investigation, though not unrealistic. Nonetheless, all

cyclones which formed during the winter of 1982-83 *were* classifiable according to

Saucier's scheme.

42

-98 -97 -96 -95 -94 -93 -92 -91 -90 -89 -88 -87 -86 -85 -84 -83 -82

Unclassifiable, September-April
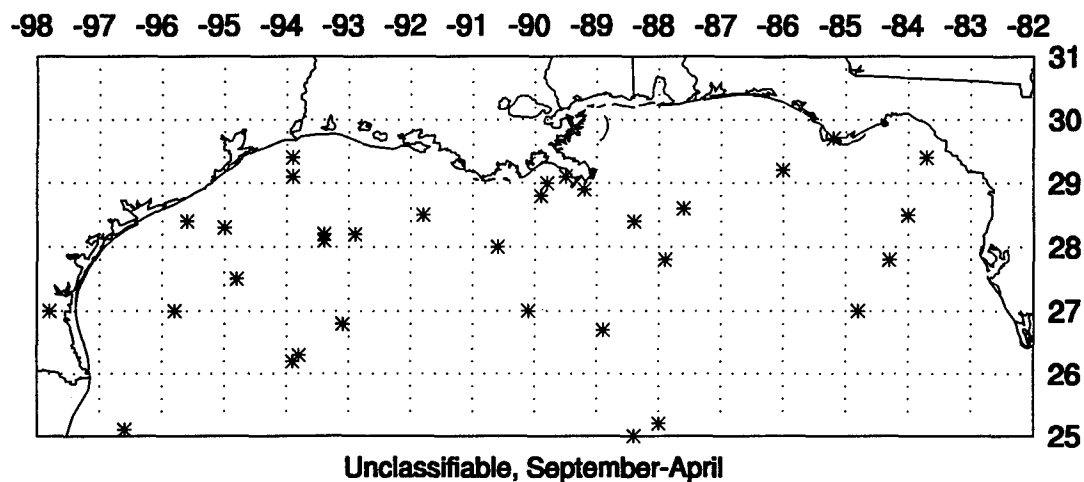
Figure 3.18. Locations of cyclogenesis for unclassifiable cyclones, 33 observations.

A New Classification

Frontal Incursions into the Gulf

As previously mentioned, Saucier (1949) contended that the "reactivation" of the

polar front is an important precondition for the initiation of Gulf cyclones. He

suggested that

> although the polar front *at the surface* usually becomes increasingly indistinct while
> moving southward over the Gulf of Mexico and neighboring regions, the solenoid
> field associated with the front in levels above the surface is maintained for a
> considerably longer period of time. Low level convergence and a usual deformed
> field of motion in a developing cyclone, placed on the temperature field near the Gulf
> Coast, can aid in the reactivation of the polar front even at times when the front has
> apparently lost most of its significance.

Saucier's description is problematic, though, since a study of 11 years of frontal

incursions into the Gulf region by Henry (1979b) showed that during the coldest

months, the majority of atmospheric fronts which migrate over the Gulf of Mexico tend

43

not to remain over the Gulf itself but rather tend to undergo frontolysis after penetrating into the Caribbean. Table 3.1 summarizes his results, which suggest that the tendency for atmospheric fronts to become stalled, or stationary, over the Gulf may not be an adequate explanation for the observed maxima in cyclogenesis frequency. Therefore, in order to determine the role of the polar front in Gulf cyclogenesis, a new classification scheme is proposed.

Table 3.1. Area where each front frontolyzed or returned as a warm front. Percentage by each month (from Henry 1979b).

	Nov	Dec	Jan	Feb
Percent frontolyzed in Gulf	31	20	18	17
Percent frontolyzed in Caribbean	55	46	59	70
Percent returned as warm fronts	14	34	23	13

Frontal Versus Nonfrontal Cyclogenesis

Frontal cyclogenesis. The classification of "frontal" was given to each cyclone which developed along an *analyzed,* pre-existing, airmass-type frontal boundary. An example of frontal cyclogenesis is provided in Figure 3.19. At 1200 UTC 21 December 1995, a stationary front was analyzed in the central Gulf, to the south of 25N latitude. This front could have been considered the boundary between tropical air to its south and modified polar air to its north. (The modification occurred as the air mass remained resident over the warmer Gulf water, a process which will be further explained in Chapter 4.) Six hours later at 1800 UTC 21 December 1995, a surface

44
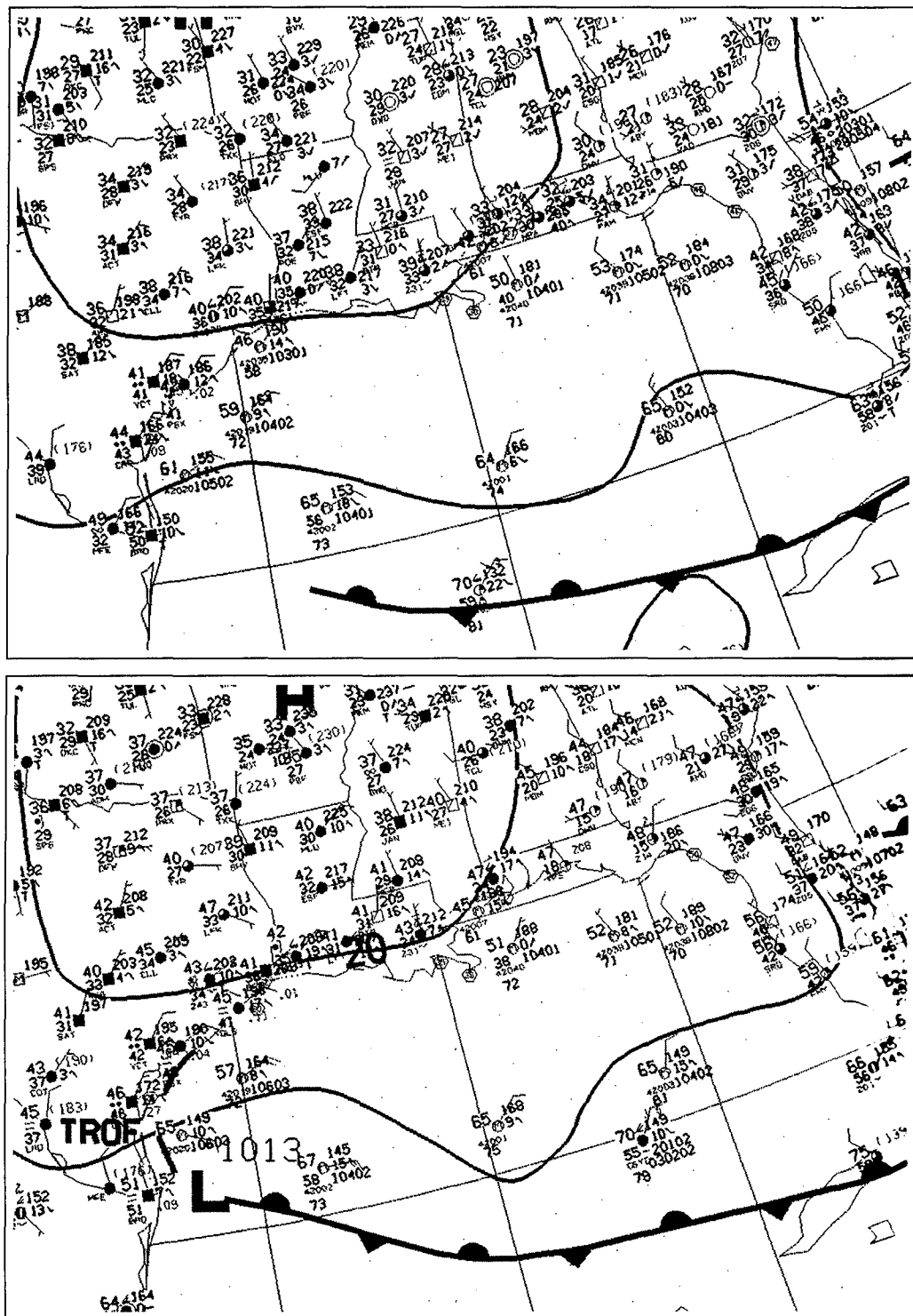
Figure 3.19. An example of frontal cyclogenesis. Surface analyses for 1200 UTC 21 December 1995 (top) and 1800 UTC 21 December 1995 (bottom).
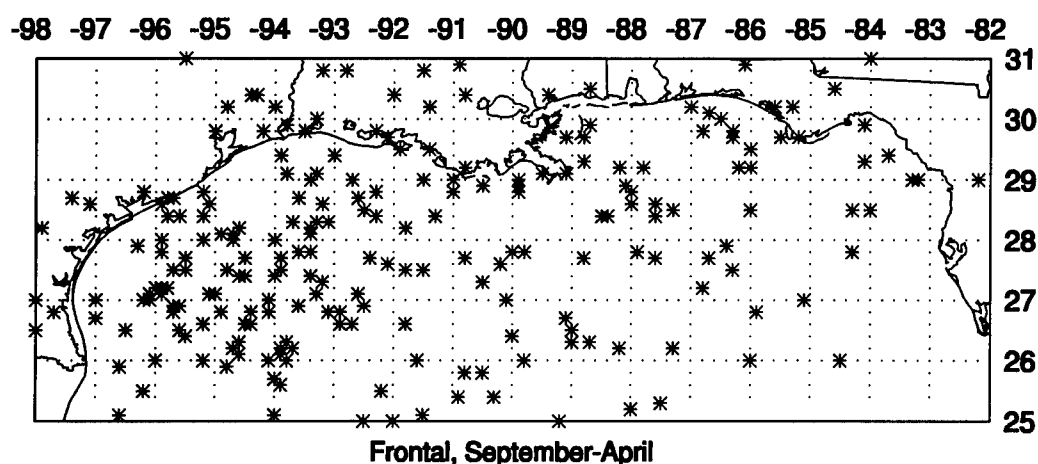
Figure 3.20. Locations of frontal cyclogenesis, 227 observations.

low was analyzed to have formed on the western edge of that front, just southeast of the Texas coast.

227 of the total 313 cyclones in the current study were classified as frontal (about 73 percent). Figure 3.20 shows the spatial distribution of those events, and indicates a high concentration of events over the open water offshore Texas, extending east-northeast over the nearshore and offshore water south of the region from the Mississippi Delta to the western Florida panhandle, with lesser concentrations to the south and east.

Again, it is useful to consider the pattern evolution during the winter season, in order to more fully understand the processes under consideration. Figure 3.21 provides bimonthly distributions of frontal cyclogenesis, excluding the transition months of September and April. A cursory inspection of these plots shows the tendency for there

46

to be a maximum in frontal cyclogenesis frequency over the open water of the northwest Gulf throughout the winter. During October-November, frontal cyclogenesis occurred at scattered locations throughout the Gulf, with some preference for the northeast Gulf coast. In December-January, the frequency maximum extends from the northwest to the north-central Gulf, particularly near the Mississippi Delta. Cyclogenesis in the northeast Gulf during this time was somewhat less preferred. During February-March, the northwest Gulf remained a preferred region for frontal cyclogenesis. In addition, there was a concentration of events over the near-coastal waters of the northeast Gulf at this time, extending southward near 86W longitude.

In summary, it appears that cyclones which form along analyzed fronts do so with highest frequency over the open water of the northwest Gulf, during the coldest months (99 observations in December-January). There also appears to be an observed tendency for cyclones to form along fronts which lie over the near-coastal waters of the northeast Gulf, particularly during the late winter months. The observed interseasonal variability of the spatial distribution of frontal cyclogenesis is supported by a study of frontal incursions into the Gulf of Mexico by DiMego et al. (1976). Their study showed that during the coldest months, a north-south maximum in the frequency of frontal passages exists over the northwest Gulf, while during the autumn and spring months, the frequency of frontal passages assumes a more "zonal" orientation (see Figure 3.22).

Nonfrontal cyclogenesis. The classification of "nonfrontal" was given to each

Frontal, October-November

Frontal, December-January

Frontal, February-March
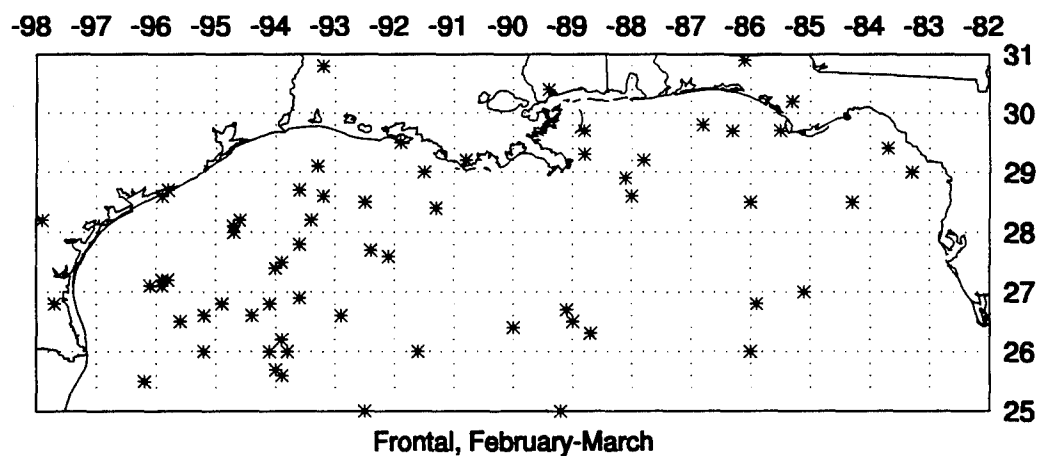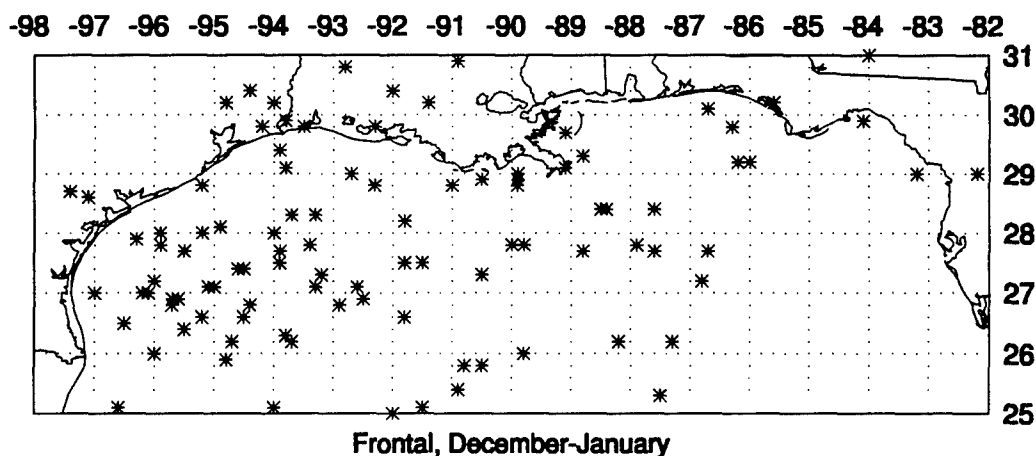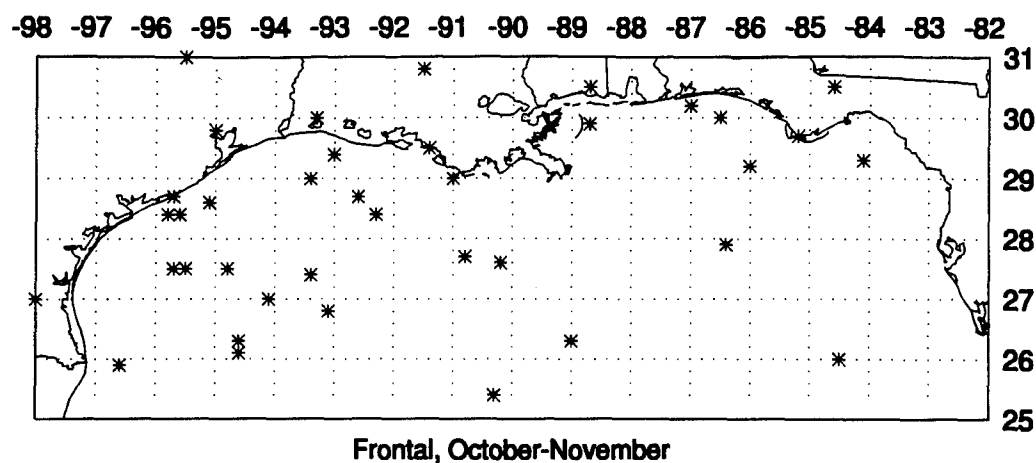
Figure 3.21. Locations of frontal cyclogenesis: October-November, 39 observations (top); December-January, 99 observations (center); and February-March, 65 observations (bottom).
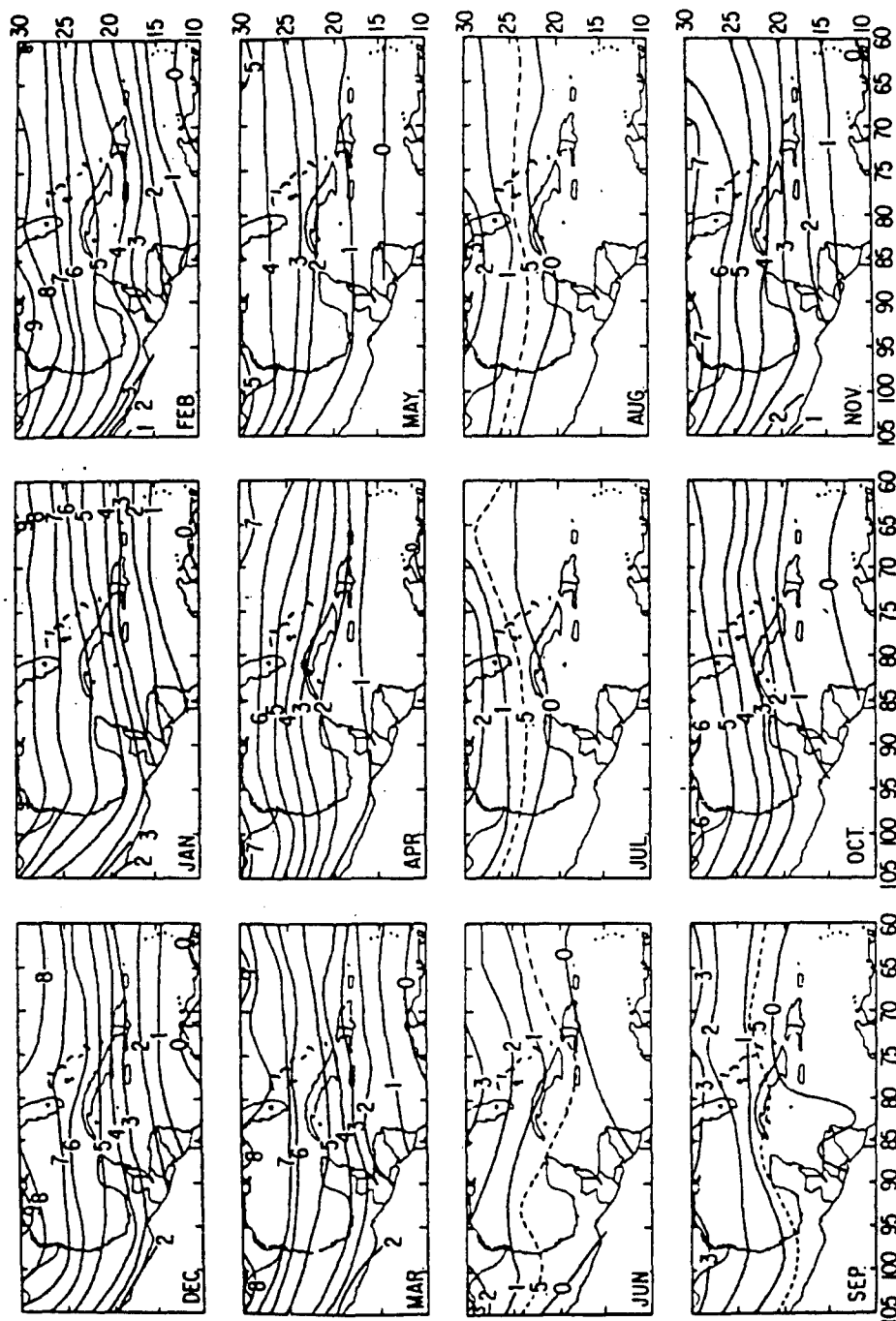
Figure 3.22. Mean-monthly frequency of frontal systems for the 1965-1972 period, expressed as the number of frontal passages per month (from DiMego et al. 1976).

49

cyclone which did *not* develop along an analyzed, pre-existing, airmass-type frontal boundary. An example of a nonfrontal cyclogenesis event is given in Figure 3.23. At 1800 UTC 5 November 1995, a stationary front dividing tropical air to its south from modified polar air to its north was analyzed well south of the study domain. A low pressure trough was analyzed in the vicinity of the Texas coast, but the subjective analysis did not explicitly indicate the presence of a boundary separating air masses of different source regions. By 0000 UTC 6 November 1995 (6 hours later), a low pressure center was analyzed over the open water offshore of the Texas coast. This surface cyclone was analyzed to form *completely within the modified polar air to the north of the quasi-stationary polar front* which had migrated south into the Caribbean. It should be noted here that the vast majority of nonfrontal cyclones in the author's study were not analyzed to form along a low pressure trough.

In the current study, 86 of the total 313 cyclones were classified as nonfrontal (about 27 percent). Their distribution is shown in Figure 3.24. Overall, it can be seen that nonfrontal events are most common over the open water of the northwest Gulf. Unlike the frontal pattern (Figure 3.20), few nonfrontal cyclogenesis events occurred over the northeast Gulf, with a noteworthy lack of observations along and to the south of the Florida panhandle. (It is understood, though, that differing numbers of observations in each classification create difficulty in drawing conclusions based solely upon pattern comparisons.)

The nonfrontal pattern's seasonal evolution (again excluding the transition
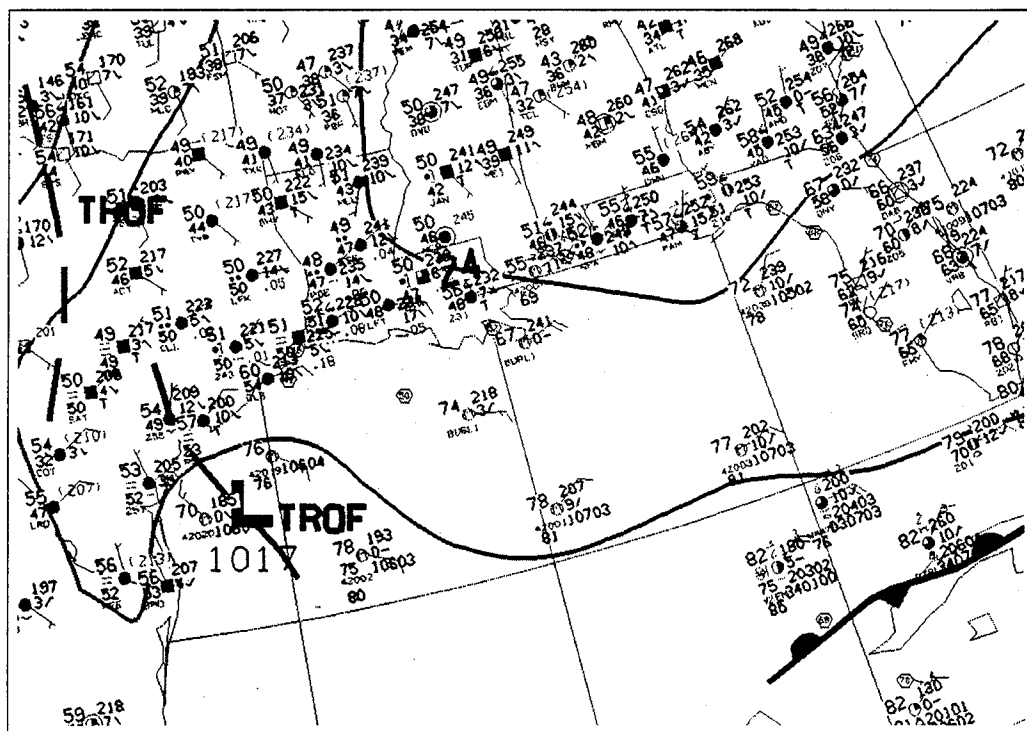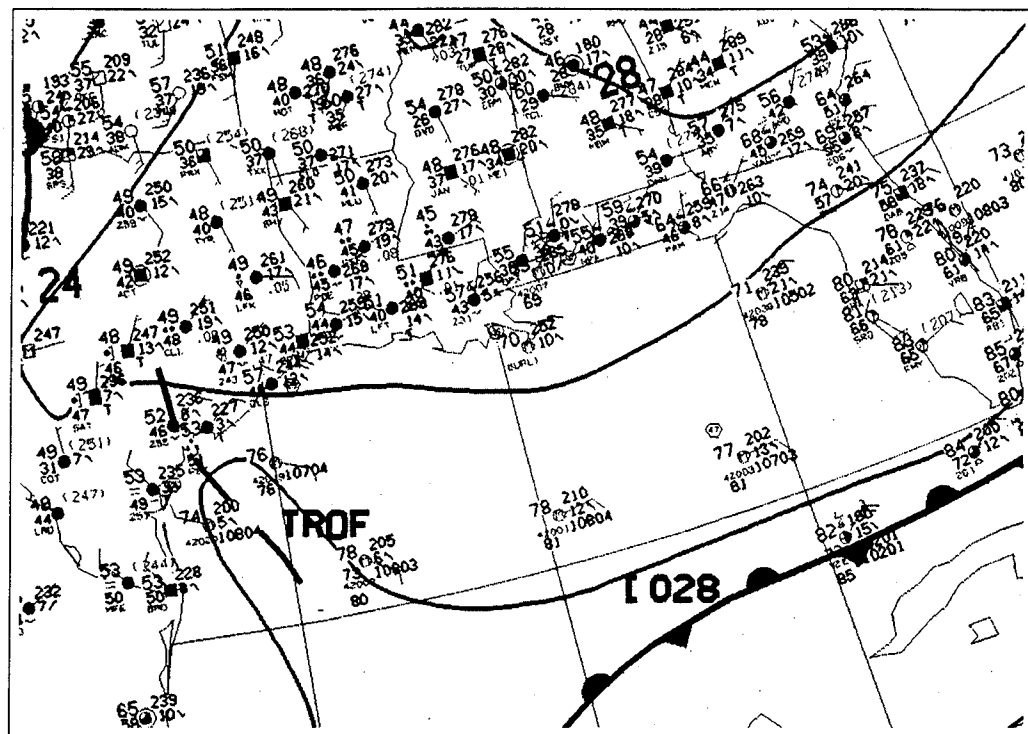
Figure 3.23. An example of nonfrontal cyclogenesis. Surface analyses for 1800 UTC 5 November 1995 (top) and 0000 UTC 6 November 1995 (bottom).
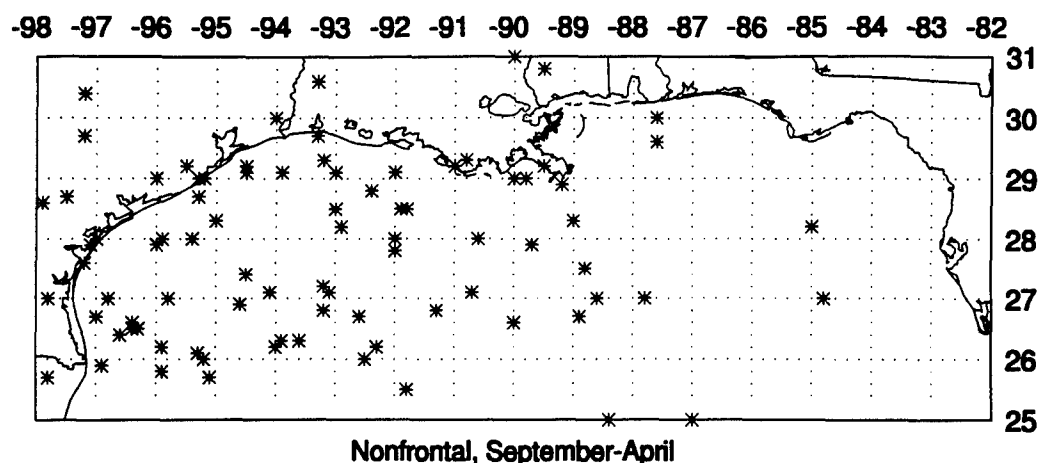
Figure 3.24. Locations of nonfrontal cyclogenesis, 86 observations.

months of September and April) is provided in Figure 3.25. Very few observations

during October-November (only 12) create difficulty in drawing reasonable

conclusions. It could be suggested, though, that a maximum does exist over the open

water of the northwest Gulf. By December-January the number of observations

increases to 40, and we see a pattern in which there is clear preference for development

over the open water of the northwest Gulf and the nearby coastal areas of Texas and

Louisiana. Most noteworthy, though, is the lack of preference for nonfrontal

cyclogenesis east of 90W longitude (the midpoint of the domain). In fact, 91 percent

of January nonfrontal cases occurred west of this longitude, while only 74 percent of

January frontal cases were observed in this region. Compare this pattern with that of

February-March. Although the number of observations during late winter is relatively

low (about half that of the prior two-month period), nonfrontal cyclogenesis appears to
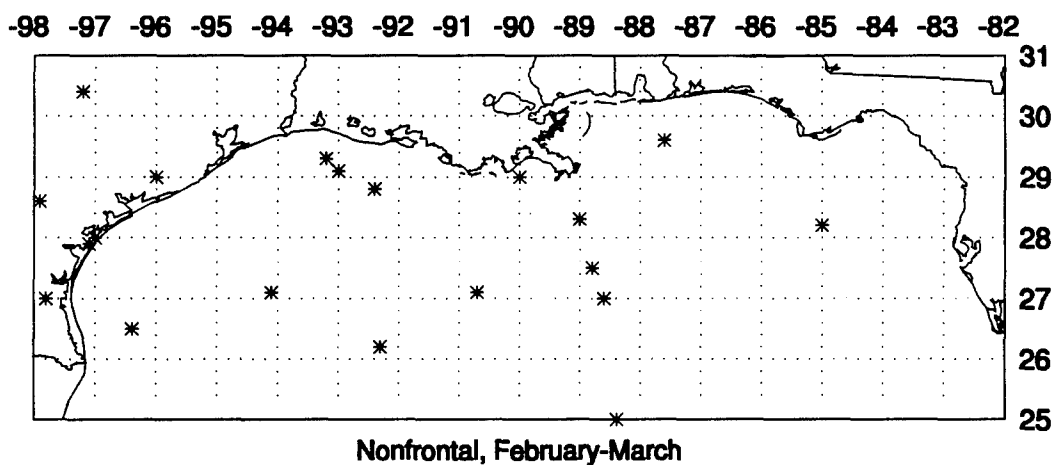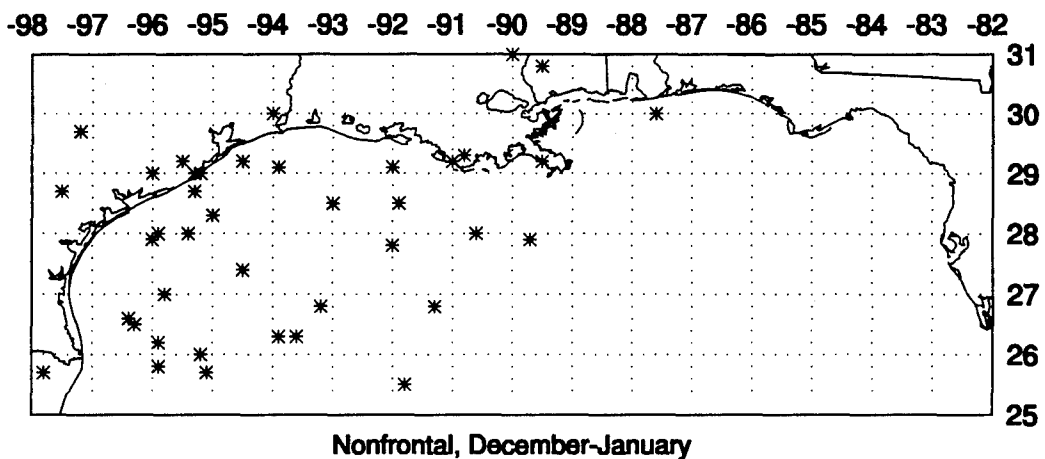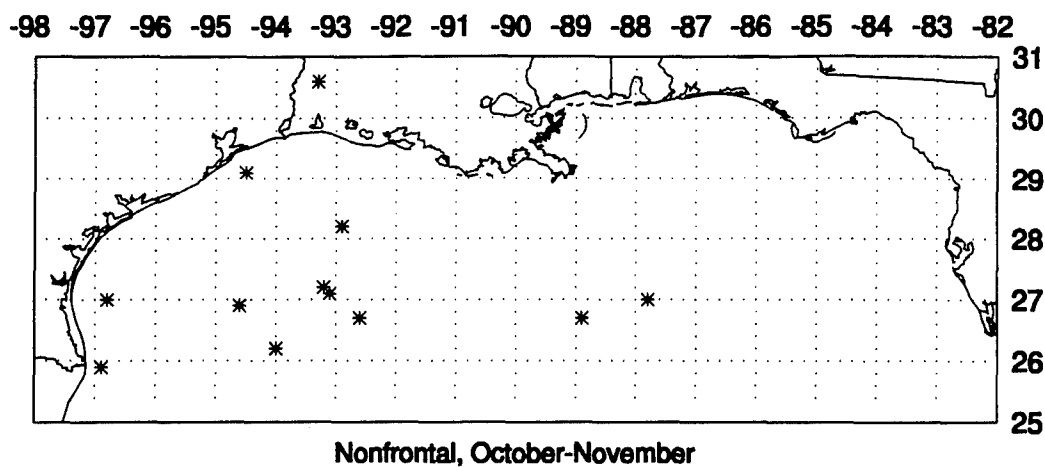
Figure 3.25. Locations of nonfrontal cyclogenesis: October-November, 12 observations (top); December-January, 40 observations (center); and February-March, 21 observations (bottom).

be about equally likely over most of the northern Gulf.

In summary, it appears that cyclones which form without the presence of analyzed frontal boundaries do so with clear preference for the northwest Gulf region during the coldest months. There is also no observed maximum south of the Gulf coast from Mississippi to the Florida panhandle during the late winter months, as observed in the frontal cases. Nonfrontal cyclogenesis cases are almost nonexistent over the eastern half of the domain during December-January.

Conclusions

It appears that Saucier's descriptions of the upper-level conditions associated with the development of Gulf cyclones are accurate, since only about 10 percent of all cyclones in the current study were unclassifiable according to his scheme, and much of that discrepancy could be related to domain differences. However, his description of the "dissolution" and "reactivation" of the polar front in association with Gulf cyclogenesis is found to be flawed, since the polar front tends to dissolve over the Caribbean Sea during the months when Gulf cyclogenesis occurs most frequently. In order to more clearly determine the role of the polar front in Gulf cyclogenesis, a new classification scheme has been proposed.

The distinction between frontal and nonfrontal cyclogenesis has been made, by definition, completely on the basis of differing low-level atmospheric conditions, as evident in surface observations. It cannot be presumed, though, that differences in the

processes which lead to these two distinct types of cyclone initiation are unique to the lowest levels of the atmosphere. It is therefore useful to investigate the upper-level conditions under which each type of development occurred.

Table 3.2. Percent of frontal and nonfrontal cyclogenesis cases which occurred under each of Saucier's synoptic classifications (Groups 1 through 5, and those which were unclassifiable).

	1	2	3	4	5	Unclassifiable
Frontal	16%	7%	48%	6%	14%	9%
Nonfrontal	15%	8%	51%	8%	3%	14%

Table 3.2 gives a comparison of the percent of frontal cyclogenesis cases and the percent of nonfrontal cyclogenesis cases which were assigned to each of Saucier's synoptic classifications (Groups 1 through 5, and those which were unclassifiable). With the exception of those cyclones classified as Group 5 (which by definition tended to be "frontal"), the frontal and nonfrontal cyclogenesis cases displayed fairly similar distributions among the synoptic classifications. In other words, it is reasonable to suggest that the upper-level flow pattern during surface cyclone initiation does not determine whether cyclogenesis will be frontal or nonfrontal. The distinction between frontal and nonfrontal cyclogenesis is, in fact, based solely on the analyzed low-level conditions.

Recall that Saucier observed that those cyclones which formed in association with the retrogressive upper trough (Group 3) did so along the "reactivated polar front," after the front had previously undergone dissolution. In the current study,

55

however, about 30 percent of all Group 3 cyclones developed *completely without the analyzed presence of the polar front*. This is a significant result, since Group 3 cyclones occur most frequently and therefore best represent the process of Gulf cyclogenesis.

The conditions which lead to cyclogenesis over the Gulf will be more fully investigated in Chapter 4. It will be suggested that the existence of an airmass-type frontal boundary defines a region which is preferable for cyclone development due to the local concentration of thermal contrast, convergence, cyclonic vorticity, and possibly convection. The observed cases of *nonfrontal* cyclogenesis, though, indicate that there may be some cyclogenetic precursors within the boundary layer that are not well-understood (or well-analyzed), particularly over the northwest Gulf during the coldest months. The remainder of this study will focus on the characteristics of the lower atmosphere which make the northwest Gulf a preferred region for cyclogenesis.

CHAPTER 4

LOW-LEVEL PROCESSES WHICH CONTRIBUTE TO

GULF OF MEXICO CYCLOGENESIS

Overview

It was shown in Chapter 3 that the northwest Gulf of Mexico is a preferred

region for cyclogenesis, particularly for those storms which develop without the

existence of analyzed, pre-existing, airmass-type frontal boundaries. This chapter

begins by presenting a brief review of the process of cyclogenesis, in order to establish

a dynamical framework for further discussion. Then, the physical characteristics of the

Gulf itself will be examined, since various case studies of cyclogenesis over the Gulf

(though limited in number) have indicated that air-sea interactions are important to

cyclone development in the region (see, for example, Bosart 1984; Hsu 1993;

Schumann et al. 1995). Finally, both theoretical and observational evidence of the

airmass modification process will be presented, and the low-level processes which

contribute to Gulf cyclogenesis will be discussed.

A Conceptual Framework for Cyclogenesis

For the purpose of the author's study, cyclogenesis was defined as the initial formation of a surface cyclone which subsequently persisted for at least 24 hours. In more general terms, however, cyclogenesis is simply the increase of cyclonic (positive) vorticity with time, and can be described by the vorticity equation,

$$
\frac{d\zeta}{dt} = -\mathbf{V} \bullet \nabla_p(\zeta + f) - \omega\frac{\delta\zeta}{\delta p} - (\zeta + f)\left(\frac{\delta u}{\delta x} + \frac{\delta v}{\delta y}\right) - \left(\frac{\delta\omega}{\delta x}\frac{\delta v}{\delta p} - \frac{\delta u}{\delta p}\frac{\delta\omega}{\delta y}\right) + \left(\frac{\delta F_x}{\delta x} + \frac{\delta F_y}{\delta y}\right),
$$

where ζ denotes the geostrophic relative vorticity, $\mathbf{V}$ is horizontal velocity vector, p is pressure, f is the Coriolis parameter, ω is the vertical wind component (in isobaric coordinates), u and v are the latitudinal and longitudinal components of the wind, respectively, and F_x and F_y are the frictional force components per unit mass in the x and y directions, respectively.

The first two terms on the right hand side (rhs) represent the horizontal and vertical advections of vorticity, which neither create nor destroy the existing vorticity field but merely move it about (Carlson 1991, chap. 3). These two terms, along with the twisting term (fourth on the rhs) and frictional effects (fifth term on the rhs) are typically small when considering synoptic-scale motions. If we replace the relative vorticity by its geostrophic value, we have a form of the quasi-geostrophic vorticity equation,

$$
\frac{d\zeta_g}{dt} = -(\zeta_g + f)\left(\frac{\delta u}{\delta x} + \frac{\delta v}{\delta y}\right).
$$

58

This equation implies that the time rate of change of geostrophic relative vorticity is the product of two kinematic properties: absolute vorticity and divergence. It demonstrates that at low levels, a local increase of cyclonic vorticity with time *must* be accompanied by low-level convergence, since absolute vorticity is normally positive at mid-latitudes. Moreover, surface development may be preferred in regions of pre-existing local absolute vorticity maxima, such as near fronts or cyclones.

Although the key to cyclone development and migration is the surface divergence pattern, convergence at the surface requires (at least) compensating divergence aloft for the maintenance of thermal wind balance. In the words of Sutcliffe (1939), "Neither the lower nor the upper member of the dynamical system can exist without the other and if a field of divergence (or convergence) can be recognized in the upper atmosphere the associated lower convergence (or divergence) completing the scheme of cyclonic (or anticyclonic) development must occur automatically." In other words, it is incorrect to disregard upper-level factors when considering the problem of surface cyclogenesis.

In Chapter 3, though, we found that the frontal and nonfrontal cyclogenesis events had similar distributions among upper-level flow patterns. It was suggested that the northwest Gulf is a preferred region for cyclogenesis primarily because of processes occurring at low levels. Therefore, in order to determine why the northwest Gulf is so prone to cyclogenesis, it is necessary to investigate those low-level processes which contribute to both pre-existing cyclonic vorticity and low-level convergence.

Physical Characteristics of the Gulf Of Mexico

Basin Depth

Figure 4.1 is a bathymetry (basin depth) map of the Gulf of Mexico. The width of the Gulf's continental shelf is highly variable, ranging from a mere 25 kilometers near Veracruz, Mexico in the southwestern corner, to over 200 kilometers off the Texas/Louisiana coast. The 200-meter isobath is often referred to as the continental shelf "break," which separates shallow shelf waters from the deeper waters of the central Gulf.

Sea Surface Temperatures

During the summer months the Gulf waters are fairly isothermal, with sea surface temperatures (SSTs) varying from about 29 to 31 degrees Celsius. During the winter months, however, the frequent incursion of cold fronts into the Gulf of Mexico region (DiMego et al. 1976; see Figure 3.22) act to cool the shelf water rapidly, mainly due to strong evaporation or latent heat flux (Hsu 1992). The Loop Current, which is the dominant circulation in the eastern Gulf (see Figure 4.2), transports warmer tropical waters from the Yucatan Channel into the interior of the eastern Gulf, and then out the Straits of Florida (Molinari 1987). This current, combined with a broad anticyclonic gyre that exists in the west-central Gulf, causes the deep waters of the central Gulf to be continuously replenished with warm, tropical water. Consequently, the cold air outbreaks which occur most frequently during the winter months are not nearly as effective in cooling the waters of the deep Gulf as they are in cooling the shallow shelf

60
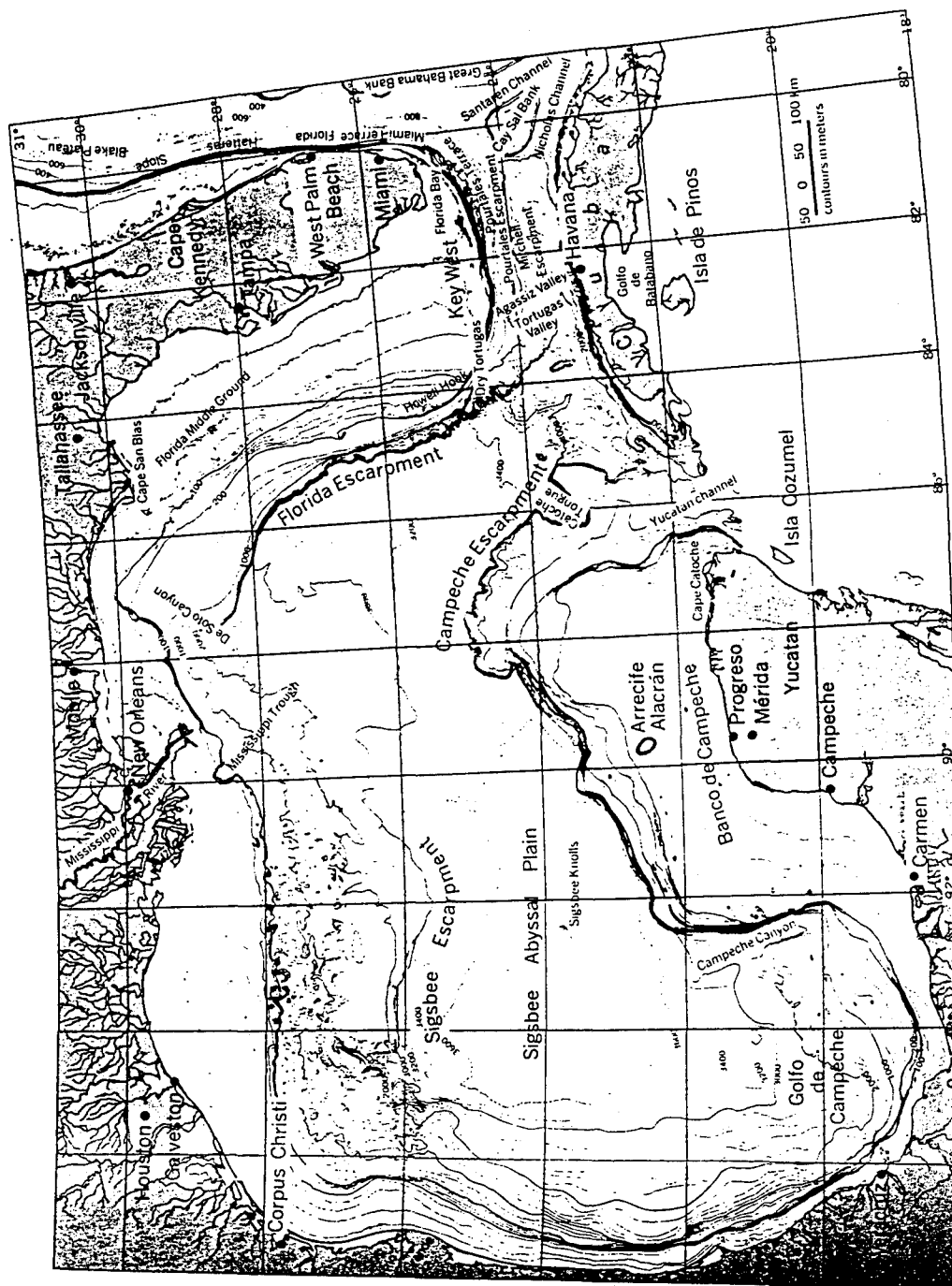
Figure 4.1. Bathymetry of the Gulf of Mexico, contoured in meters (from McGraw-Hill 1980).

61

waters. In addition, atmospheric wind direction also plays a role in the SST pattern of

the shelf waters, since strong offshore flows tend to cause upwelling of colder waters

beneath the surface (Thompson 1994). In fact, the dynamic response of the relatively

warm water to a flow of cold air over it may be the establishment of a thermally

indirect circulation (cold water rising and warm water sinking) which acts to enhance,

or at least maintain, the initial SST distribution (Adamec and Elsberry 1985).

The resulting winter SST distribution (for example, the mean SST for February,

provided in Figure 4.3) shows a pattern in which the isotherms tend to parallel the

contours of basin depth (and the coastline), with spatial variations in temperature that

are roughly twice the magnitude of those found in the open ocean at a similar latitude

(Griffiths 1976). On any given day, though, the SST pattern can deviate far from the
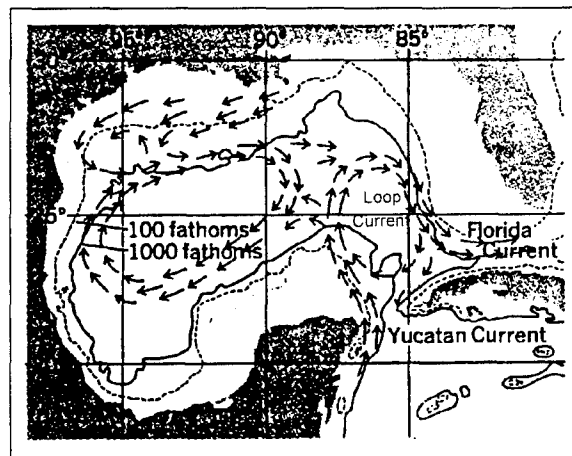
Figure 4.2. Basic surface circulation of the Gulf of Mexico (from McGraw-Hill 1980).
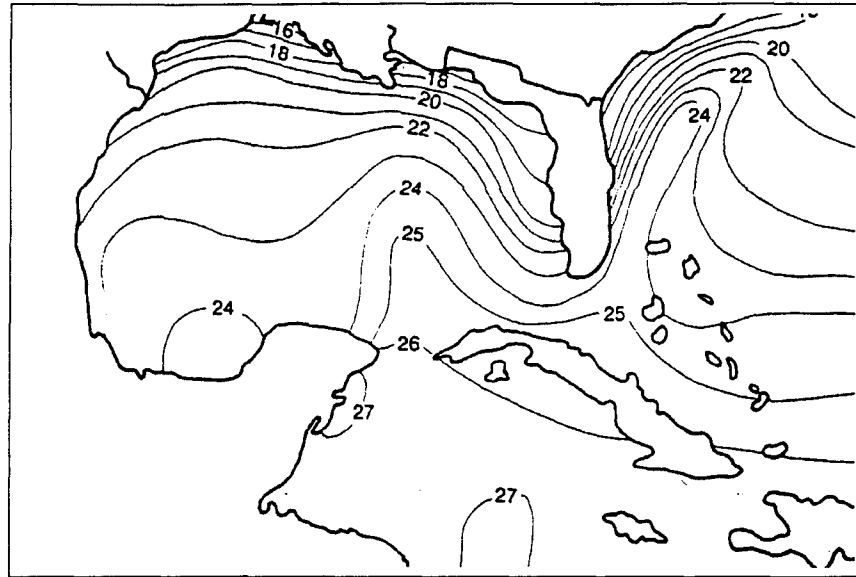
Figure 4.3. Climatological sea surface temperature (degrees Celsius) for February, from the atlases of the U.S. Navy (U.S. Navy 1985). (Figure obtained from Lewis and Crisp 1992.)
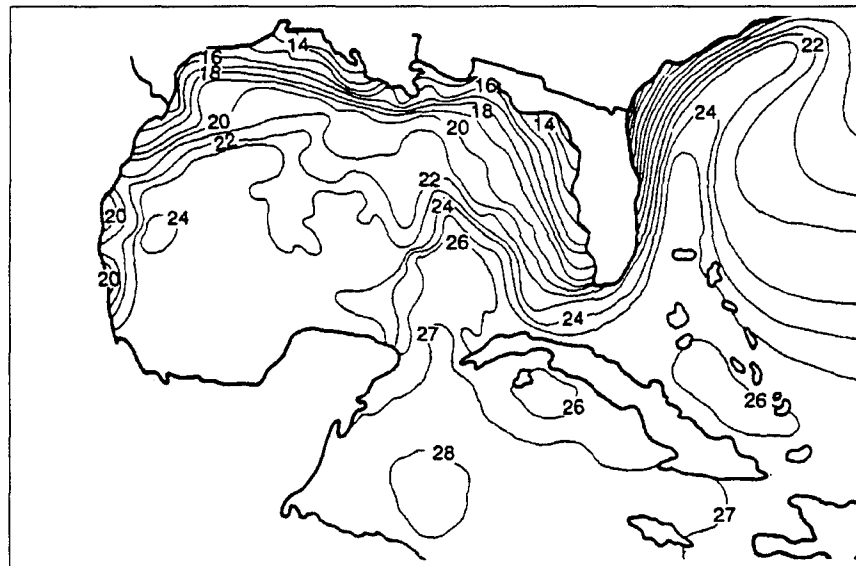
Figure 4.4. Sea surface temperature (degrees Celsius) for 22 February 1988, produced at the National Hurricane Center. (Figure obtained from Lewis and Crisp 1992.)

mean, as shown on the chart for 22 February 1988 (Figure 4.4). Note how in this case

the combination of cooler-than-average shelf waters near the coast of Mexico and

warmer-than-average waters offshore create an SST *gradient* which is much stronger

than that which is observed in the mean. Although such a detailed pattern may have

significant consequences with respect to cyclogenesis, most modeling studies of

airmass modification do not incorporate SST data of such a high spatial and temporal

resolution (see, e.g., Mailhot 1992; Warner et al. 1990).

The strongest SST gradient which exists during the winter months lies near the

shelf break (Burk and Thompson 1992; Hsu 1992). The waters of the northwest Gulf's

continental shelf have been observed to exhibit temperature gradients of about .5

degree Celsius per kilometer (Nowlin and Parker 1974), and the temperature difference

between waters near the Texas/Louisiana coast and waters those near the shelf break is

about 7 degrees Celsius, even for the January mean (Hsu 1992).

Airmass Modification

Overview

In recent years, a great deal of research has focused on the modification of polar

air masses which reside over the relatively warm waters of the Gulf during the winter

months. The Gulf of Mexico Experiment (GUFMEX) was conducted in

February-March 1988 in order to "gather data on two phenomena: airmass

modification over the Loop Current, and return flow characteristics of modified polar

air returning to the southern shores of the United States" (Lewis et al. 1989). Airmass modification over the Gulf has a profound effect on the forecasting of not only ceiling, visibility, fog, and steady precipitation at locations near the coast or over shelf waters, but also on forecasting the initiation of elevated convection and severe weather outbreaks over the southern and central Plains (see, e.g., Burk and Thompson 1992; Crisp and Lewis 1992; Janish and Lyons 1992; Lewis and Crisp 1992; Liu et al. 1992; Mailhot 1992; Merrill 1987, 1992; Muller 1977; Thompson 1994; Weiss 1992).

The frequent cold air outbreaks over the Gulf of Mexico during winter cause an SST front to develop near the continental shelf break. As air resides for an extended period over such an SST distribution, differential fluxes of heat and moisture from the sea surface to the atmosphere result in the formation of an atmospheric baroclinic zone which may lie well to the north of any airmass-type frontal boundary analyzed on surface synoptic charts. This region is an ideal location for nonfrontal cyclogenesis, since the presence of the polar front is not required for the development of significant low-level baroclinicity.

Differential Diabatic Warming of the Boundary Layer

Nowlin and Parker (1974) studied the effects of a cold air outbreak on the boundary layer sensible and evaporative heat fluxes over the northwest Gulf. Prior to a cold air outbreak which occurred during January, 1966, SST contours generally paralleled the shore, with a maximum observed gradient of 0.14 degrees Celsius per kilometer. Fifteen days after the outbreak (and still under the outbreak's influence), the
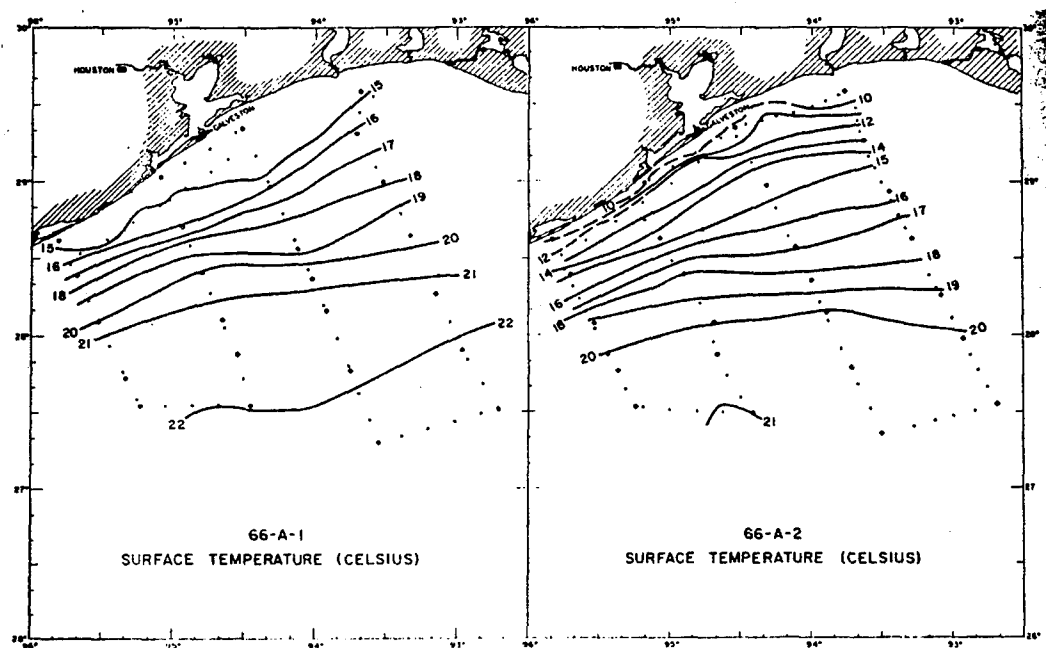
Figure 4.5. Distribution of sea surface temperature (Celsius) as observed before (left) and after (right) the cold air outbreak (from Nowlin And Parker 1974).

SST contours remained parallel to the coast, but the maximum observed gradient had increased to .43 degrees Celsius per kilometer (Figure 4.5). Net local SST changes after the outbreak were found to be greatest in the nearshore region (about 4 degrees Celsius), and decreased with distance from shore to about 1 degree Celsius near the boundary of the study domain.

Prior to the outbreak, air-sea temperature differences were generally less than 1 degree Celsius (Figure 4.6). After the outbreak, however, the air was cooler than the water over the entire region, and the air-sea temperature contrast increased with distance from shore to about 10 degrees Celsius. As a result, the distributions of
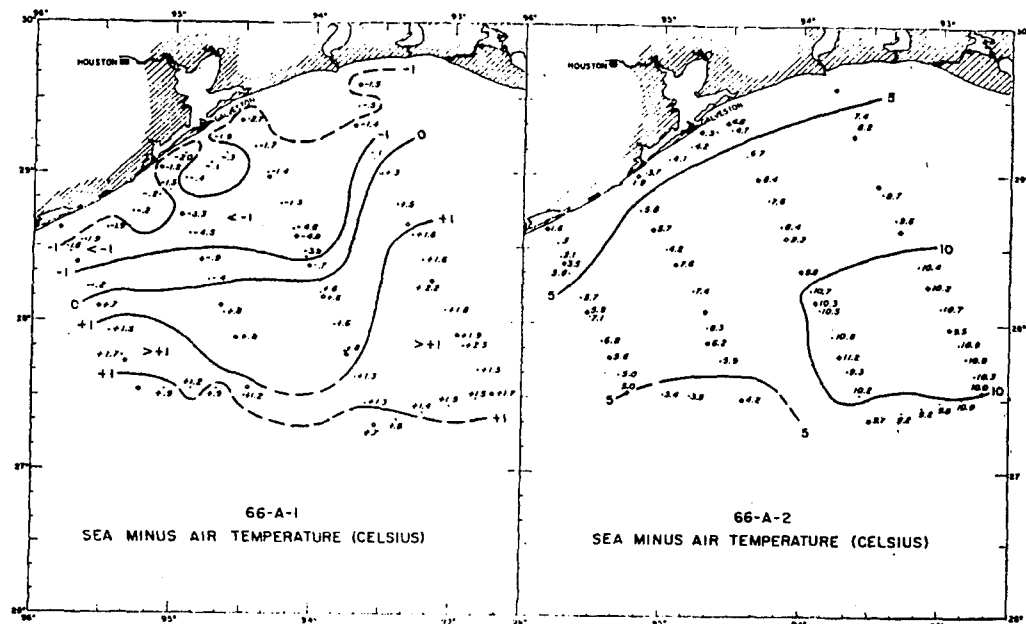
Figure 4.6. Sea surface temperature minus air temperature (Celsius) as observed before (left) and after (right) the cold air outbreak (from Nowlin and Parker 1974).

sensible and evaporative heat fluxes also changed dramatically through the course of the outbreak. Even after some general cooling of the Gulf surface and warming of the boundary layer, estimated sensible heat exchange from the water to the atmosphere showed dramatic increases well offshore (Figure 4.7), from about 30 calories centimeter^{-2} day^{-1} before the outbreak to about 500 calories centimeter^{-2} day^{-1} afterward, while a much smaller change was observed in the nearshore region. Similar to the sensible heating distribution, evaporative heat exchange from the ocean to the atmosphere also changed dramatically after the cold air outbreak, with about a three-fold increase in latent heating well offshore, but much smaller net changes in the nearshore region.

67
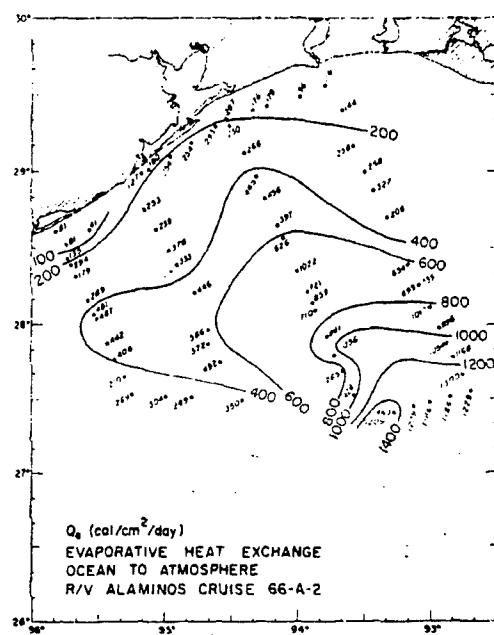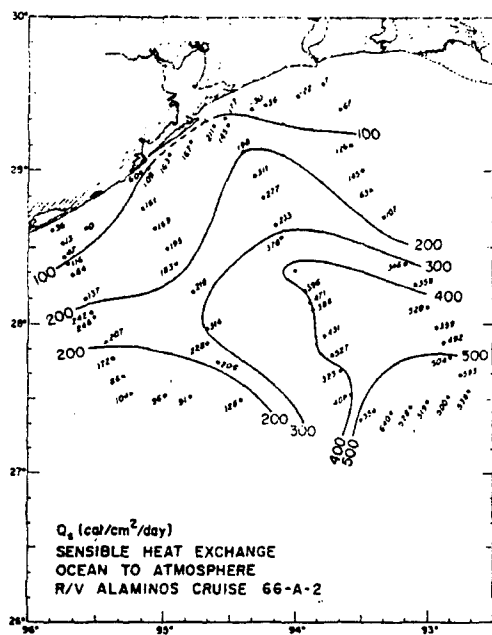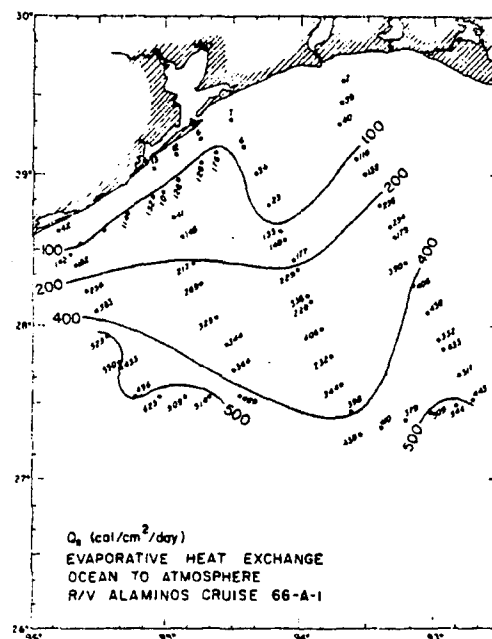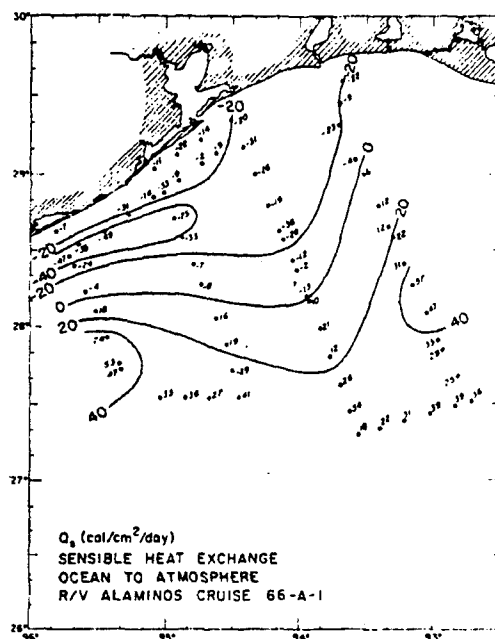
Figure 4.7. Distributions of sensible heat flux (left) and evaporative heat flux (right) from ocean to atmosphere, before (top) and after (bottom) the cold air outbreak (from Nowlin and Parker 1974).

68

Generation of Cyclonic Vorticity within the Boundary Layer

Hsu (1992) used monthly mean air temperatures compiled from both onshore stations and offshore buoys to develop a climatology of air temperature variations from the deep Gulf to the coast. See Figure 4.8 for a plot of station locations used. Figure 4.9 shows that during the winter season 1989-1990, the average air temperature variation from Shreveport, Louisiana (SHV) to National Data Buoy Center buoy station 42002 in the deep Gulf increased from about 5 degrees Celsius in September to a maximum difference of about 14 degrees Celsius in December. Hsu determined that from January through May, all monthly mean air temperatures from the land and shelf stations were practically identical, while the deep Gulf waters remained warm (see Figure 4.10). He therefore concluded that "the orientation of the shelf break from January through May is the more important 'demarcation' line in baroclinicity than the physical coastline" (Hsu 1992).

From the climatological air temperature data, Hsu used a 5-point stencil (see Figure 4.8) to calculate the Laplacian of the temperature field, which is a measure of the vorticity of the thermal wind. He defined the geostrophic relative vorticity as

$$\zeta = \frac{\nabla^2 p}{\rho f} \, ,$$

where p is pressure, f is the Coriolis parameter ($\approx 6 \times 10^{-5} s^{-1}$ at 30N latitude), and ρ is air density. Using $p = \rho R T$, where R is the gas constant and T is the air temperature, he calculated the geostrophic relative vorticity in finite-difference form by

69
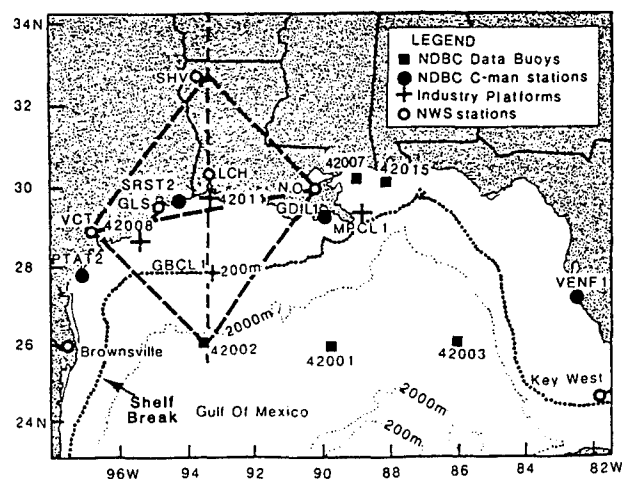
Figure 4.8. Station locations for onshore and offshore temperature distribution used in Figures 4.9 and 4.10, and calculations of vorticity. A five-point stencil (see the rhombus with its center approximately over buoy station 42011) was used for the computation of the Laplacian of temperature field to obtain the relative or local vorticity (from Hsu 1992).
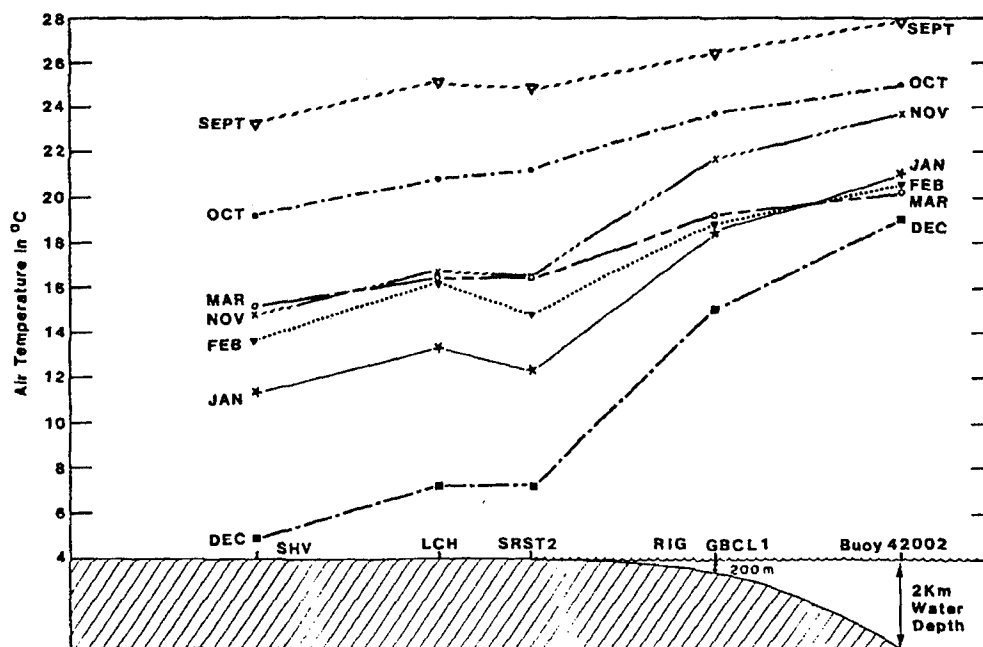
Figure 4.9. Monthly variations of air temperature from deep Gulf to Shreveport, Louisiana, via stations near the shelf break and coastal areas, from September 1989 through March 1990 (from Hsu 1992).

70
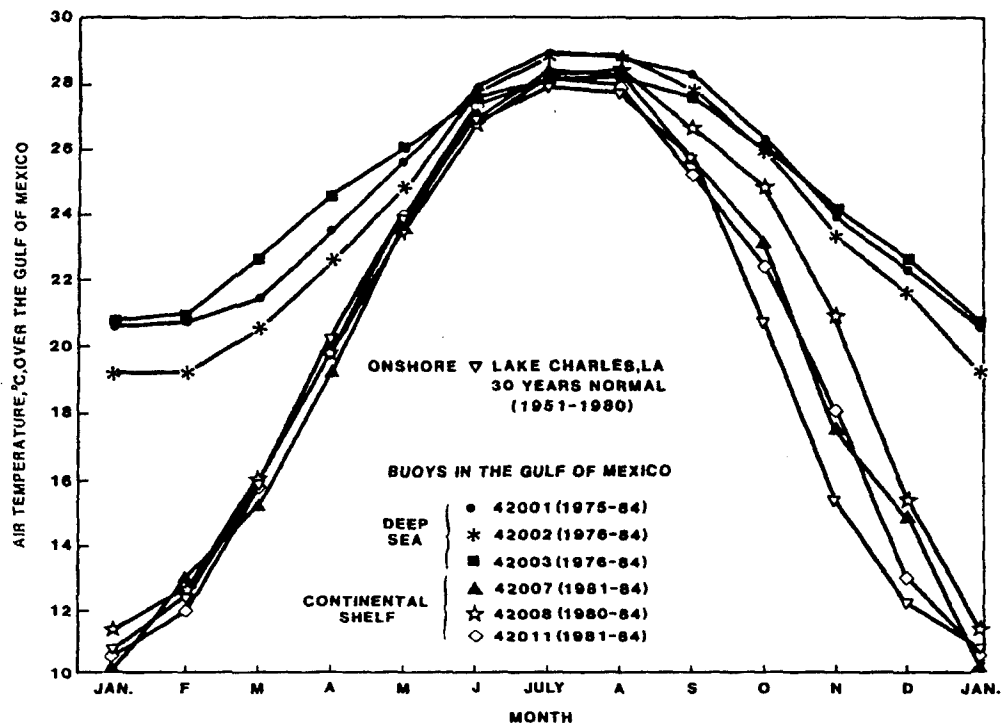
Figure 4.10. Comparison of air temperature measurements over the deep Gulf, the inner continental shelf, and Lake Charles, Louisiana (from Lewis and Hsu 1992).

using

$$\zeta \cong \frac{R\left[\sum_{i=1}^{4} T_i - 4T_0\right]}{d^2 f} ,$$

where T_i, $i = 1, ..., 4$, are the temperatures at the four corners of the rhombus, T_0 is the

temperature at the center, and d is the distance between corners and the rhombus

center. The resulting monthly values of geostrophic vorticity are given in Table 4.1. It

can be seen that his method shows a substantial increase of what might be called

"ambient" vorticity in October and November, with relatively high values continuing

71

through March. Based on this finding, Hsu concluded that the horizontal air temperature gradient between the warmer deep Gulf and the colder shelf waters should create a region where surface cyclogenesis is preferred, given sufficient upper-level support.

Table 4.1. Geostrophic relative vorticity, $(10^{-5}\ s^{-1})$, in the lower levels of the atmosphere for the northwestern Gulf as calculated using mean monthly air temperature data from the stations forming the rhombus shown in Figure 4.8 (from Hsu 1992).

Month	Vorticity
January	24.50
February	20.60
March	15.50
April	7.20
May	4.00
June	4.00
July	8.30
August	9.00
September	8.70
October	17.70
November	26.00
December	27.80

Surface Convergence in the Boundary Layer

In their seminal work on mesoscale frontogenesis along the southeastern New England coast, Bosart et al. (1972) suggested that friction, orography, coastal configuration, and land-ocean thermal contrast are all important factors in the development of the commonly observed New England coastal front. More recent studies, however, have determined that in other geographic regions which commonly

experience coastal frontogenesis (such as the Carolinas), diabatic effects (differential surface heating, for example) are the primary causes of mesoscale convergence in the near-coastal marine atmospheric boundary layer, while the effects of differential friction and other factors are secondary in importance (Riordan 1996).

Although (to this author's knowledge) there have been no extensive field experiments or numerical simulations documenting coastal frontogenesis over the northwest Gulf, the existence of a coastal front which is mesoscale in its along-front direction would provide a reasonable explanation for the observed nonfrontal cyclogenesis events in this region. In order to better understand how diabatic processes may contribute to surface convergence -- and ultimately cyclogenesis -- over the northwest Gulf, the results of a numerical experiment for a similar problem will be summarized.

Boundary Layer Circulations Forced by Gulf Stream SST Gradients

As mentioned in the historical review of North American cyclogenesis in Chapter 2, it has been known for some time that a distinct maximum in observed cyclogenesis frequency exists near the Atlantic coastline or over the Gulf Stream. Studies of rapidly deepening cyclones (Sanders and Gyakum 1980; Sanders 1987; Roebber 1993) have shown that these meteorological "bombs" preferentially migrate along the axis of the Gulf Stream. Such observations suggest that an inherent mechanism in the initiation, development, and movement of marine cyclones must be the air-sea interactions which occur in regions of strong oceanic and ocean-atmosphere
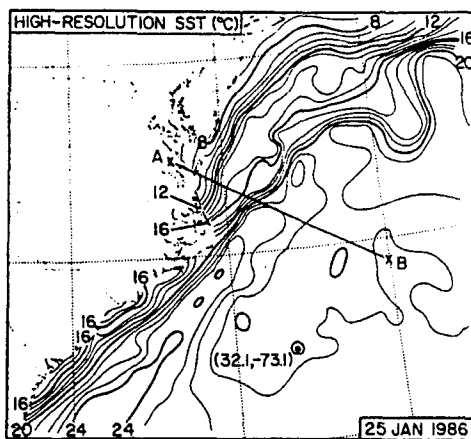
Figure 4.11.   Sea surface temperature (Celsius) field based on the NOAA 14-km high-resolution analysis for 25 January 1986. The line A-B shows the orientation of a vertical cross section on which the model solutions are displayed (from Warner et al. 1990).
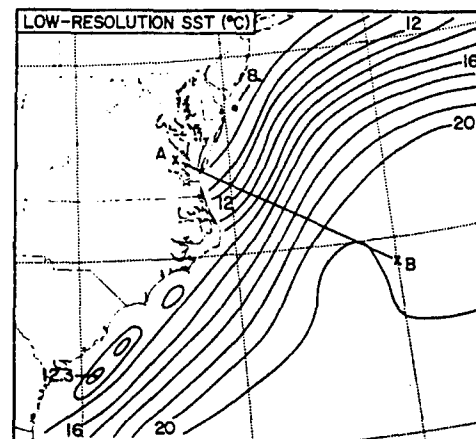
Figure 4.12.   Sea surface temperature (Celsius) field based on the 381-km grid-increment analysis from the Navy's Fleet Numerical Oceanography Center. The line A-B shows the orientation of a vertical cross section on which the model solutions are displayed (from Warner et al. 1990).

thermal contrast.

In order to quantify the interplay between the atmosphere and the ocean in such regions, Warner et al. (1990) used the Penn State/National Center for Atmospheric Research mesoscale model to simulate the evolution of the marine atmospheric boundary layer in the vicinity of the Gulf Stream. They initialized the model with calm winds everywhere and a uniform sea level pressure of 1000 millibars. Terrain elevations were set to zero. The initially horizontally uniform temperature and moisture fields were derived from a maritime sounding obtained from the Genesis of Atlantic Lows Experiment during Intense Observation Period 2 (see Dirks et al. 1988). The effects of two SST distributions were modeled. The control was a high-resolution

74

SST analysis based on satellite radiometer data and corrected with available *in situ* measurements (Figure 4.11). The other was a much smoother (yet more readily available) analysis by the Navy's Fleet Numerical Oceanography Center (Figure 4.12). Initial air-sea temperature differences had a maximum of about 7.5 degrees Celsius over the warmest water. The results of these experiments (all for 12 hours into the simulations) are displayed in Figures 4.13 through 4.17, and are summarized below.

Boundary layer temperature (Figure 4.13). Air temperatures rose from their initially uniform value of about 15 degrees Celsius to in excess of 19 degrees Celsius over the core of the Gulf Stream. There was little increase in temperature over the waters of the continental shelf, while temperature rose about 2 degrees Celsius to the southeast of the warmest water.

Boundary layer pressure (Figure 4.14). The greatest sea-level pressure falls were about 1.5 mb in magnitude, and located over the core of the Gulf Stream. This may appear to be a small perturbation, but is actually significant, given the horizontal scale. The pressure field induced a northeasterly surface geostrophic flow in excess of 10 meters second^{-1} on the northwest side of the pressure trough (near the north wall of the Gulf Stream).

Boundary layer winds (Figure 4.15). A region of upward motion (7 microbars second^{-1}) developed over the Gulf Stream, with subsidence to the northwest and southeast. Low-level streamlines show a general inflow to the region of greatest ascent.

Figure 4.13. Temperature (Celsius) from the lowest model level (~50 meters AGL) after 12 hours of the control simulation. The initially uniform value was ~15 degrees Celsius (from Warner et al. 1990).

Figure 4.14. Sea level pressure (millibars) after 12 hours of the control simulation. The initially uniform value was 1000 millibars (from Warner et al. 1990).

Figure 4.15. Vertical velocity (microbars second^{-1}) at 900 millibars, and streamlines of horizontal motion at 975 millibars after 12 hours of the control simulation (from Warner et al. 1990).

Figure 4.16. Relative vorticity (times 10^{-5} second^{-1}) at 975 millibars after 12 hours of the control simulation (from Warner et al. 1990).

76

Figure 4.17. Precipitable water (centimeters) after 12 hours of the control simulation. The initially uniform value was 1.4 centimeters (from Warner et al. 1990).

Boundary layer relative vorticity (Figure 4.16). By the 12-hour point, low-level

flow developed a significant cyclonic rotation, as relative vorticity increased from an

initially uniform value of zero to in excess of 8 units, centered over the Gulf Stream.

Boundary layer precipitable water (Figure 4.17). Low-level moisture

convergence increased the total column precipitable water from 1.4 centimeters to

more than 2.4 centimeters just to the warm side of the north wall of the Gulf Stream.

Precipitation (not shown) existed along the entire axis of the Gulf Stream at this time.

The marine atmospheric boundary layer front which was found to develop by the

12-hour point is shown in the cross section of Figure 4.18. Note the presence of a front

of about 2 degrees Celsius amplitude, which was located just on the cool side of the

greatest initial surface sensible heat flux, and extends up to about 1 kilometer (through

the lowest 100 millibars). Compare this front with that which developed in the smooth

77
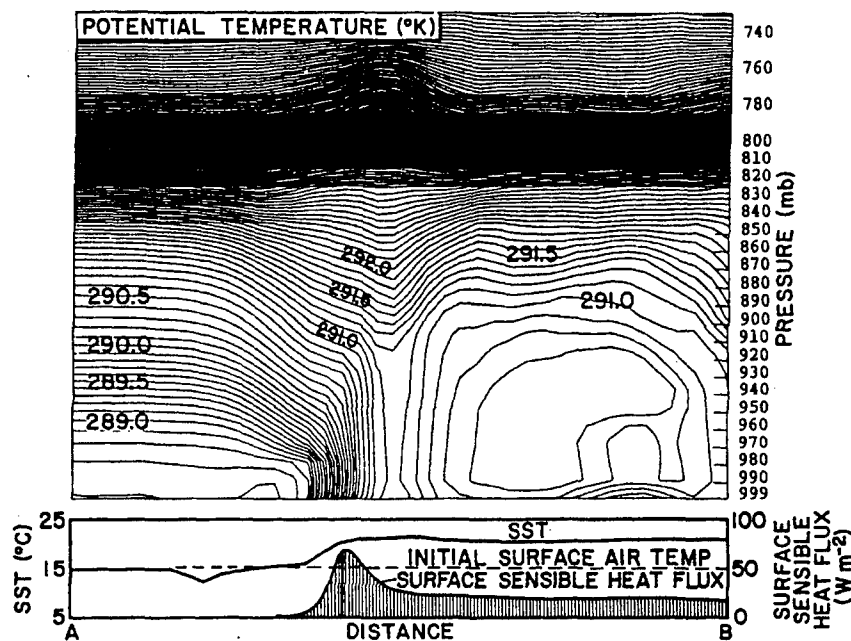
Figure 4.18. Potential temperature (Kelvin) cross section along the line A-B (Figure 4.11) after 12 hours of the control simulation. At the bottom are shown the SST, the 12-hour surface sensible heat flux (Watts meter^{-2}) and the initial surface air temperature (Celsius) (from Warner, et al. 1990).
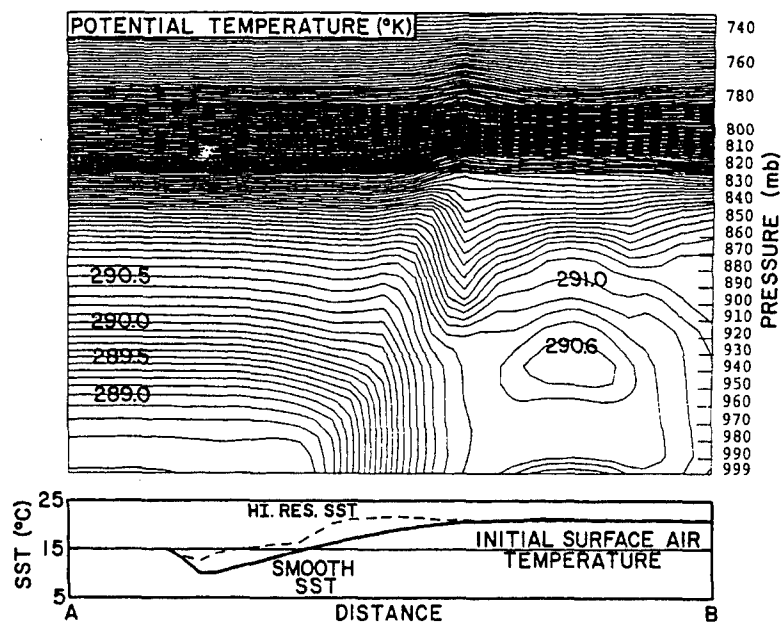
Figure 4.19. Same as Figure 4.18, except for the smooth SST field experiment (from Warner, et al. 1990).

SST simulation (Figure 4.19), which is *three to four times weaker*.

Table 4.2 summarizes the findings of Warner et al. A marine atmospheric boundary layer circulation was found to be forced by the air-sea temperature differences associated with the Gulf Stream. The strength of the resulting atmospheric front was directly related to the strength of the SST gradient and the inclusion of the effects of latent heating. Overall, the boundary layer modifications which occurred during their simulations created a low-level environment which is favorable for cyclogenesis, due in large part to enhanced surface convergence and diabatic warming. It should be noted here that the simulated mesoscale process was not under the influence of any synoptic-scale atmospheric forcing. It is expected from dynamic arguments that such an SST-induced boundary layer circulation would be very sensitive to the synoptic-scale wind (Sublette and Young 1996).

Table 4.2. Comparison of 12-hour model simulations (from Warner et al. 1990).

Parameter	Control	Smooth SST	No latent heating
Coastal trough amplitude (millibars)	1.50	0.40	0.80
Relative vorticity maximum (10^{-5} second^{-1})	14.10	2.42	0.70
Vertical velocity maximum (microbars second^{-1})	-8.30	-2.88	-0.52
Maximum horizontal velocity	7.40	2.06	1.67
Surface frontal strength relative to control	1.00	0.25	0.90
Maximum surface pressure gradient near the front in terms of geostrophic wind speed (meters second^{-1})	12.22	3.83	2.81
Total (12-hour) rainfall maximum along front (centimeters)	3.64	1.94	--

Observations of Frontogenesis along the Shelf Break

Although the numerical simulations discussed above describe a type of coastal frontogenesis which occurs near the Gulf Stream, it is reasonable to suggest that a similar process occurs near the strong SST gradient associated with the shelf break of the northwest Gulf. It is also reasonable to believe that if an atmospheric front tends to develop near the shelf break following cold air outbreaks, then surface observations should indicate its presence.

Evidence of the "Shelf Break Trough" from Surface Charts

Norris (1992) observed that surface synoptic charts often indicate the presence of a trough of low pressure either along the Texas/Louisiana coastline, or offshore and parallel to the physical coastline. She proposed that the trough should not be analyzed in that location, but that it should rather be analyzed near the shelf break, with a similar orientation. The mis-analysis, according to Norris, was due to both the lack of surface data over the Gulf and "traditional thinking whereby the land-sea temperature gradient and the shape of the coastline are the primary causes of Gulf cyclogenesis."

A review of 41 years of synoptic surface charts revealed that the analysis of a trough of low pressure which lies slightly offshore and parallel to the Texas/Louisiana coast is, in fact, a fairly common occurrence during the winter months. An example of such a feature is provided in Figure 4.20, which is the surface map for 1200 UTC 5 November 1995. Note that later on this day, cyclogenesis occurred along the analyzed trough, and was the chosen example of nonfrontal cyclogenesis shown in Figure 3.23.
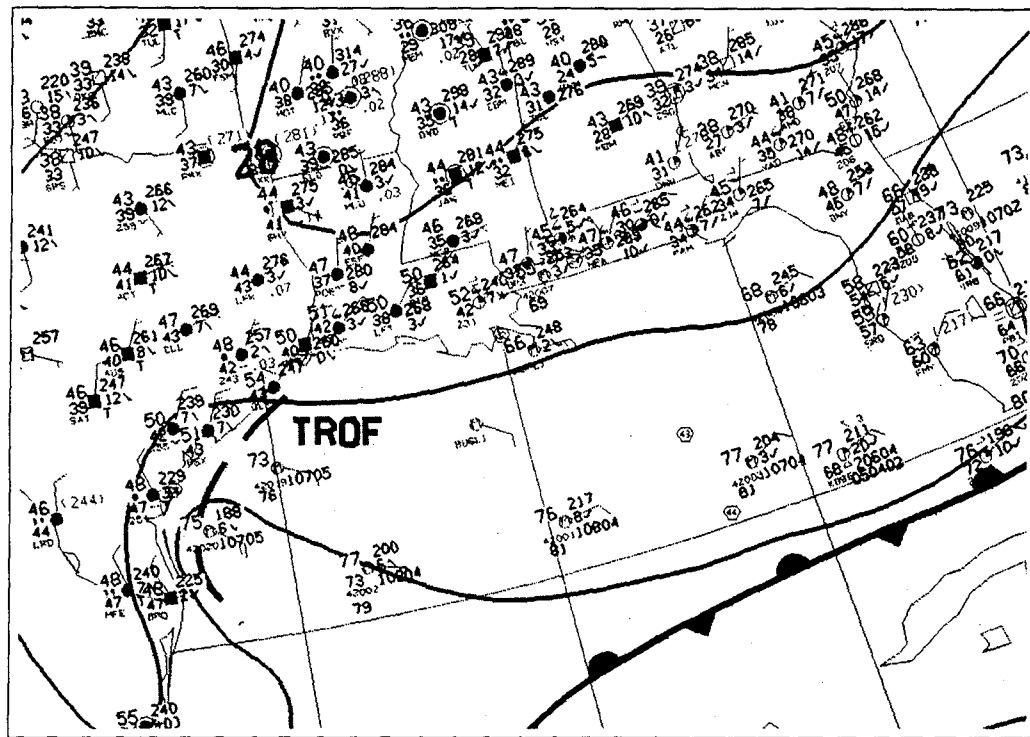
Figure 4.20. An example of a shelf break trough. Surface analysis for 1200 UTC 5 November 1995 (see Figure 3.23 for subsequent analyses).

To the east of this trough, temperatures and dewpoints (Fahrenheit) were in the 70s, and winds were from the east-southeast. To the west, temperatures were near 50, dewpoints were in the 40s, and winds varied from north-northeast to north-northwest. Skies were overcast to the west, and many stations were reporting light precipitation. Although the feature was analyzed as simply a trough in the surface pressure field, a strong argument could be made for the analysis of a stationary front, since the temperature contrast was so strong. Hsu (1992) defined "frontal overrunning" as occurring "when a polar front is nearly stationary along the central Gulf coast or over the northern Gulf of Mexico. Typically observed overrunning conditions are heavy cloud cover and precipitation." Indeed, such conditions did exist at this time, but the

81

Number of Pressure Troughs Identified
Off the Texas/Louisiana Coast
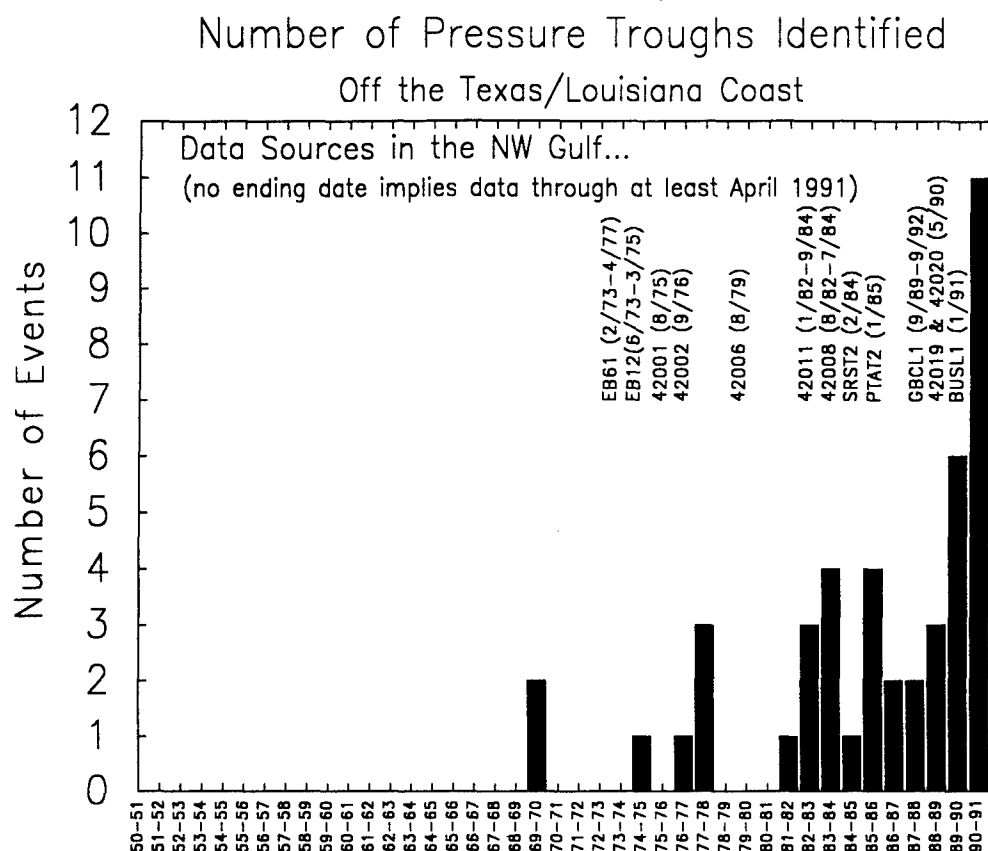
Figure 4.21. Number of pressure troughs or stationary fronts per winter season which were analyzed on daily surface synoptic charts to lie slightly offshore and nearly parallel to the Texas-Louisiana coast during the months of September through April, 1950-1991. The dates in the figure indicate approximate time periods when the referenced data buoys were active. See Figure 3.5 for buoy locations.

boundary was clearly *not the polar front*, which, in this case, was well to the south.

As was mentioned, the author's inspection of daily weather maps revealed that this feature has been observed repeatedly. The frequency of this occurrence was noted, and the result is plotted in Figure 4.21. There were a few instances when the pressure trough was analyzed as a stationary or warm front. These situations were included, since they represent the same meteorological phenomenon.

82

At first glance, it appears as though the shelf break trough never developed prior to 1969! However, recall from Chapter 3 that prior to the early 1970s, data buoys had not yet been deployed into the Gulf. Although the introduction of surface data sources was shown not to have significantly affected the frequency of analyses of Gulf cyclogenesis, it appears as though resolution of the shelf break trough, or front, (which tends to be found within the West Gulf region of Figure 3.6) is closely related to the spatial resolution of data. Indeed, the scarcity of marine observations and the lack of understanding of the marine atmospheric boundary layer has caused features such as the coastal front to be omitted or misanalyzed throughout the history of synoptic analysis (Riordan 1996).

Evidence of the "Shelf Break Trough" from Satellite Imagery

Since readily available surface observations do not consistently indicate the presence of the shelf break front, it is necessary to investigate other data sources for their utility in resolving this problem. One proposed data source, which is commonly available to operational meteorologists, is high-resolution visible satellite imagery.

The New England Winter Storms Experiment of 1983 was the first to provide detailed information on the vertical structure of the New England coastal front (Nielsen and Neilley 1990). The front which was observed showed a "structure remarkably similar to that of a density current. At its leading edge, the sharp frontal zone was nearly vertical or rose abruptly from the surface to 200 to 300 meters. Behind this 'head' region, the frontal zone was nearly horizontal" (Riordan 1996).

83

Case 1. GOES-8 visible imagery from 1800 UTC 4 December 1995 (Figure 4.22) indicated the existence of a rope cloud over the northwest Gulf. A rope cloud is a line of cumulus which forms along the hydraulic head of a density current (Houze 1993, pp. 475-478), and has been observed to form in connection with the atmospheric circulations of the boundary layer convergence zone which can often be found along the north wall of the Gulf Stream (Sublette and Young 1996). The orientation of the cloud band was roughly parallel to the Texas coast, but well offshore. To the west of the band, cloud features were stratiform, indicating a relatively high level of atmospheric stability. To the east, clouds were convective in nature. Strongest convection was evident in a northwest-southeast line south of Louisiana.

The most striking aspect of this feature to the author was its persistence throughout the day, with hourly visible satellite images showing it to remain in approximately the same location, with the same orientation, during each of the daylight hours. Infrared satellite imagery (not shown) displayed this feature much less vividly, owing to the low altitude and relatively warm temperatures at cloud top -- indicative of shallow, small-scale convection.

The surface analysis for 1200 UTC 4 December 1995 (Figure 4.23) showed a weak cold front moving off the Texas coast, with light northwesterly winds in its wake. Since winds were so weak at this time, the lower temperatures behind the front were likely more a reflection of radiational cooling than of significant cold air advection. Offshore, winds were generally southwesterly at speeds of 10 knots or less, and
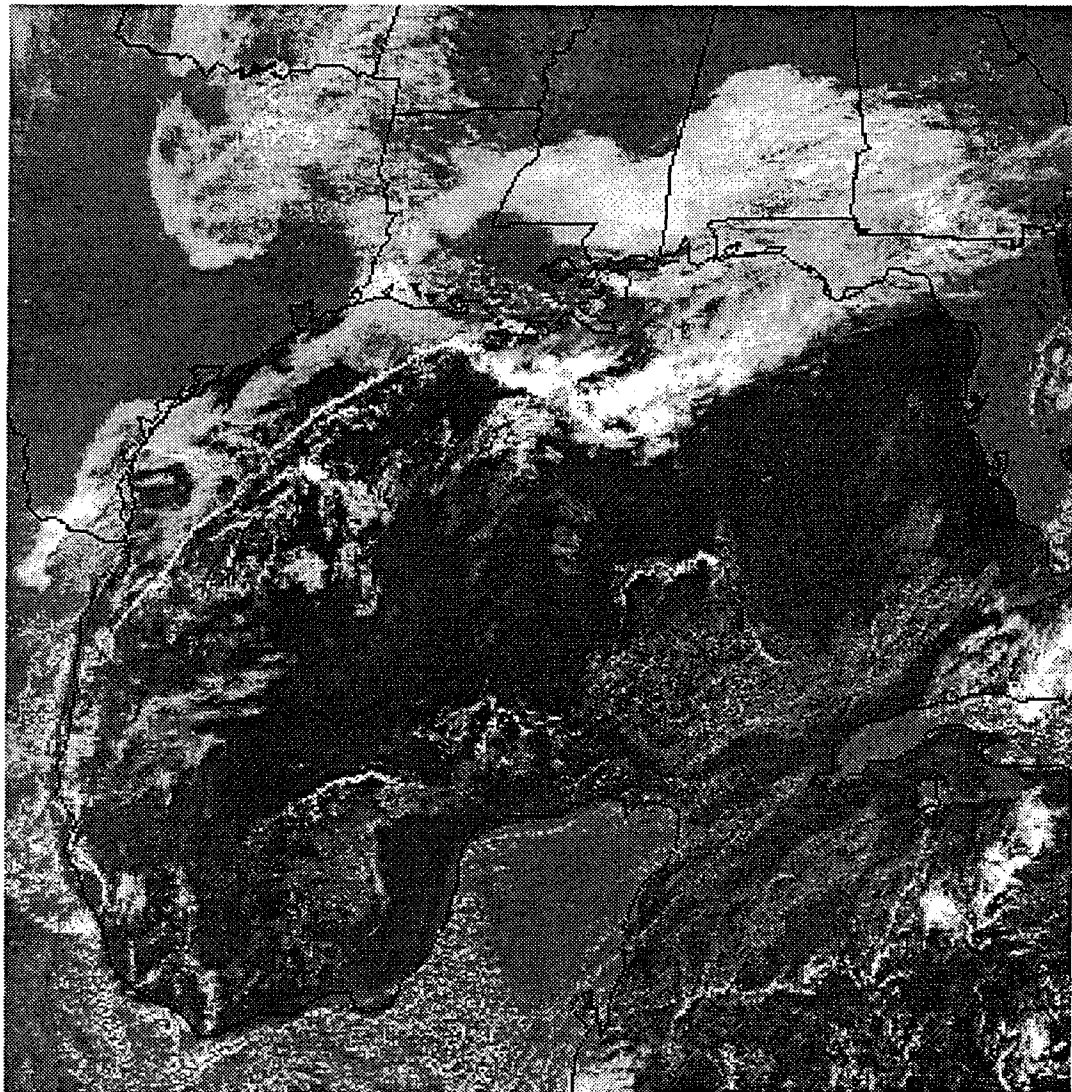
Figure 4.22. GOES-8 visible satellite imagery for 1800 UTC 4 December 1995.
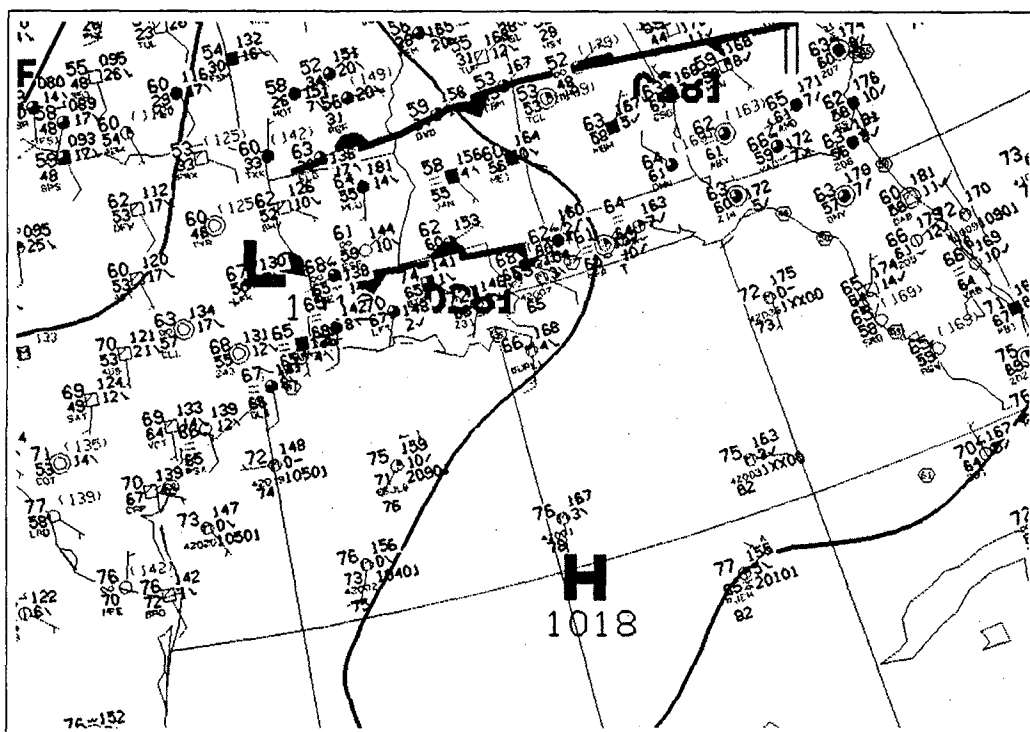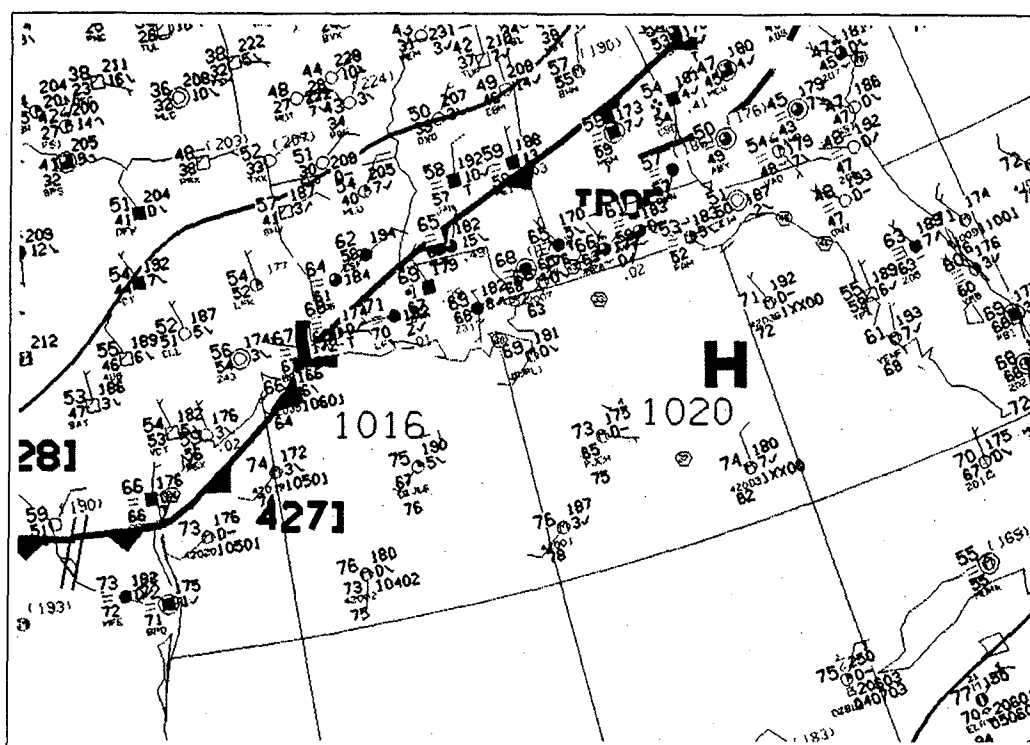
Figure 4.23. Surface analyses for 1200 UTC 4 December 1995 (top) and 0000 UTC 5 December 1995 (bottom).

temperatures were about 20 degrees (Fahrenheit) greater than over land. By 0000 UTC

5 December 1995, the cold front was no longer analyzed, and winds over eastern Texas

were 10 knots or less, and from the south. Immediately offshore, winds were light and

variable, while the buoys to the east indicated light southwesterly winds. The

temperature difference between the land and Gulf stations was generally about 5

degrees. Average sea surface temperatures for the week of 6 December 1995 (Figure

4.24) depict that the coolest water existed along the immediate Gulf coast. The SST

isotherms over the northwest Gulf were aligned fairly parallel to orientation of the rope

cloud, though data resolution is insufficient for the depiction of a strong SST gradient

near the shelf break.

The Rapid Update Cycle (RUC) (Benjamin et al. 1994) appears to have handled

this situation well. Plots of 1000-mb streamlines from the 1200 UTC 4 December

1995 model run depicted an asymptote of confluence offshore Texas and Louisiana in

the model analysis, and in the 3- and 6-hour forecasts (Figure 4.25a, b, and c,

respectively). The model even resolved a mesoscale cyclonic eddy which developed to

the east of extreme south Texas, which is discernible in the stratiform cloudiness in the

1800 UTC satellite image (Figure 4.22), and was clearly evident in satellite image

loops.

The 1000-mb moisture convergence field (Figure 4.26) was a maximum in the

region of the rope cloud. Along and to the east of the region of maximum moisture

convergence, a tongue of maximum equivalent potential temperature (theta-e) (Figure

87
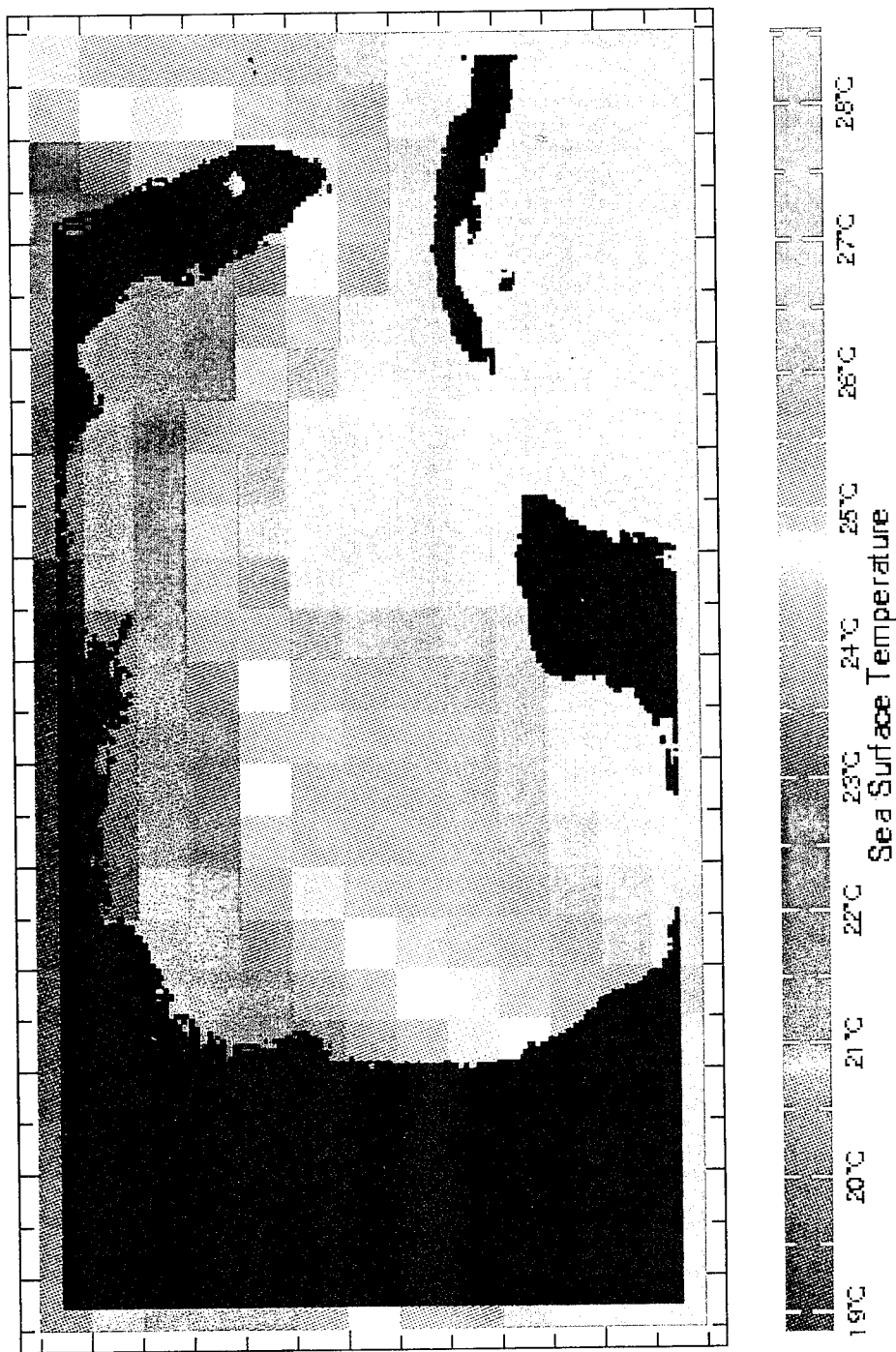
Figure 4.24. Mean sea surface temperatures for the week of 6 December 1995, created on a 1-degree latitude-longitude grid by blending *in situ* and satellite-derived SSTs (Reynolds and Smith, 1994). Obtained via the internet from the Integrated Global Ocean Services Systems (IGOSS), cited 1996: http://rainbow.idgo.columbia.edu/igoss/productsbulletin/ .
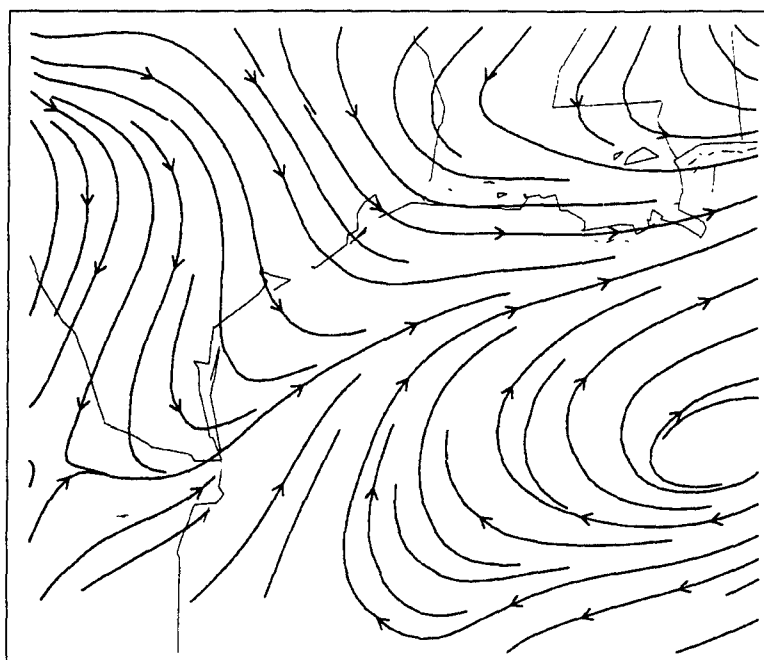
Figure 4.25a. Streamlines at 1000 mb, from the 1200 UTC 4 December 1995 RUC: model initialization valid 1200 UTC 4 December 1995.
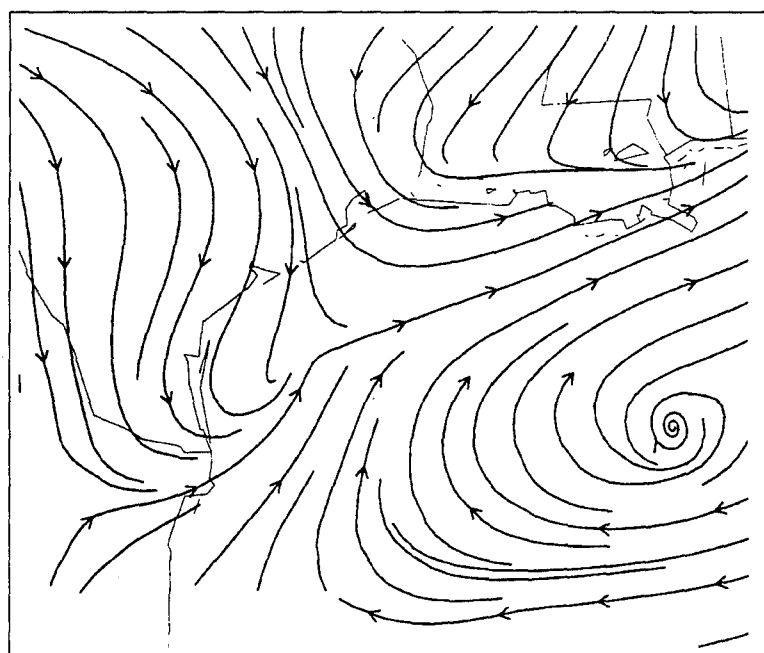
Figure 4.25b. Same as Figure 4.24a, except for 3-hour forecast valid 1500 UTC 4 December 1995.

89
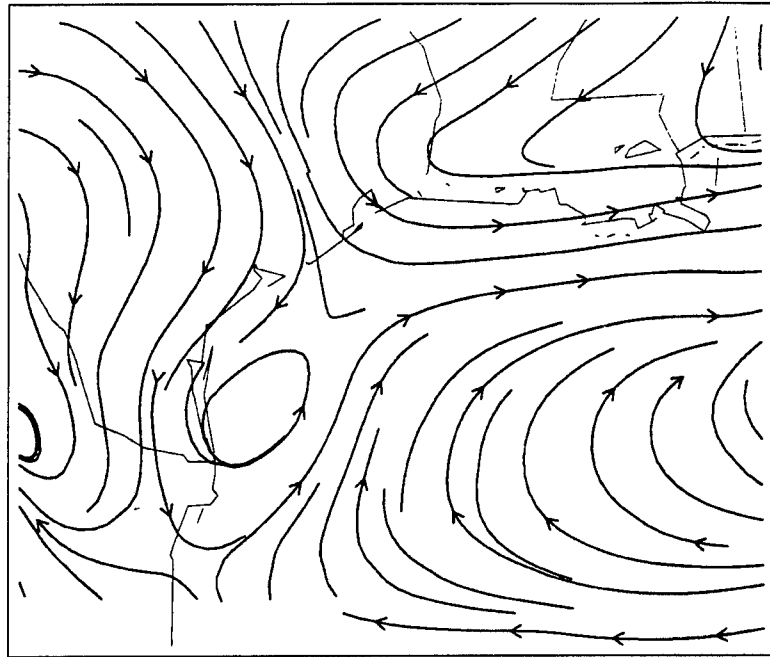
Figure 4.25c. Same as Figure 4.24a, except for 6-hour forecast valid 1800 UTC 4 December 1995.
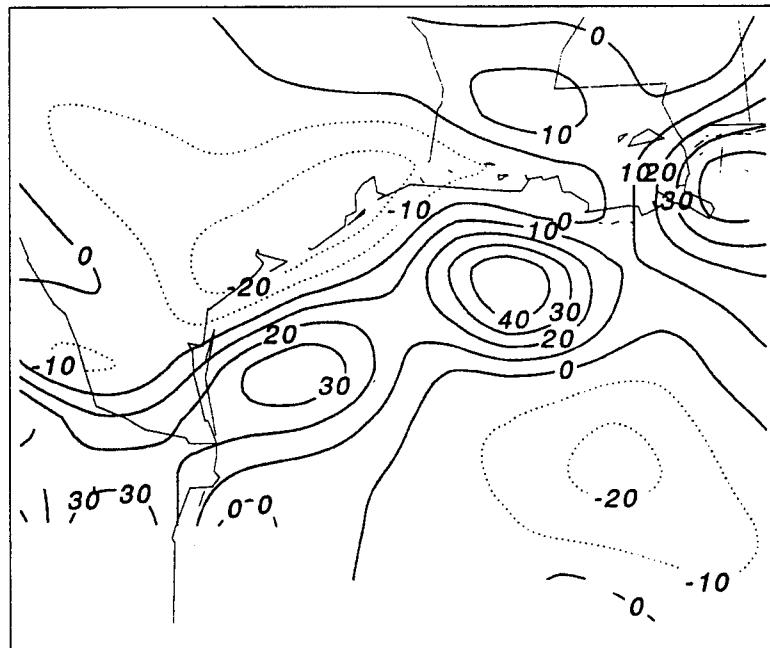
Figure 4.26. 1000-mb moisture convergence, from the 1200 UTC 4 December 1995 RUC: model initialization valid 1200 UTC 4 December 1995. Contour interval is 10×10^{-8} g kg^{-1} s^{-1}; positive values indicated by solid lines.
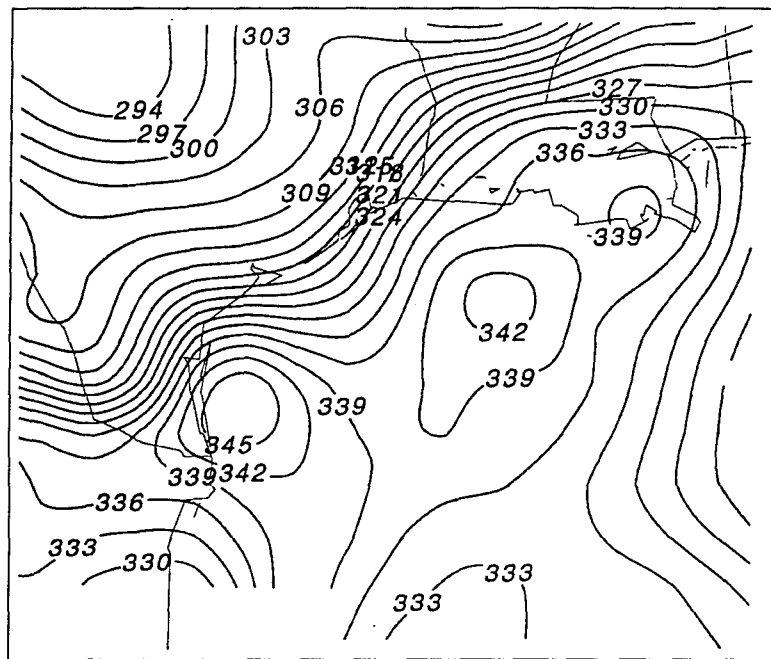
Figure 4.27. 1000-mb equivalent potential temperature (Kelvin), from the 1200 UTC 4 December 1995 RUC: model initialization valid 1200 UTC 4 December 1995.

4.27) extended into southeastern Louisiana. Persistent convection was observed where this theta-e ridge intersected the confluence line, to the south of eastern Louisiana.

A cross section which is oriented approximately normal to the confluence line and the theta-e ridge (see Figure 4.28a) shows the vertical arrangement of the potential temperature and theta-e isopleths (Figure 4.28b). Both parameters are plotted in order to show the influence of the moisture profile on atmospheric stability. The theta-e isotherms wedged upward and to the left (northwestward), with the maximum value occurring near the 1000-mb confluence line. Above this wedge and below about 800 mb, there was a strong decrease of theta-e with height, indicating potential instability. Below this wedge, the atmosphere was strongly stable, while weaker stabilities were

91
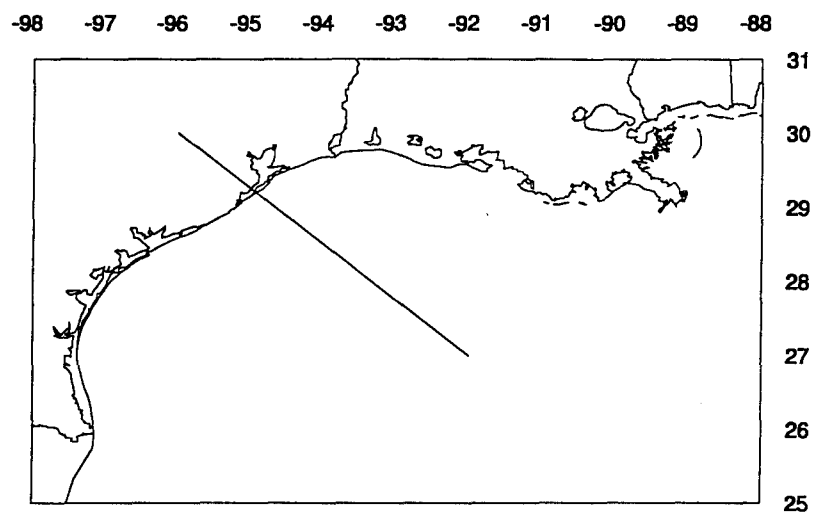
Figure 4.28a. Horizontal location of cross section.
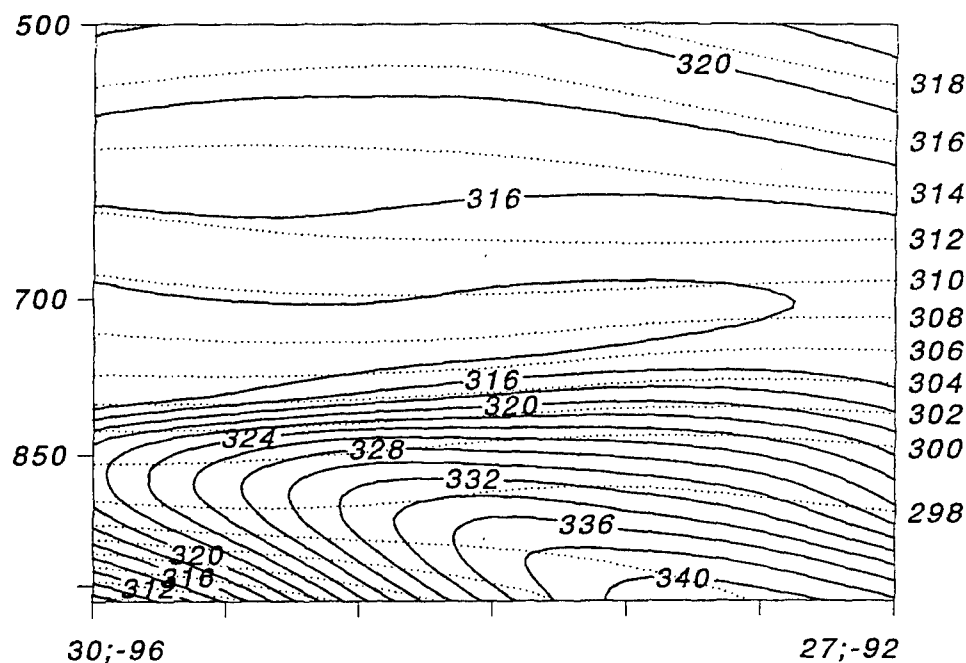
Figure 4.28b. Cross section of equivalent potential temperature (solid lines; contours are labeled within the plot) and potential temperature (dotted lines; contours are labeled along the right vertical axis), (Kelvin), from the 1200 UTC 4 December 1995 RUC: model initialization valid 1200 UTC 4 December 1995. The horizontal location of the cross section is plotted in Figure 4.28a. The vertical axis is pressure (mb; labeled on the left).

92

observed above 700 mb.

The rope cloud which existed at the "head" of this density current could certainly not be depicted by the RUC due to insufficient resolution. Nonetheless, the model output did indicate that the distinct boundary separating the stratiform and cumuliform regions observed on satellite imagery was a function of the strong horizontal differential of atmospheric stability within the boundary layer. This finding is significant, since vertical motion and cyclonic development are strongly dependent on atmospheric stability (see, e.g., Zwack and Okossi 1986).

Case 2. GOES-8 visible imagery from 2000 UTC 5 January 1996 (Figure 4.29) showed a rope cloud which extended from the western Bay of Campeche near 20S latitude, northward to the Texas coast, crossing the coastline near Victoria (VCT), and bending back toward the northeast. North of Victoria, the feature was nearly parallel to the coast, but *onshore*. Further south, however, the feature was located in the vicinity of the shelf break, and more closely resembled the rope cloud shown in Case 1 (Figure 4.22). Offshore Texas and Louisiana, a stratus cloud deck shrouded the shelf waters.

The surface analysis for 1800 UTC 5 January 1996 (Figure 4.31, bottom) shows that the onshore portion of the feature was analyzed as a trough of low pressure, while the offshore segment to the south was not analyzed. In fact, when comparing the surface pressure at buoy 42020 (1017.4 mb) with surrounding pressures, it appears that the trough *should* have been analyzed to be offshore in that area. This mis-analysis was consistent with a similar mis-analysis at 1200 UTC (Figure 4.31, top), and may

93
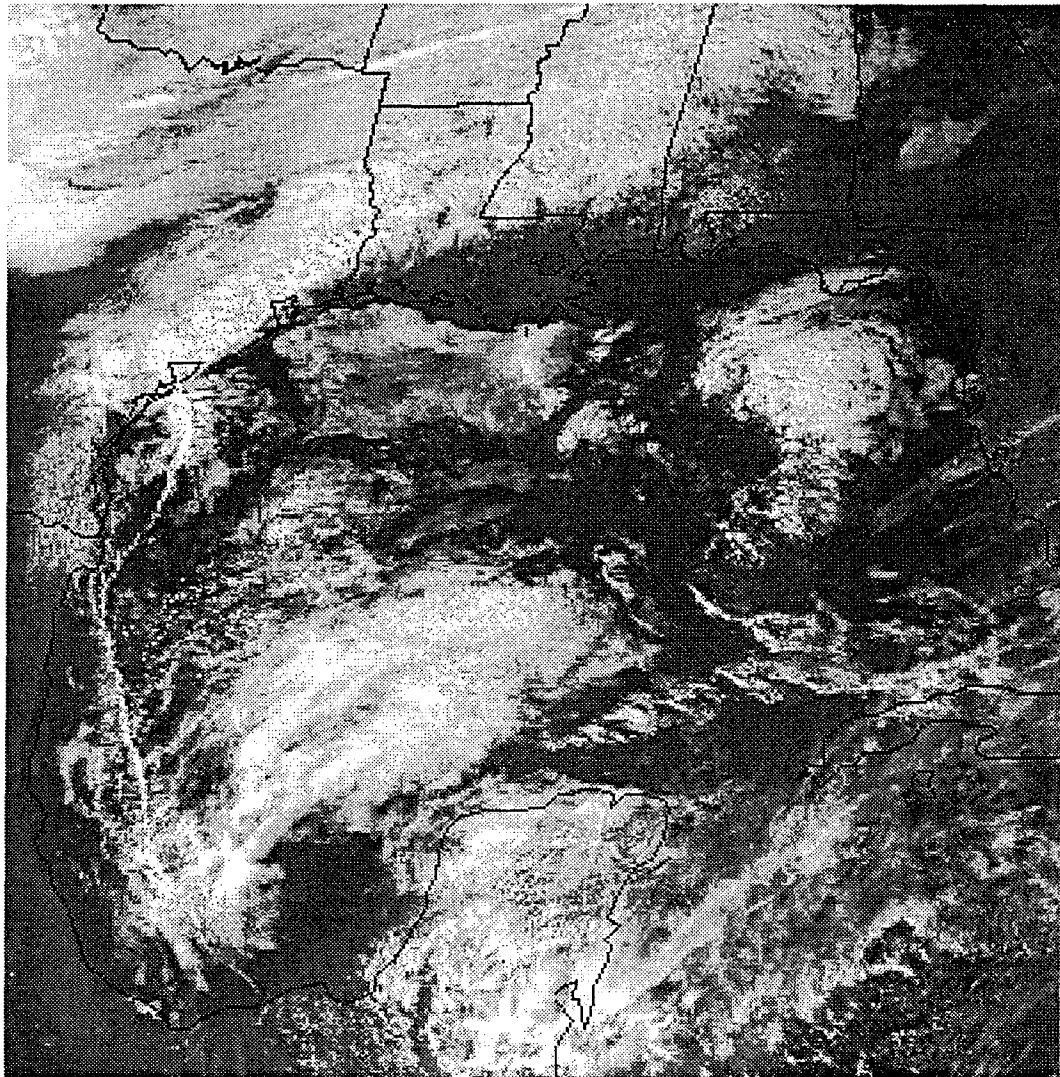
Figure 4.29. GOES-8 visible satellite imagery for 2000 UTC 5 January 1996.
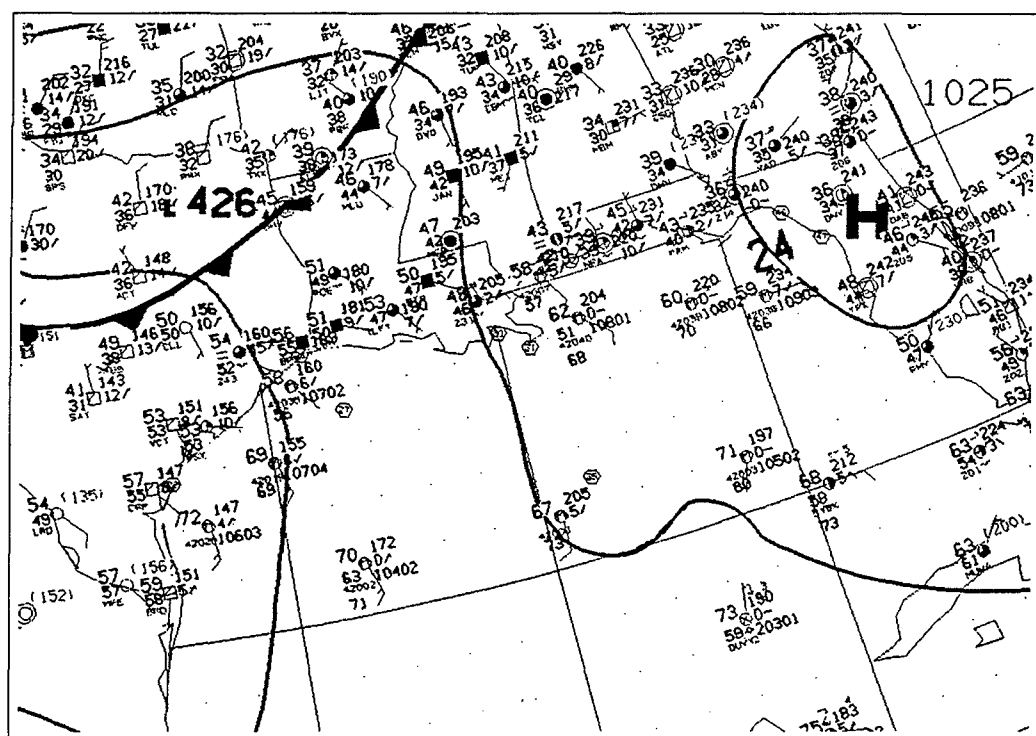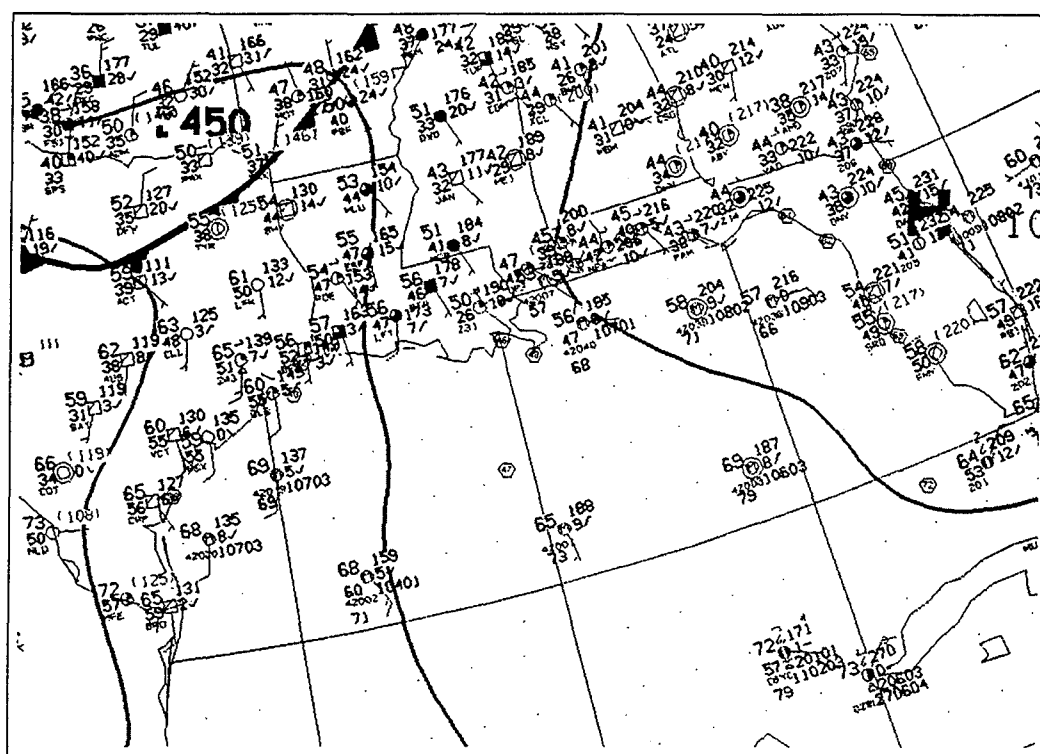
Figure 4.30. Surface analyses for 5 January 1996: 0000 UTC (top), and 0600 UTC (bottom).
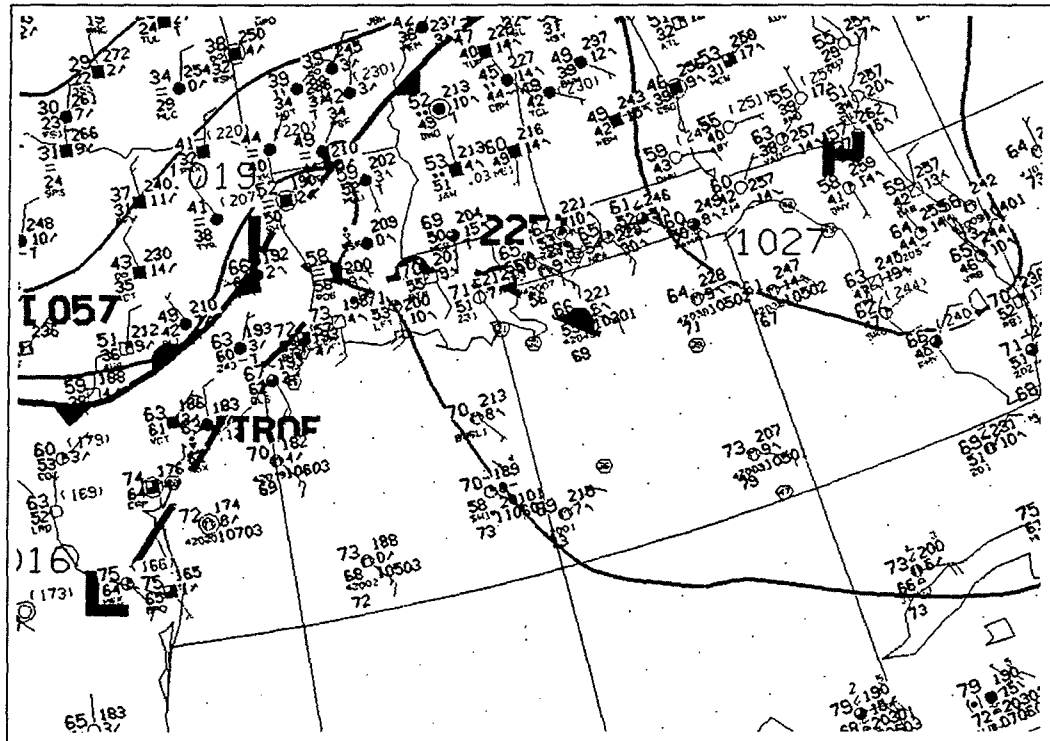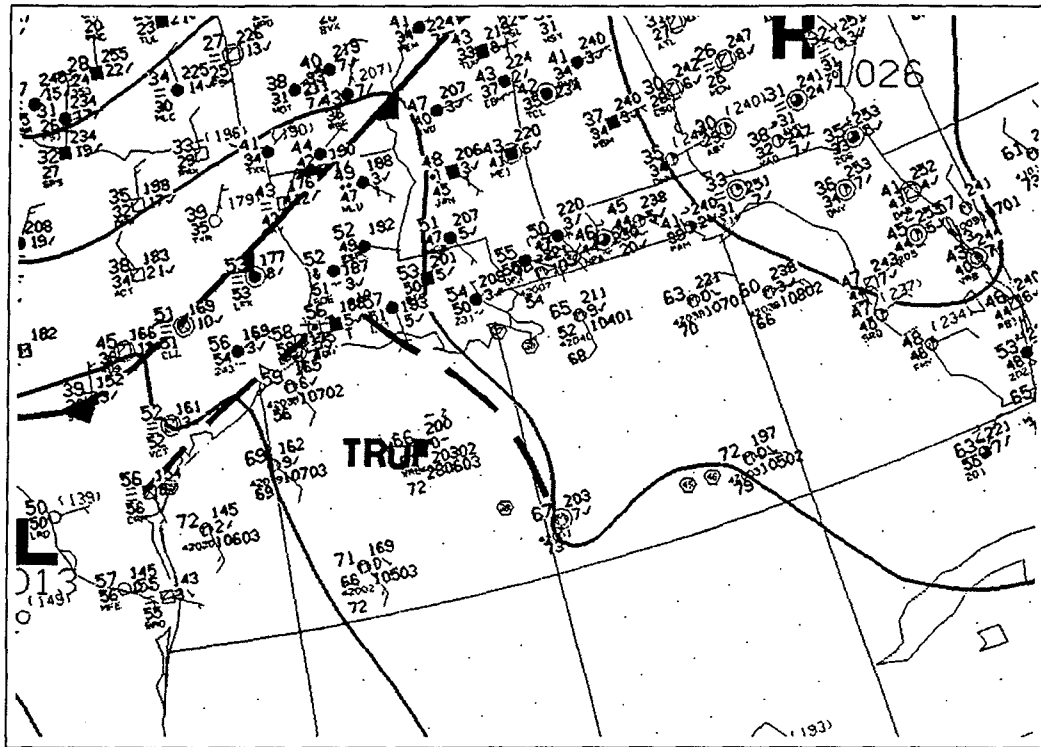
Figure 4.31. Surface analyses for 5 January 1996: 1200 UTC (top), and 1800 UTC (bottom).

have been an attempt to connect the pressure trough with an analyzed center of low pressure in extreme northeast Mexico.

The rope cloud which existed over the Gulf was present in a quasi-stationary position throughout the course of the day. In fact, it was evident in the previous day's satellite imagery as well (not shown), though not as clearly defined or well-organized, especially over the northwest Gulf. Interestingly, a weak disturbance was observed (from satellite imagery) to propagate northward along the convergence line, from about 22N latitude at 0100 UTC 4 January 1996, to Victoria at 1900 UTC 5 January 1996. The 18-hour evolution of this wave and convergence line is provided in Figure 4.32. Most of the locations were determined using infrared satellite imagery, which was somewhat ambiguous at times, again, due to the relatively high temperatures at cloud top.

The northern segment of the front migrated (or continually reformed) slightly to the northwest during each successive analysis, first coming ashore between Palacios, Texas (PSX) and Galveston, Texas (GLS) at about 0700 UTC. As the frontal wave propagated northward, it resembled the typical open wave structure of a synoptic-scale front. Convection was enhanced in the vicinity of the wave, but was observed to occur along the front everywhere north of the wave. A loop of higher-resolution visible images at 15-minute intervals (see, e.g., Figure 4.33) indicated that individual convective elements also moved northward along the front, repeatedly crossing the coastline. This situation resembled one studied by Bosart et al. (1992) in which there
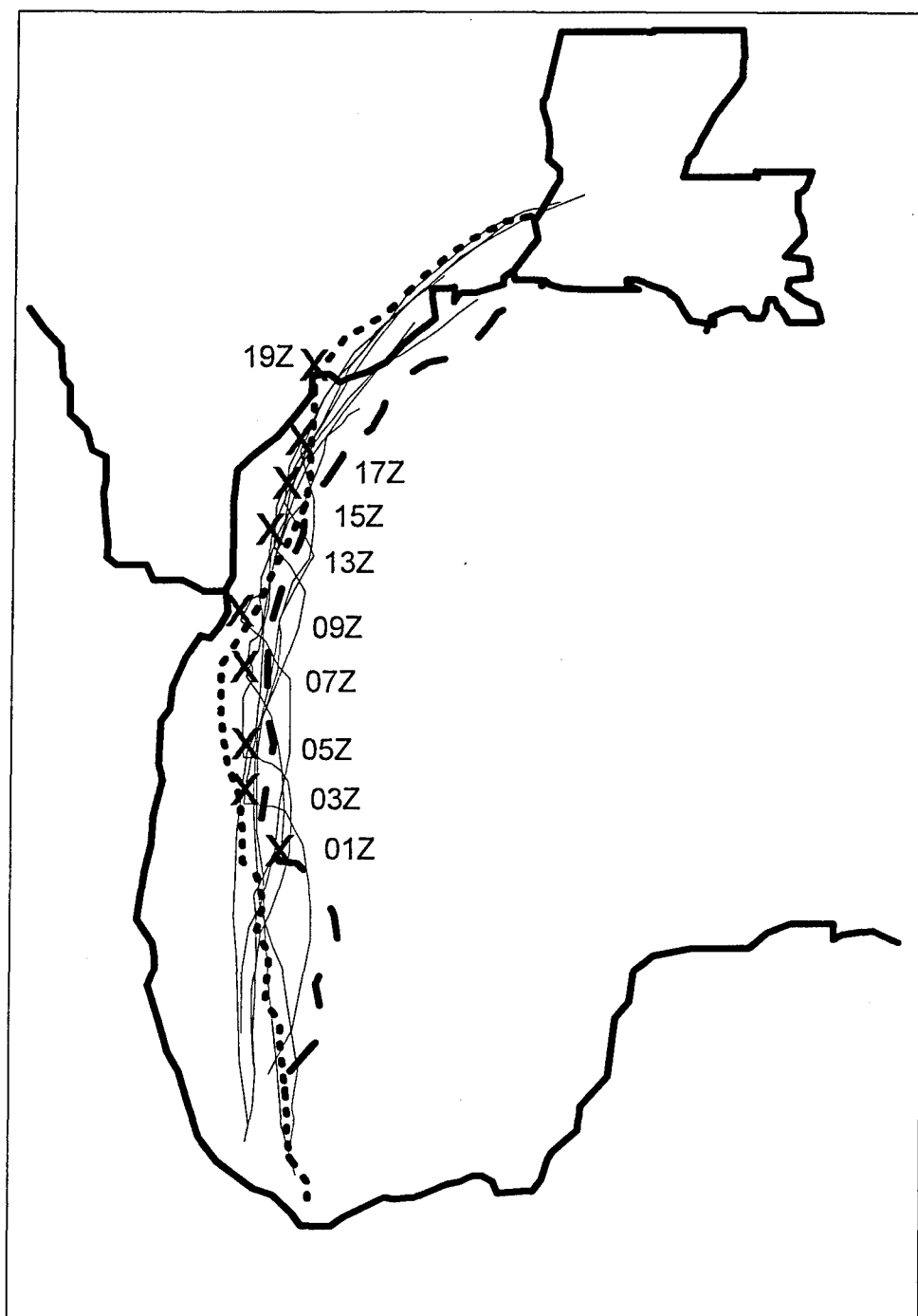
Figure 4.32. Locations of the coastal front and frontal wave from 0100 UTC to 1900 UTC 5 January 1996, as interpreted by satellite imagery. The initial and final locations of the coastal front are denoted by heavy long dashes and heavy short dashes, respectively. The locations of the frontal wave at successive times are given by the "x".

98
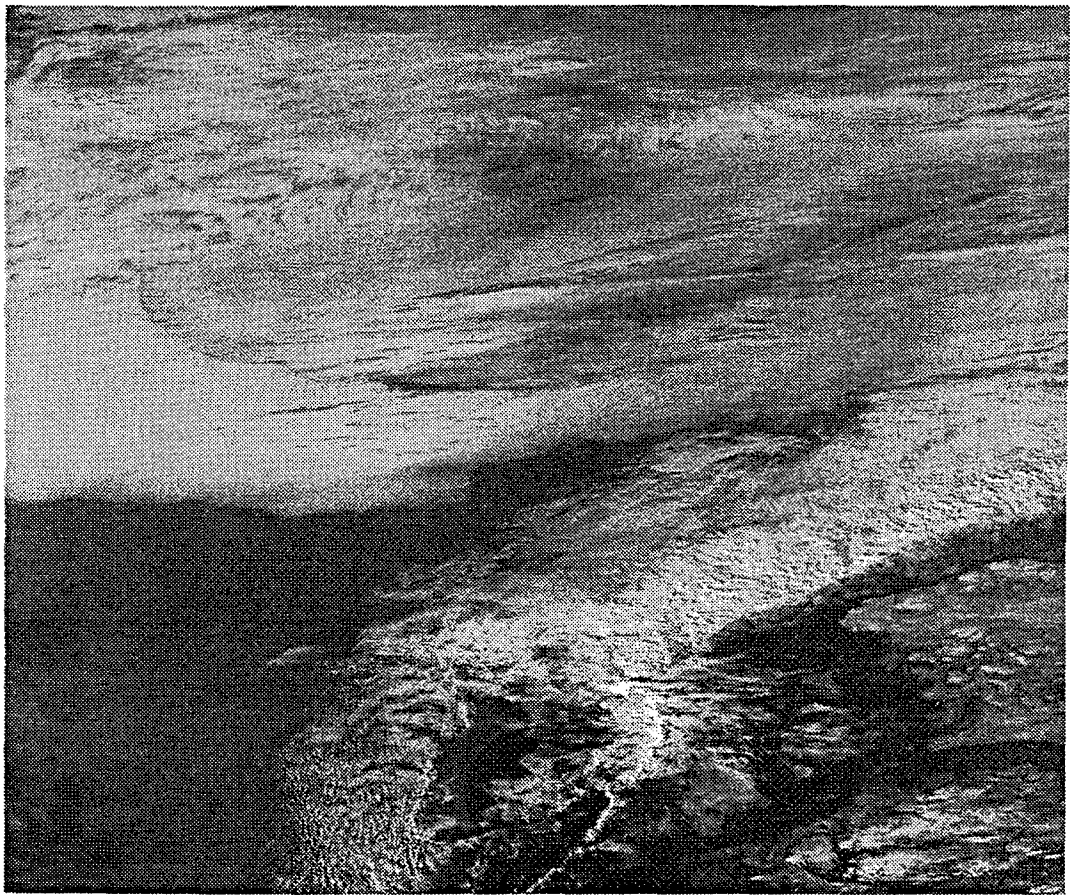
Figure 4.33. GOES-8 visible satellite imagery for 1900 UTC 5 January 1996.

99

was weak cyclogenesis and heavy coastal precipitation.

It is difficult to determine whether the northern portion of the front *propagated* onshore, or whether it was *produced locally* near the coast. The argument, though, may simply be one of semantics, with both premises containing an element of truth. The 0000 UTC 5 January 1996 surface analysis (Figure 4.30, top) (20 hours prior to the satellite image in Figure 4.29) shows that winds over southeast Texas and immediately offshore were generally southerly at 10 knots or less, to the east of a weak, but broad area of low pressure, and to the south of an advancing cold front. No pressure trough was analyzed near the Texas coast -- nor does the data suggest that one should have been. Temperature differences between offshore and onshore stations were about 5-10 degrees Fahrenheit.

By 0600 UTC 5 January 1996 (Figure 4.30, bottom), though, there was a substantial cyclonic turning of the surface winds at the Texas coastline. The land-ocean thermal contrast had increased by this time, solely due to radiational cooling over the landmass. The cyclonic vorticity at the coastline increased over the following 12 hours, and a coastal trough was first analyzed at 1200 UTC 5 January 1996 (Figure 4.31, top).

The cyclonic turning of the winds which occurred near the coast *could have* been produced by differential friction between (rough) land and (smooth) water. In the case of onshore flow, cross-isobar flow toward lower pressure is greater over land than over sea, which induces surface convergence and cyclonic vorticity at the coastline (Bosart

et al. 1972). The 0000 UTC 5 January 1996 surface analysis (Figure 4.30, top), though, indicates neither a cyclonic turning of the onshore winds, nor any noticeable decrease in velocity as winds reached the coast. The coastal vorticity was produced during the nighttime, when boundary layer cooling occurred over the landmass, but not over the water. Thus, it is presumed that the thermodynamic structure of the boundary layer enhanced coastal convergence, as warm, moist air from the deep Gulf was advected northward, and was forced to rise over the cool, stable air which was forming over southeast Texas during the night. Once lifted, this air reached its level of free convection, and an elevated convective line was formed (Colman 1990). This convective line further enhanced low-level convergence and cyclonic vorticity (as evident by the continued cyclonic turning of the winds evident at 1800 UTC 5 January 1996), which, in turn, increased the flow of warm, moist air northward (note the increase in the velocity of the winds offshore by 1800 UTC 5 January 1996). In addition, it should be emphasized that the front which developed along the Texas coast formed a continuous line with the feature off the Mexican coast, where there was clearly no differential friction.

The stratiform cloud which was present immediately south of Texas and Louisiana was advection fog, formed as the synoptic-scale flow advected warm, moist air from the deep Gulf region over the cool waters of the continental shelf. Sea surface temperatures are provided in Figure 4.34. When compared with the SST distribution of one month earlier (Figure 4.24), it is evident that the Loop Current had made a slight
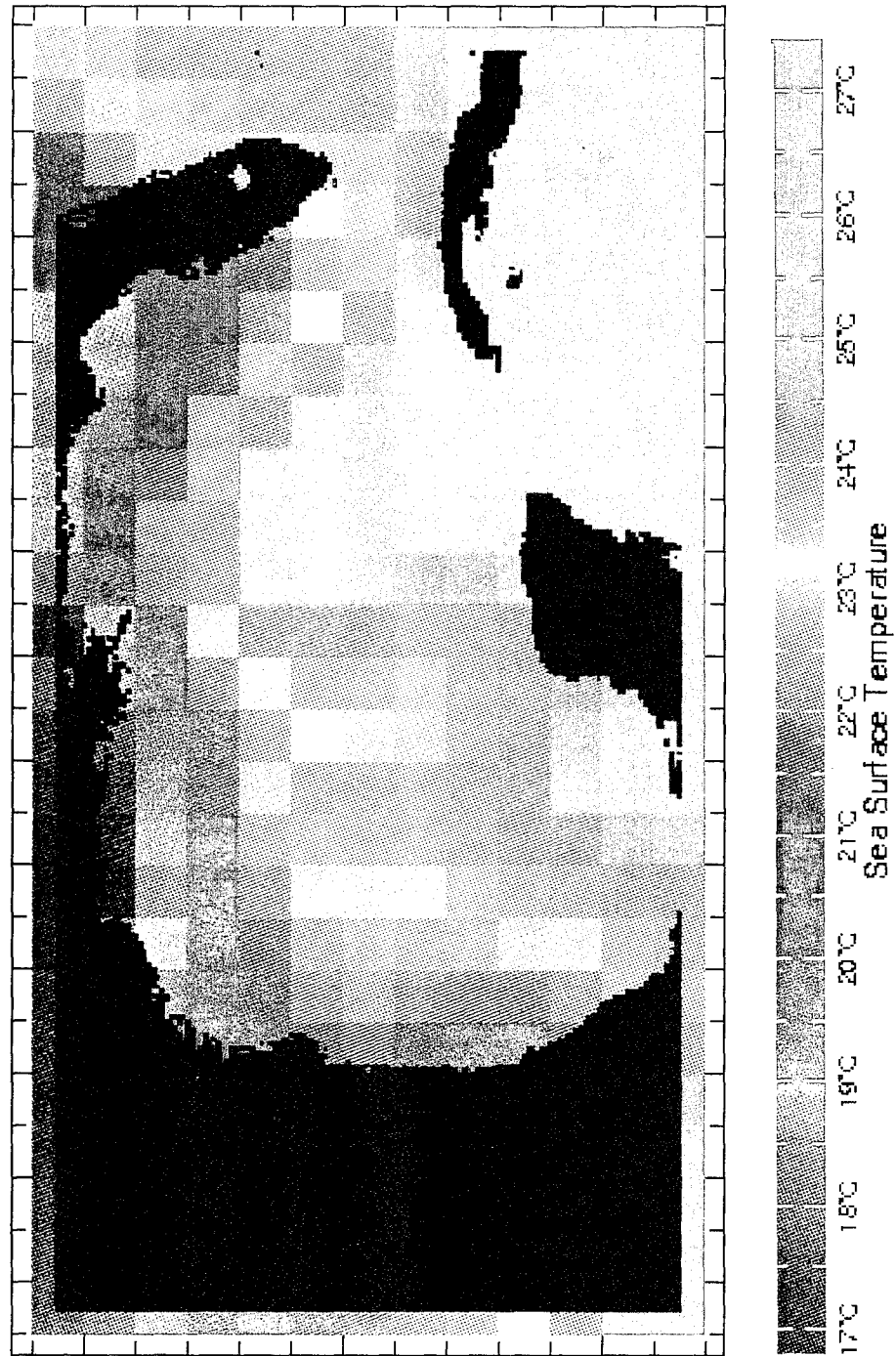
Figure 4.34. Same as Figure 4.24, except for the week of 3 January 1996.

advancement to the northwest, and that the waters of the Mexican continental shelf had

cooled significantly. Along the Mexican and extreme southeastern Texas continental

shelf, SSTs generally paralleled the orientation of the rope cloud. To the north,

however, the rope cloud was not oriented along the shelf break, indicating that

advection of warm air from the regions of the deeper Gulf was significant, and played a

role in the northwestward migration of this feature.

The 1200 UTC 5 January 1996 RUC initialization and 6-hour forecast of

1000-mb streamlines (Figures 4.35a and b, respectively) did not indicate the cyclonic

turning of the winds at the coast which was evident at those times. Rather, the cyclonic

vorticity in the RUC output was associated with the cold front which was advancing

from the north. Since this feature was not resolved well, it is presumed that the fairly

accurate 6-hour forecast of 1000-mb moisture convergence (Figure 4.36), which

displayed a maximum along the Texas coast, was a "lucky guess," since it was more

likely associated with the synoptic-scale cold front than with the coastal front. A cross

section of the 6-hour forecast of theta-e (Figure 4.37) is taken in the same location as in

Case 1 (see Figure 4.28a), and shows a similar structure: the theta-e isotherms wedged

upward and to the left (northwestward), with a potentially unstable layer above the

wedge, and a stable stratification below. In this case, though, the maximum value was

not coincident with any convergence line near the shelf break, but rather occurred in a

broad, deeper layer, over the shelf waters and just onshore. Obviously, this high

theta-e valued air was not being produced locally, since the presence of stratiform
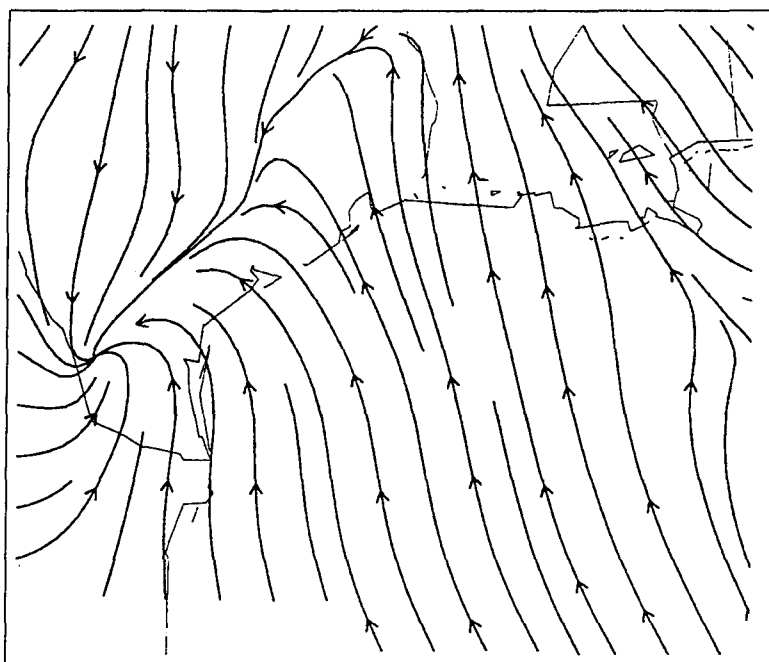
Figure 4.35a. Streamlines at 1000 mb, from the 1200 UTC 5 January 1996 RUC: model initialization valid 1200 UTC 5 January 1996.
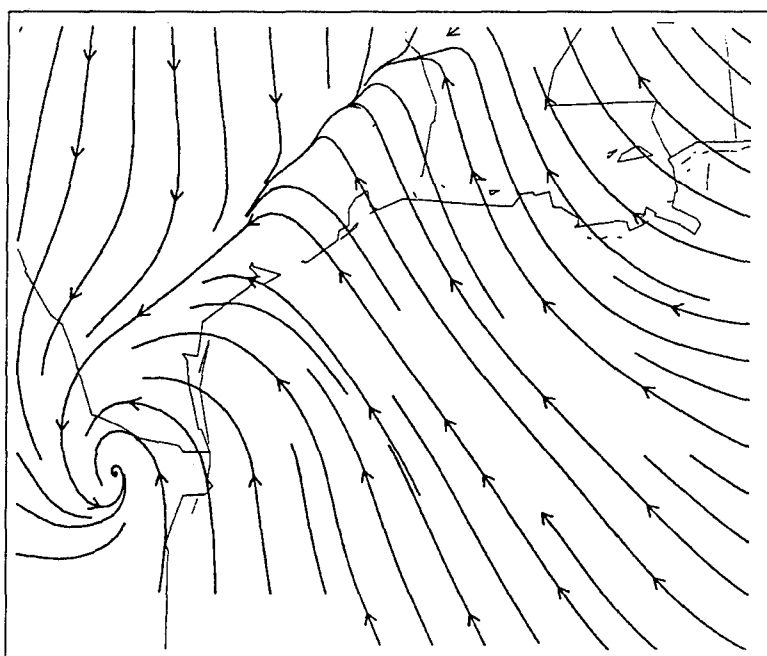
Figure 4.35b. Same as Figure 4.34a, except for 6-hour forecast valid 1800 UTC 5 January 1996.
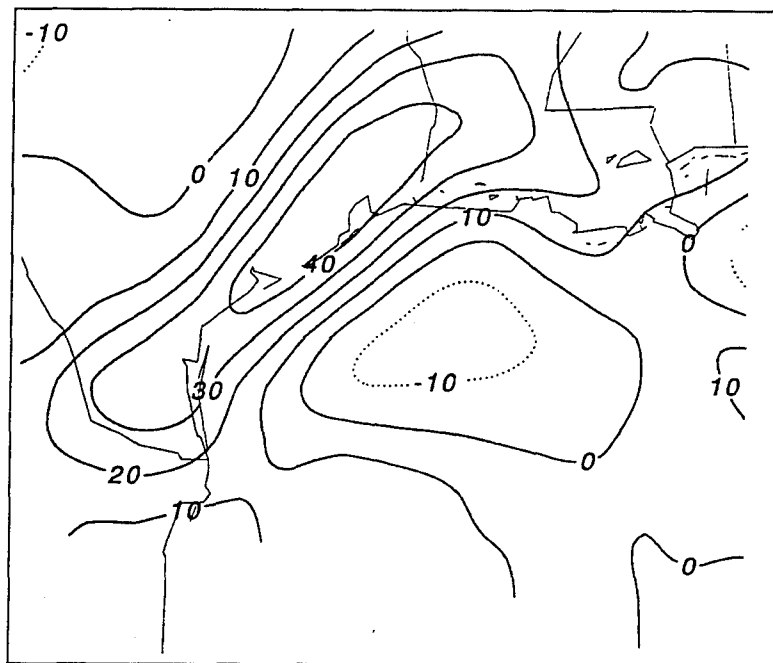
Figure 4.36. 1000-mb moisture convergence, from the 1200 UTC 5 January 1996 RUC: 6-hour forecast valid 1800 UTC 5 January 1996. Contour interval is 10 x 10^{-8} g kg^{-1} s^{-1}; positive values indicated by solid lines.
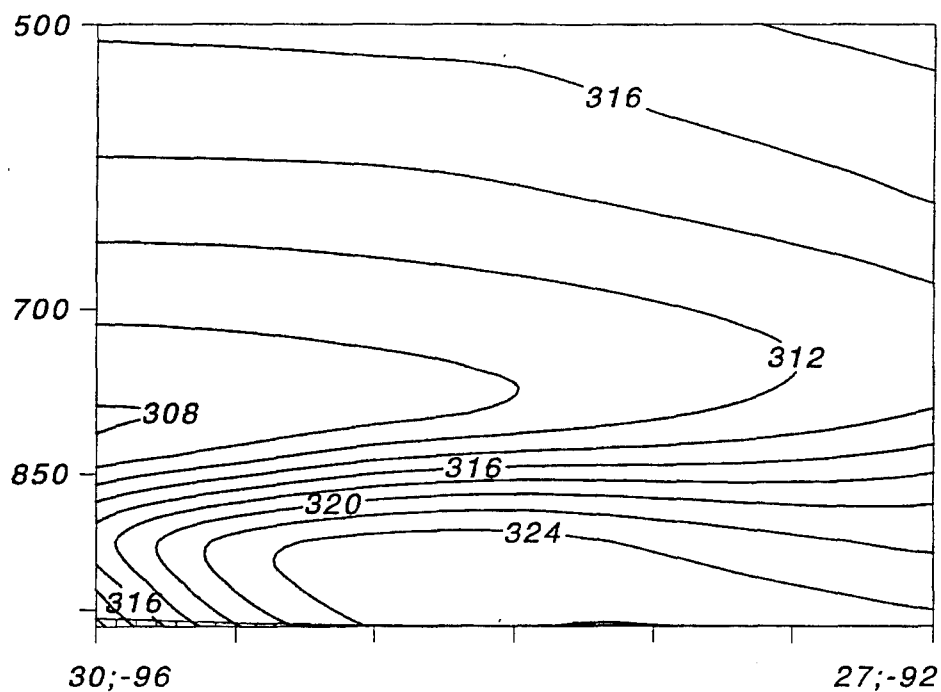
Figure 4.37. Cross section of equivalent potential temperature (Kelvin), from the 1200 UTC 5 January 1996 RUC: 6-hour forecast valid 1800 UTC 5 January 1996.

105

clouds indicated that diabatic cooling was actually occurring over the shelf. Therefore, it is apparent that the RUC accurately forecasted a synoptic-scale flow which was sufficiently strong to continuously advect high theta-e valued air over the cold shelf water, so that the atmospheric boundary layer did not reach thermodynamic equilibrium with the underlying water. As a result, the areas of maximum thermal contrast, mesoscale convergence, and cyclonic vorticity did not form along the shelf break as they had in Case 1, but frontogenesis occurred at the land-sea boundary. In this sense, it is suggested that the development of what might be called the "shelf break front" is highly sensitive to the synoptic-scale flow.

Case 3. GOES-8 visible imagery from 2000 UTC 21 January 1996 (Figure 4.38) showed a rope cloud which was well offshore the Texas/Louisiana coast, continuing southward off the Mexican coast, and then eastward over the open water toward the Yucatan peninsula. In fact, it was located in the vicinity of the continental shelf break over the entire periphery of the western Gulf. As in Cases 1 and 2, it remained quasi-stationary through the course of the day, as indicated by imagery loops.

A detailed analysis of this Case will not be presented, since the factors which contributed to its existence were found to be similar to those previously described. The RUC indicated confluent flow and moisture convergence in the region of the rope cloud, and an axis of maximum 1000-mb theta-e along it and to its east. It also showed a vertical wedge of high theta-e values which was maximized at the confluence line, with a shallow potentially unstable layer above the wedge, and a more stable
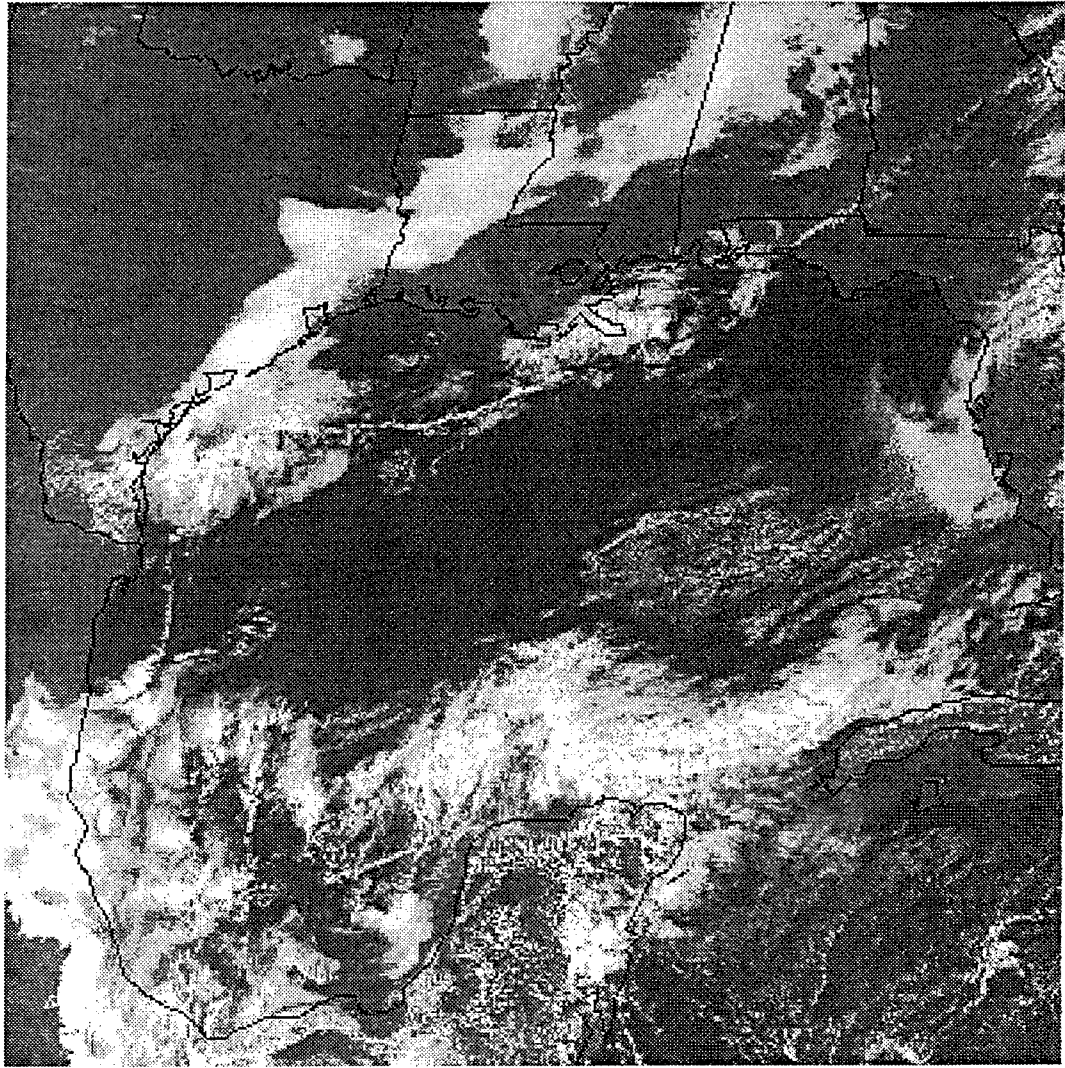
Figure 4.38. GOES-8 visible satellite imagery for 2000 UTC 21 January 1996.
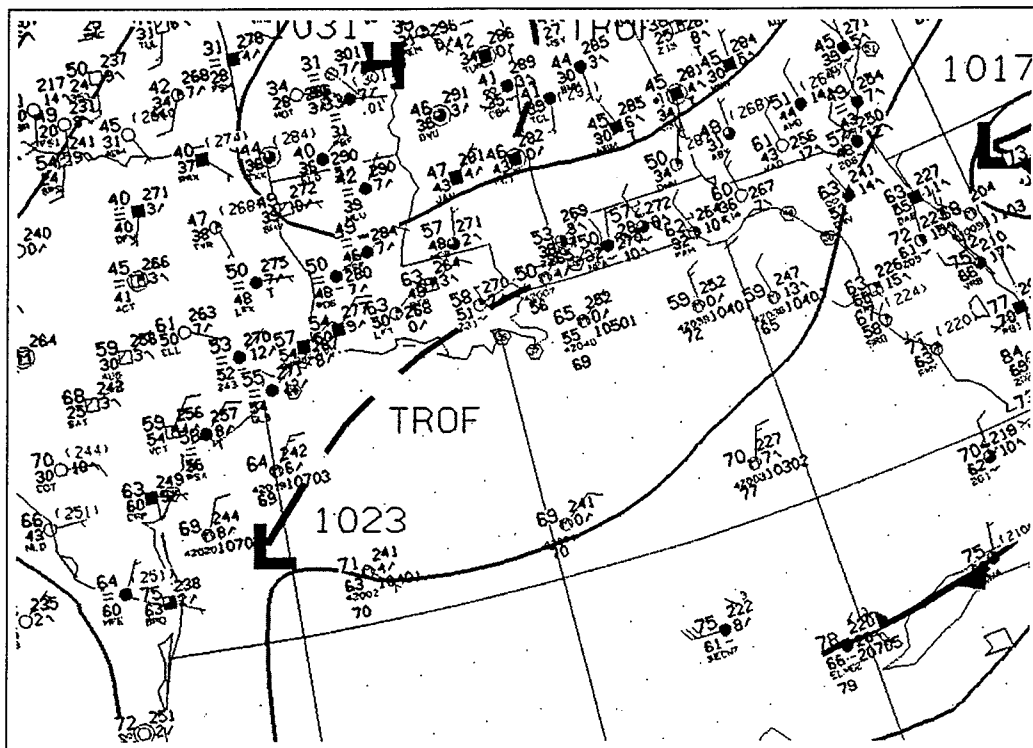
Figure 4.39. Surface analyses for 1800 UTC 21 January 1996.

stratification below. The surface analysis for 1800 UTC 21 January 1996 (Figure 4.39)

did indicate a trough of low pressure over the northwest Gulf. Had the analyst

recognized this feature on visible satellite imagery, however, its orientation might have

been drawn more accurately. Indeed, the trough should also have been extended well

south, paralleling the Mexican coast. Sea surface temperatures over the western Gulf

(Figure 4.40) were closer to isothermal than in the previous cases, but an SST gradient

could still be observed along the continental shelf.

The weak center of low pressure off the Texas coast was analyzed to have

formed at 1200 UTC 21 January 1996, to the north of a stationary front over the
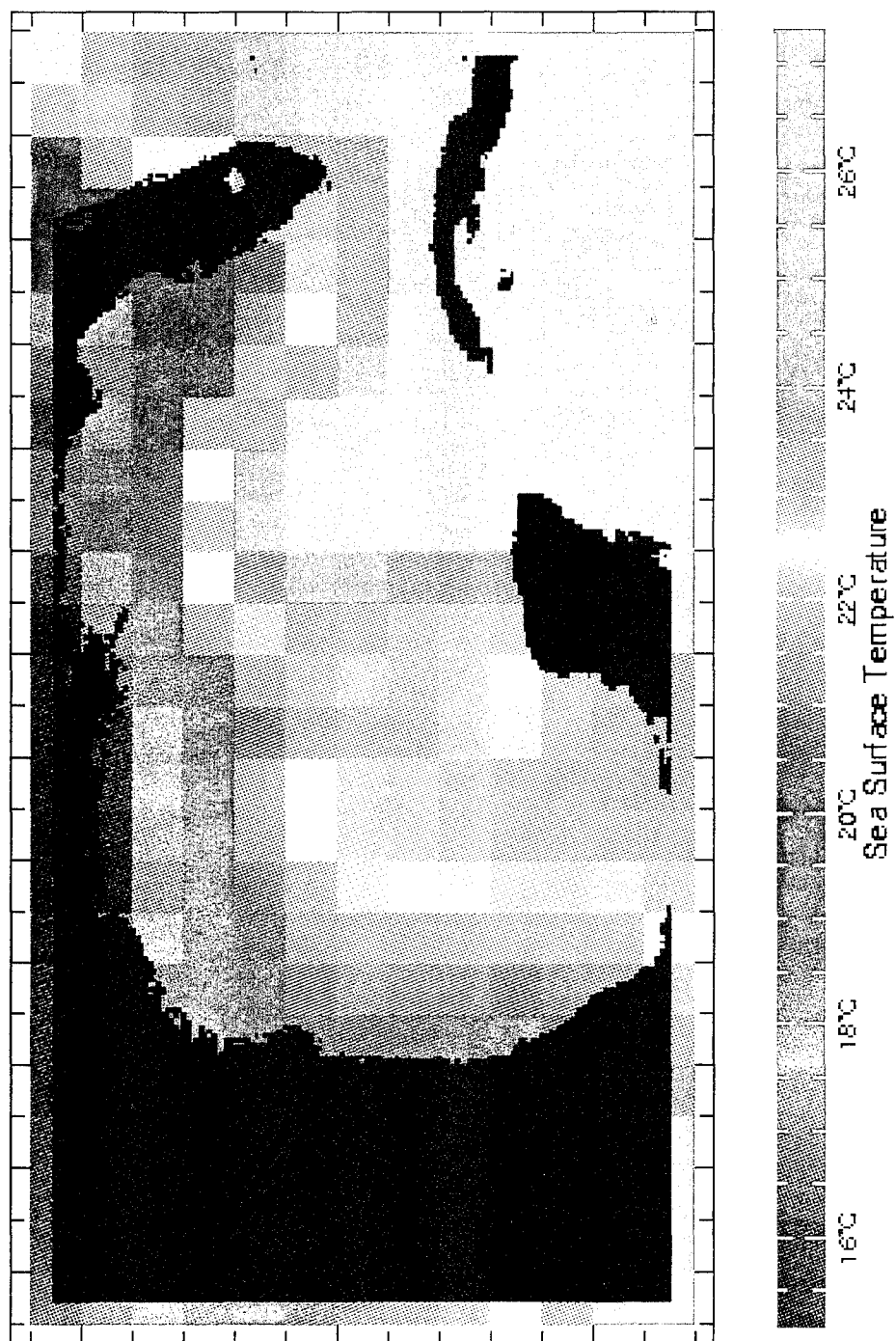
Figure 4.40. Same as Figure 4.24, except for the week of 17 January 1996.

southern Gulf and western Caribbean. This front had departed the Texas coast 66 hours earlier, on 1800 UTC 18 January 1996, with northwesterly winds in excess of 30 knots in its wake. Thus, the surface low was analyzed to form completely within the modified polar air to the north of this front, and as such, is an example of nonfrontal cyclogenesis. Although the synoptic-scale flow did not allow for further development of this cyclone (it was dropped from the analysis a mere 12 hours after its inception), its presence, along with that of the rope cloud, indicates that the low-level circulations which develop over the northwest Gulf and adjacent coastal region in the wake of a cold-air outbreak make this region an ideal one for the inception and subsequent development of winter extratropical cyclones.

Summary

The polar front has historically been an accepted mechanism for cyclogenesis over the northwest Gulf. Even Hsu (1992), who introduced the concept of the continental shelf break as a region of strong atmospheric baroclinicity, stated that "the orientation of the shelf break is a very important baroclinic characteristic because fronts tend to stall there rather than at the physical coastline." As mentioned earlier, he described "frontal overrunning" as occurring "when a polar front is nearly stationary along the central Gulf coast or over the northern Gulf of Mexico. Typically observed overrunning conditions are heavy cloud cover and precipitation." Indeed, the atmospheric baroclinicity near the shelf break is certainly important, but primarily

because of the *in situ* frontogenesis which can occur there. The case studies presented in this section show that the air-sea interactions which occur during the winter over the Gulf of Mexico's continental shelf result in the establishment of a low-level environment which is ideal for the development of extratropical cyclones. Therefore, the presence of the polar front has been determined not to be a necessary precondition for cyclogenesis in this region.

It has been proposed (Johnson et al. 1984; Lewis and Hsu 1992) that the combination of coastal shape (*not* bathymetry) and the SST pattern provides an opportunity for the establishment of a low-level mesoscale circulation as a result of differential heating due to horizontal variations in the length of the path air parcels leaving a curved coastline travel over a horizontally-varying SST distribution (Atlas et al. 1983). This premise is flawed, though, since during the coldest months -- when cyclogenesis frequency is greatest -- air flowing offshore behind a cold front is not significantly colder than the already cool shelf waters. In this scenario, the effect of differential diabatic warming would be relatively small until the air reaches the shelf break. It would therefore be necessary to consider the overwater path length with reference to the *shelf break*, and not the *physical coastline*. Incipient low pressure fields *do* form over the northwest Gulf following cold air outbreaks, but not with sea-level isobars that "tend to parallel the shape of the coast, with lower atmospheric pressure being further offshore" in the manner proposed by Atlas et al. (1983), and referenced by Johnson et al. (1984) and Lewis and Hsu (1992). As suggested by the

111

modeling experiment of Warner at al. (1990) and as shown in surface observations for the northwest Gulf, a local minimum in the sea-level pressure field and an area of cyclonic vorticity can develop along the shelf break after a cold air outbreak, simply due to spatial variations in the fluxes of latent and sensible heating. Thus, with regard to the air-sea interaction process, the shape and orientation of the coastline *during the coldest months* may be largely coincidental.

Earlier in the season, though, when cold fronts first migrate over the Gulf, the surface waters of the northwest Gulf are fairly isothermal. Thus, the relatively cold air which resides over this SST pattern after frontal passage may be *uniformly* modified by the warm waters beneath. In such cases, the shape of the coastline itself may be significant, since the Laplacian of diabatic warming due to sensible heat flux is maximized offshore, contributing to cyclonic vorticity and low-level height falls in accordance with the method discussed by Bosart (1984), and depicted in Figure 4.41.

The air-sea interaction processes of the northwest Gulf region may have significant implications with regard to the "return flow" conceptual model. Crisp and Lewis (1992) defined the offshore- and onshore-flow phases during a return flow event based on trends in the observed surface winds at each of three stations along the Texas-Louisiana Gulf coast (Brownsville, Texas; Victoria, Texas; and Lake Charles, Louisiana) during February-March. The offshore-flow phase begins when the first of these stations exhibits a component of flow toward the Gulf, while the onshore-flow phase commences when the first of the three stations exhibits a component of flow
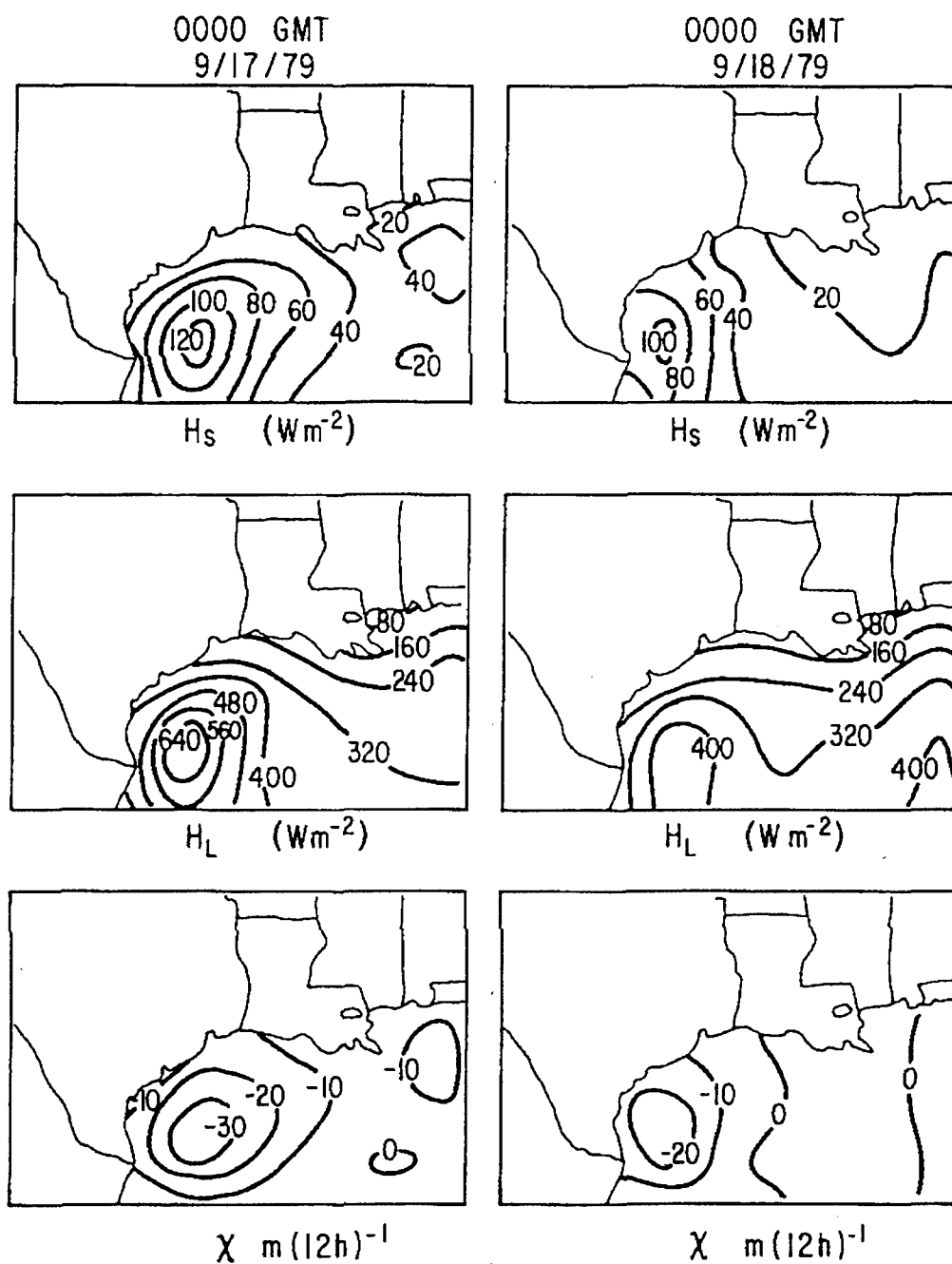
Figure 4.41. Sensible heat flux (top), latent heat flux (middle), and 1000-mb height tendency due to sensible heating (bottom) for 0000 UTC 17 September 1979 (left) and 0000 UTC 18 September 1979 (right). Units are watts meter^{-2} except meters (12 hour)$^{-1}$ for the 1000-mb height tendency (from Bosart 1984).

113
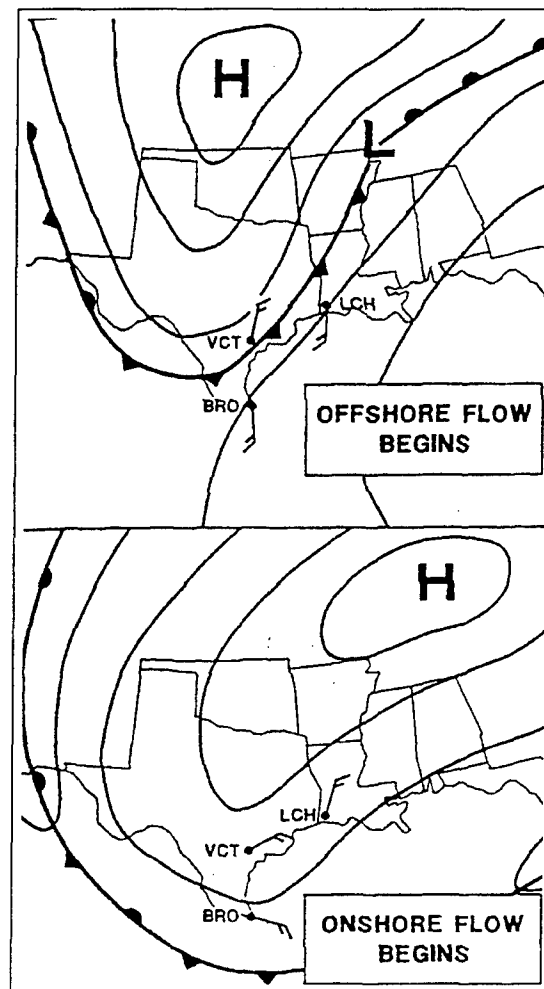
Figure 4.42. Typical synoptic patterns associated with the offshore- and onshore-flow phases of a return flow event. The upper-air stations used to determine the onset of each phase are shown: BRO (Brownsville, Texas), VCT (Victoria, Texas), and LCH (Lake Charles, Louisiana) (from Crisp and Lewis 1992).

toward land (see Figure 4.42). However, Case 1 indicates that the normal pattern

associated with return flow might be disrupted when cool, highly stable air resides over

the continental shelf. During such an event, the warm, moist, modified polar air which

is being steered toward the continent by the synoptic regime may be deflected slightly

eastward and forced to rise over the stable air covering the shelf waters. Although

114
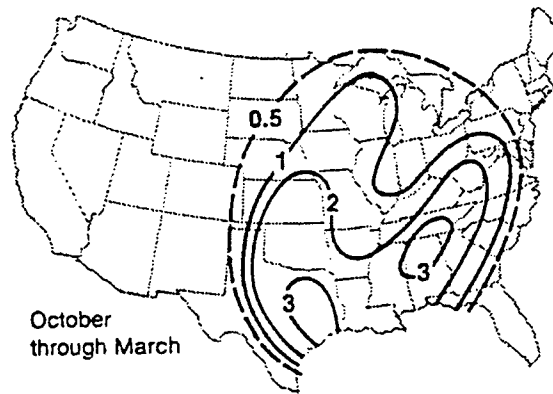
Figure 4.43. The number of elevated thunderstorms (reports/station) identified during October-March between September, 1978 and August, 1982 (from Colman 1990).

observations at coastal stations may indicate an *offshore* flow at the surface and a stable boundary layer, potential instability may be released in the return flow *aloft*, resulting in elevated convection. It is likely that the high frequency "bullet" of elevated convection near the Gulf coast during the winter months (Figure 4.43) extends to the shelf break, and is not principally a reflection of the "temperature contrast between the land and the water" (Colman 1990).

In addition to the air-sea interaction process, there are certainly other factors which need to be investigated for a more complete understanding of Gulf cyclogenesis. The orientation and shape of the coastline relative to the synoptic wind regime may locally enhance frontogenesis due to the effects of differential friction (Bosart 1984; Bosart et al. 1992). Orography, too, may play a role in cyclogenesis over the western Gulf, since the Sierra Madre Oriental are an extension of the Rocky Mountains along

115

Mexico's Gulf coast (Figure 4.44). The effects of orography may be directly related through lee cyclogenesis (Clark 1990; Pierrehumbert 1986), or indirectly through the southward displacement of polar air, which not only contributes to low-level baroclinicity (Bosart et al. 1992) and upslope flow, but also may further cool the shelf waters near the Mexican coast, enhancing the local SST gradient. Radiational cooling over the landmass, which was suggested as a primary contributor to the coastal frontogenesis in Case 2, may also be significant. Interestingly, the processes contributing to Gulf cyclogenesis are notably similar to those which create the Australian east coast cyclones, which form preferentially at night (Holland et al. 1987).
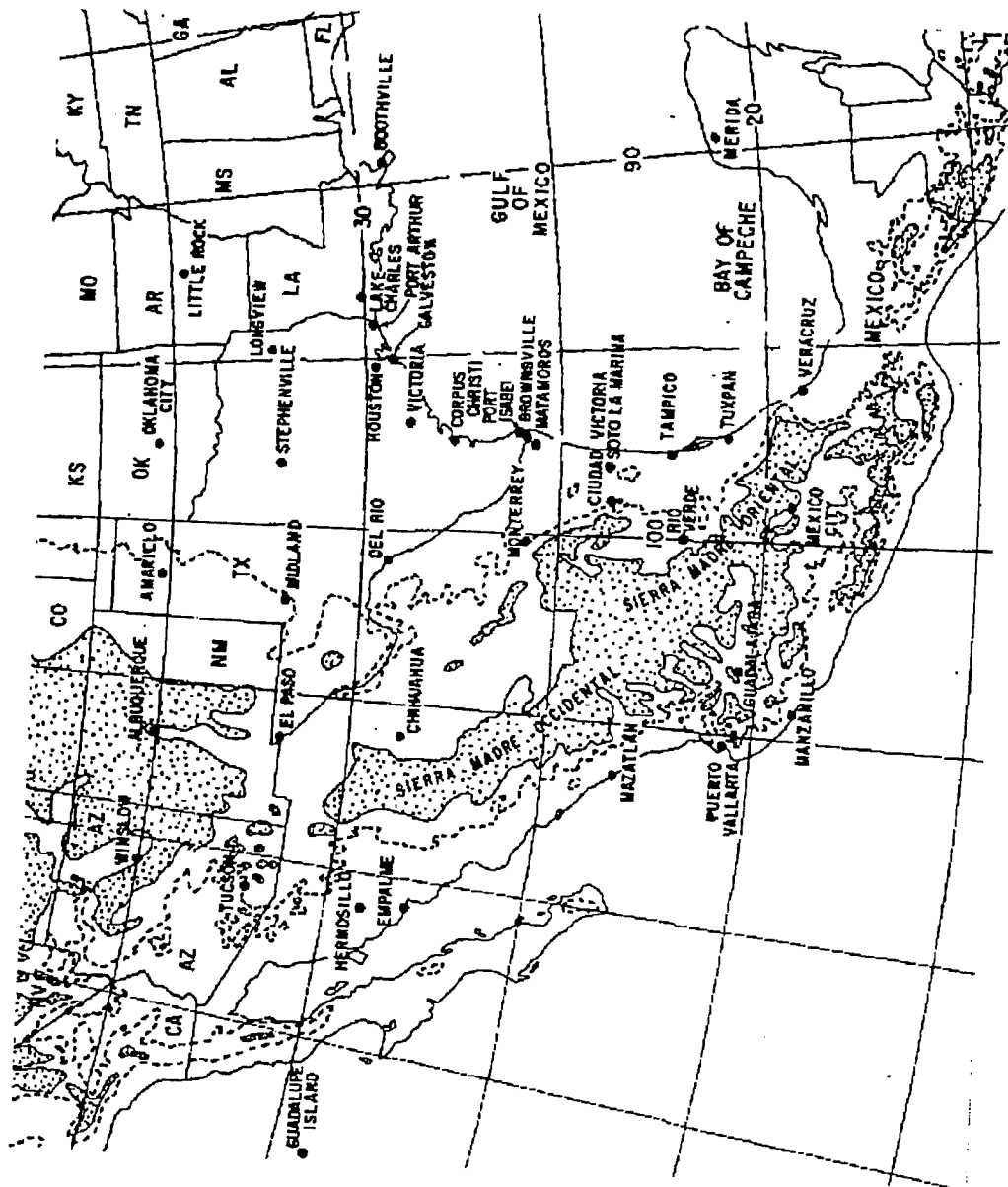
Figure 4.44. Station locator and simplified terrain map. Dashed contour indicates elevations greater than 900 meters, while elevations greater than 1800 meters are stippled (from Bosart et al. 1992).

117

CHAPTER 5

CONCLUSION

Summary

Winter extratropical cyclogenesis over the Gulf of Mexico has been examined by assigning a synoptic classification to each cyclone which developed during the 41-season period 1950-51 to 1990-91. The classifications of "frontal" and "nonfrontal" cyclogenesis were used to differentiate between those cyclones which were analyzed to have formed along pre-existing, airmass-type frontal boundaries, and those which developed in the absence of such boundaries. Since the frontal and the nonfrontal events showed similar distributions among various upper-level patterns, it is felt that the real distinction between these two types of cyclone development lies in the characteristics of the lower atmosphere during cyclogenesis.

Spatial distributions of cyclogenesis events indicated that the open water of the northwest Gulf tends to be a preferred region for cyclone initiation, for both the frontal and the nonfrontal cases. This is particularly evident during the coldest months, when sea surface temperatures exhibit a strong gradient along the continental shelf break.

Through the process of airmass modification, a continental air mass which

118

resides over the strong SST gradients of the northwest Gulf develops an internal solenoidal circulation, resulting in a local increase of convergence and cyclonic vorticity within the boundary layer. A strong horizontal gradient in atmospheric stability is also found to develop in the vicinity of the continental shelf break. Surface charts have indicated the presence of such a circulation through the repeated analysis of a trough of low pressure offshore, and approximately parallel to, the Texas/Louisiana coast. The ultimate location and orientation of the feature, however, is believed to be sensitive to the large-scale flow.

A mesoscale convergence line may be observed on visible satellite imagery due to its frequent association with a rope cloud or a stronger line of convection. Since there is a lack of surface data sources in the Gulf, it is suggested that satellite imagery may be a useful supplement to other data for the analysis of this feature.

Gulf Cyclogenesis: The Frontal Case

It was suggested in Chapter 3 that the interseasonal variability in the spatial distributions of frontal cyclogenesis is related to the frequency with which cold fronts penetrate the Gulf, since atmospheric fronts provide low-level environments which are suitable for cyclone development. Consequently, the relatively high frequency of frontal *passage* over the northwest Gulf during the winter months provides a sufficient explanation for the observed high frequency of frontal *cyclogenesis* over the region. In other words, the northwest Gulf *could* be a preferred region for frontal cyclogenesis

119

even without the existence of the continental shelf break and associated SST gradient. This premise, however, is believed to be flawed.

During the coldest months, a cold front initially penetrating the Gulf may collide with a cool, stable layer of air over the shelf waters (recall, e.g., Figure 4.28), resulting in little or no convection or enhancement of cyclogenesis. When the front reaches the shelf break, however, it collides with air that has relatively low static stability, so that resistance to ascent is minimized, free convection is more likely to occur, and surface cyclogenesis is common. Observations have shown that low static stability exists over the entire length of the continental shelf break, where average monthly air-sea temperature differences are maximized (Lewis and Hsu 1992). Thus, the atmospheric instability which exists near the shelf break, even over the northeast Gulf, may make a very real contribution to the high frequency of frontal cyclogenesis in that region.

Errors in analysis may have also contributed to the observed high frequency of frontal cyclogenesis near the shelf break. It was found in the author's study that fronts which became stationary over the northern half of the Gulf (rather than migrating to the Caribbean) tended with time to assume an orientation along the shelf break. This transition was frequently observed to occur between two consecutive analyses, and is therefore termed "frontal jumping." Although it is likely that in reality, the initial front underwent dissolution while frontogenesis occurred near the shelf break, the lack of data offshore (or the introduction of a new analyst) contributed to the surface chart's misleading indication of a migrating front. If cyclogenesis were to have occurred

along this front, the author was forced (by the constraints of his own definition) to include it in the "frontal" category, though the development *process* was more likely "nonfrontal" in nature. Consider, for example, the author's chosen example of frontal cyclogenesis (Figure 3.19). Prior to the analysis of the surface low southeast of the Texas coast at 1800 UTC 21 December 1995, there was clearly *in situ* frontogenesis along the Texas coast, along with "overrunning" precipitation. The northwestward extension of the quasi-stationary polar front is not apparent from the available data, and may have been an attempt to depict the surface low as a frontal wave with weather. Despite the potentially strong influence of the SST gradient at this time on cyclogenesis, this cyclone falls into the "frontal" category.

Inadequate surface analysis was probably the primary reason why Saucier (1949) felt that the polar front played such a critical role in the development of Gulf cyclones. His chosen example of Group 3 cyclogenesis (Figure 5.1) demonstrates how frontal "jumping" can lead to a misinterpretation of the processes contributing to cyclone formation in this region. Note, for example, the northwesterly flow along the south Texas coast at 0630 UTC 19 December 1946. This strongly ageostrophic flow of cold air does not support the analysis of a dissolving cold front just to the southeast. In addition, the observed wind field does not support the conceptual model of return flow (see Figure 4.41). This model would depict the wind over south Texas to have either an onshore component or to be parallel to the coast out of the northeast, given the synoptic regime. Rather, the surface wind at Brownsville is indicative of low pressure
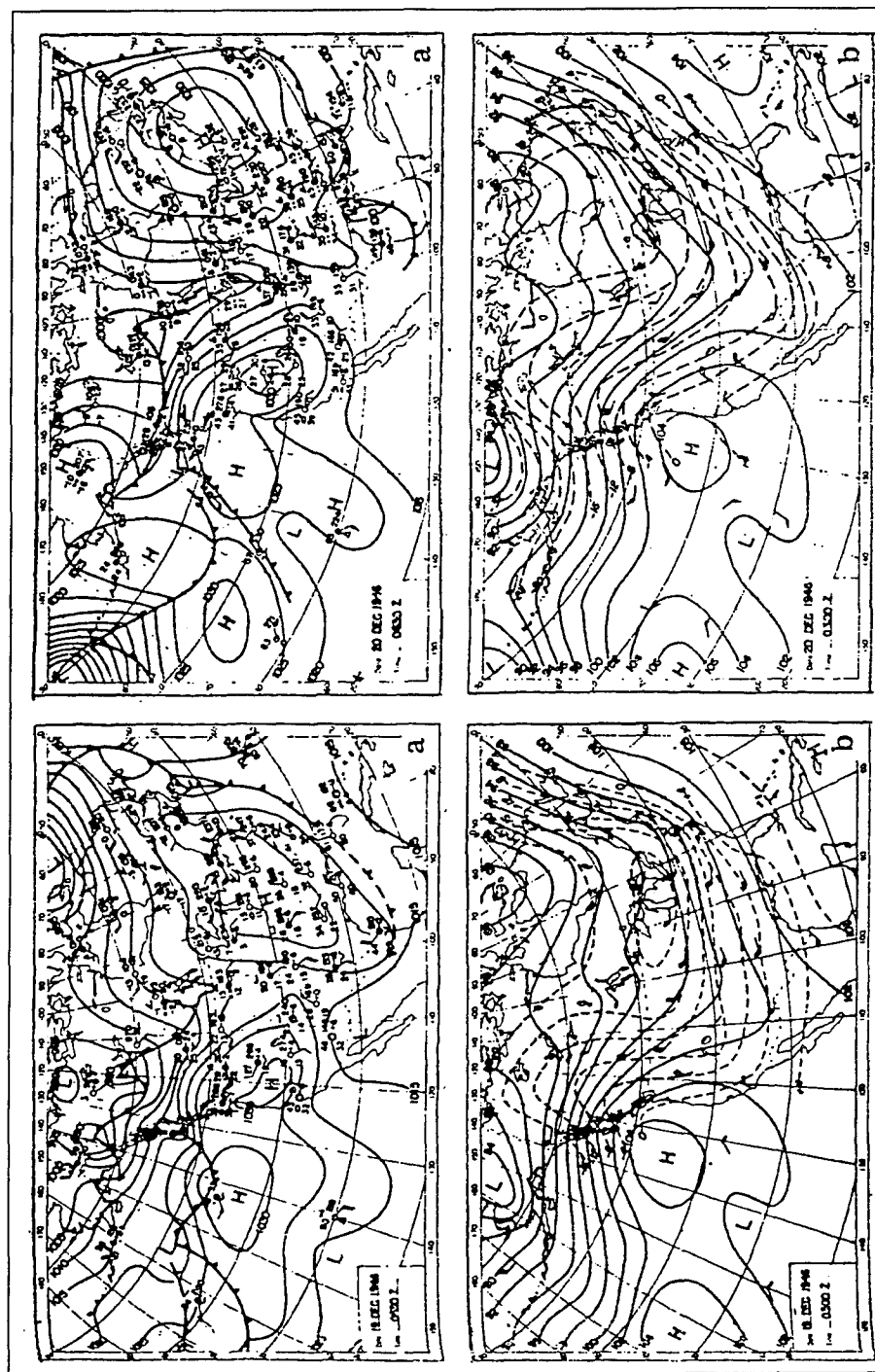
Figure 5.1. Sequences in the development of a typical Group 3 cyclone. Sea level weather maps for 0630 UTC (a) and 700-mb charts for 0300 UTC (b), on 19 December 1946 (bottom) and 20 December 1946 (top). On the surface charts, solid lines are pressure contours. On the 700-mb charts, solid lines are height contours (labeled in hundreds of feet), and dashed lines are isotherms (Celsius) (from Saucier 1949).

developing just offshore, well to the north of the actual surface location of the quasi-stationary polar front.

Saucier stated that Group 3 cyclones, which were most representative of the sequences of Gulf cyclogenesis, had a preferred region of development over the coastal waters of the northwest Gulf -- a premise which has been verified in this author's work. He suggested that Group 3 cyclones formed most frequently during the coldest months, following a cold air outbreak and subsequent "dissolution" and "reactivation" of the polar front. Henry (1979), though, showed that *it is precisely during the coldest months when the polar front is least likely to become stalled over the northern Gulf.* This verified the earlier work of DiMego et al. (1976). Indeed, Saucier's conceptual model of Gulf cyclogenesis was based in part on the flawed premise that "the frequency with which the polar front is in the vicinity of the north Gulf coast and the natural land-water temperature contrast in winter make the coast a semi-permanent low-level frontal zone." It was thus necessary to review the processes which lead to the development of Gulf cyclones, placing an emphasis on the low-level preconditions for cyclogenesis, and in particular, the air-sea interaction process.

Gulf Cyclogenesis: The Nonfrontal Case

Clearly, the nonfrontal cyclones developed, at least in part, due to the strong low-level atmospheric baroclinicity which exists over the northwest Gulf during the winter months. The mesoscale convergence lines (i.e., pressure troughs, shelf break

123

fronts, coastal fronts) which are frequently observed over the northwest Gulf are reflections of the thermal contrast which characterizes the region, and of the boundary layer circulations which are forced by the "turbulent transport of heat originating from the sea surface" (Mailhot 1992). The northwest Gulf does represent a "semi-permanent low-level frontal zone" (Saucier 1949) during the winter months, but it is neither the stalling nor the reactivation of the polar front which contributes to this enhanced baroclinicity. Pre-existing *in situ* diabatic warming, surface convergence, and cyclonic vorticity on the mesoscale make this region a preferential location for cyclone intensification, provided that the upper-level pattern is also favorable. According to Carlson (1991),

> That cyclogenesis tends to favor certain geographical locations is due to the tremendous inhomogeneity of lower-tropospheric baroclinicity and static stability...Cyclogenesis does not occur continuously following the movement of a seemingly potent 500 mb trough but occurs preferentially in certain locations. This suggests that there are regions where the atmosphere is much more efficient in allowing 500 mb absolute vorticity and 1000-500 mb thickness advections to be realized as stronger vertical motions and surface pressure tendencies.

The case studies presented in chapter 4 clearly indicate that the northwest Gulf of Mexico is such a region.

As previously mentioned, atmospheric stability is low, though, along the entire length of the continental shelf break during the winter months, with instability values over the northeast Gulf which actually exceed those over the northwest Gulf due to the strong thermal contrast between cool shelf waters and the Loop Current (and its eddies) (Lewis and Hsu 1992). Lewis and Hsu found the observation of low stability over the northeast Gulf to be "quite unexpected, since no trend in wintertime storm

124

```
                              │
                              ▼
                  CYCLONIC GEOSTROPHIC VORTICITY
                        IN FRICTION LAYER
                              │
                              ▼
                      EKMAN PUMPING
                              │
                              ▼
              ┌──►  CUMULUS CONVECTION
              │               │
              │               ▼
              │       LATENT HEAT RELEASE
              │               │
              │               ▼
              └──────  MORE RISING MOTION
                              │
                              ▼
                  MORE LOW-LEVEL CONVERGENCE
```
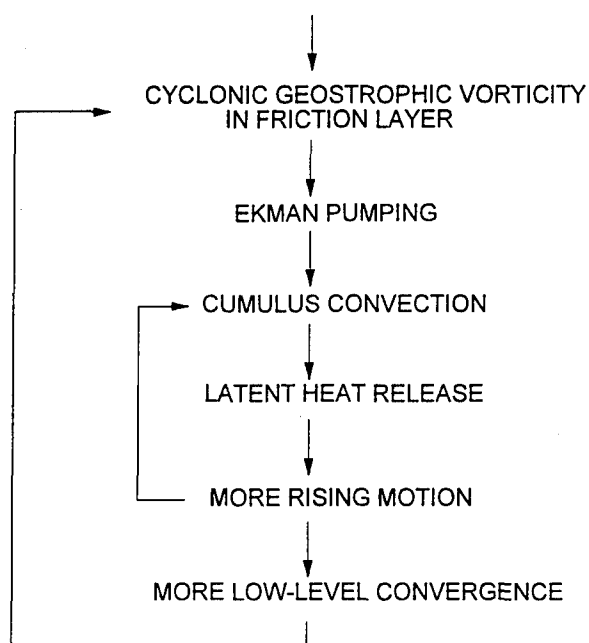
Figure 5.2. Schematic diagram of conditional instability of the second kind (from Bluestein 1993, pp. 16-19).

development has ever been established for that region." Indeed, although the present

study has indicated a fairly high frequency of *frontal* cyclogenesis in this region,

nonfrontal cyclogenesis was seldom observed over the northeast Gulf.

Lewis and Hsu attempt to resolve this difficulty by suggesting that "the spatially

limited and more linear character of the shelf break likely limits the effect of any strong

shelf break free convection on enhancing cyclogenesis." This author disagrees, noting

that strong shelf break convection has indeed been observed to be associated with

surface cyclogenesis (see, e.g., Bosart 1981; Bosart et al. 1992). Although the

relationship between convection and cyclogenesis along the shelf break may pose a

classic chicken-and-egg argument, the process is best described by "conditional

125

instability of the second kind," which suggests that convection and cyclogenesis are mutually-amplifying processes (see Figure 5.2).

The lack of nonfrontal cyclogenesis cases over the northeast Gulf, and even the observed tendency for established cyclones not to undergo deepening in that region (Businger 1990; Colucci 1976), can be explained within the quasi-geostrophic framework. When the shelf break front develops off the Texas coast, it does so with warm air (higher thicknesses) to its south and east, and cold air (lower thicknesses) to its north and west. If an eastward-propagating upper-tropospheric disturbance migrates over this region, cyclonic vorticity advection ahead of the disturbance induces ascent both over the surface disturbance, and to the east, where there is already low-level warm air advection (and low static stability). Anticyclonic vorticity advection induces descent to the west, where there is already cold air advection (and high static stability). This configuration results in the conversion of potential energy to kinetic energy, and the surface low deepens, and begins to migrate. Thus, the westward tilt with height of the entire system is a *necessary condition* for surface development to continue.

It has been observed by the author that the phase lag between the upper and lower disturbances must be present for a relatively long amount of time before nonfrontal cyclones show significant development. Although the lowest levels of the atmosphere may have become "ripened" for cyclogenesis through airmass modification, upper-level disturbances which migrate quickly over the near-stationary surface baroclinic zone often fail to deepen the surface low, despite their dynamical

126

vigor.

The continental shelf break of the *northeast* Gulf, though, separates cool shelf waters to its *east* from warm deep waters, and the Loop Current, to its *west*. After sufficient airmass modification in the boundary layer, eastward moving upper-tropospheric disturbances which migrate over this region attempt to induce ascent in the cool, stable air to the east, and descent in the warm, unstable air to the west. In this configuration, the dynamic and thermodynamic forcings of vertical motion act to negate the effects of each other, and cyclogenesis is inhibited.

The paradox of the "nonfrontal" classification is that many (if not all) of the nonfrontal cyclones may, in fact, have developed along pre-existing (though not analyzed) atmospheric frontal boundaries! The *processes* which contribute to baroclinicity and the generation of cyclonic vorticity along the shelf break are indeed very real and do often result in the initiation of surface cyclones. The *classification* of "nonfrontal cyclogenesis," however, and the historical misinterpretation of Gulf cyclogenesis from Saucier's time to the present day may merely be a result of poor analyses due to inadequate data. These data are capable of resolving the surface pressure patterns and low-level circulations associated with a developing cyclone, but are insufficient in the detection of subsynoptic convergence and thermal contrast. Indeed, a data set which has a higher spatial resolution than that which is currently available would be invaluable to understanding the complex processes which contribute to winter extratropical cyclogenesis over the Gulf of Mexico.

SELECTED BIBLIOGRAPHY

Adamec, D., and R. L. Elsberry, 1985: Response of an intense oceanic current to cross-stream cooling events. *J. Phys. Oceanogr.*, **15**, 273-287.

Atlas, D., W. P. Byerly, and S. H. Chou, 1983: The influence of coastal shape on winter mesoscale air-sea interaction. *Mon. Wea. Rev.*, **111**, 245-252.

Bane, J. M. and K. E. Osgood, 1989: Wintertime air-sea interaction processes across the Gulf Stream. *J. Geophys. Res.*, **94**, 755-772.

Benjamin, S. G., K. J. Brundage, and L. L. Morone, 1994: Implementation of the Rapid Update Cycle Part I: Analysis/Model Description. NOAA/NWS Tech. Proc. Bulletin Draft-16 June, 18 pp.

Bennetts, D. A., J. R. Grant, and E. McCallum, 1988: An introductory review of fronts. Part I: Theory and observations. *Meteor. Mag.*, **117**, 357-370.

_____, _____, and _____, 1988: An introductory review of fronts. Part II: A case-study. *Meteor. Mag.*, **117**, 370-374.

Bleck, R., 1990: Depiction of Upper/lower vortex interaction associated with extratropical cyclogenesis. *Mon. Wea. Rev.*, **118**, 573-585.

Bluestein, H., 1993: *Synoptic-Dynamic Meteorology in Midlatitudes, Vol. II.* New York: Oxford University Press.

Bosart, L. F., 1981: The Presidents' Day Snowstorm of 18-19 February 1979: A subsynoptic-scale event. *Mon. Wea. Rev.*, **108**, 1542-1566.

_____, 1984: The Texas coastal rainstorm of 17-21 September 1979: An example of synoptic-mesoscale interaction. *Mon. Wea. Rev.*, **112**, 1108-1133.

_____, 1994: Observed cyclone life cycles. *The Life Cycles of Extratropical Cyclones, Vol. 3*, S. Gronas and M. A. Shapiro, Eds., Bergen-Norway, 111-148.

_____, C. J. Vaudo, and J. H. Helsdon Jr., 1972: Coastal frontogenesis. *J. Appl. Meteor.*, **11**, 1236-1258.

_____, C. Lai, and R. Weisman, 1992: A case study of heavy rainfall associated with weak cyclogenesis in the northwest Gulf of Mexico. *Mon. Wea. Rev.*, **120**, 2469-2500.

_____, M. A. Bedrick, W. E. Bracken, M. J. Dickinson, G. H. Hakim, D. M. Schultz, and K. Tyle, 1994: Large-scale antecedent conditions associated with the 12-14 March 1993 cyclone ("Superstorm '93") over eastern North America. *Preprints, 14th Conf. on Weather Analysis and Forecasting*, Dallas, TX, Amer. Meteor. Soc., 7-12.

Burk, S. D., and W. T. Thompson, 1992: Airmass transformation over the Gulf of Mexico: Mesoscale model and airmass transformation model forecasts. *J. Appl. Meteor.*, **31**, 925-937.

Businger, S., D. I. Knapp, and G. F. Watson, 1990: Storm following climatology of precipitation associated with winter cyclones originating over the Gulf of Mexico. *Wea. Forecasting*, **5**, 378-403.

Carlson, T. N., 1991: *Mid-latitude Weather Systems*. New York: Harper Collins.

Chou, S. H., and D. Atlas, 1982: Satellite estimates of ocean-air heat fluxes during cold air outbreaks. *Mon. Wea. Rev.*, **110**, 1434-1450.

Cione, J.J., and S. Raman, 1994: A three dimensional investigation of surface-induced coastal cyclogenesis near the Gulf Stream. *The Life Cycles of Extratropical Cyclones, Vol. 3*, S. Gronas and M. A. Shapiro, Eds., Bergen-Norway, 52-56.

_____, S. Raman, and L. J. Pietrafesa, 1993: The effect of Gulf Stream-induced baroclinicity on U.S. east coast winter cyclones. *Mon. Wea. Rev.*, **121**, 421-430.

Clark, D. A., 1983: A comparative study of coastal frontogenesis. M. S. Thesis, Massachusetts Institute of Technology, Cambridge, MA, 86 pp.

Clark, J. H. E., 1990: An observational and theoretical study of Colorado lee cyclogenesis. *J. Atmos. Sci.*, **47**, 1541-1561.

Colman, B. R., 1990: Thunderstorms above frontal surfaces in environments without positive CAPE. Part I: A climatology. *Mon. Wea. Rev.*, **118**, 1103-1121.

Colucci, S. J., 1976: Winter cyclone frequencies over the eastern United States and adjacent western Atlantic. *Bull. Amer. Meteor. Soc.*, **57**, 548-553.

Crisp, C. A., and J. M. Lewis, 1992: Return flow in the Gulf of Mexico. Part I: A classificatory approach with a global historical perspective. *J. Appl. Meteor.*, **31**, 868-881.

Daily Weather Maps, Weekly Series, 1968-1991: NOAA, U.S. Government Printing Office.

Davis, C. A., and K. Emmanuel, 1988: Observational evidence for the influence of surface heat fluxes on rapid maritime cyclogenesis. *Mon. Wea. Rev.*, **116**, 2649-2659.

_____, and _____, 1991: Potential vorticity diagnostics of cyclogenesis. *Mon. Wea. Rev.*, **119**, 1929-1953.

Davis, R. E., R. Dolan, and G. Demme, 1993: Synoptic Climatology of Atlantic coast north-easters. *Int. J. Climatol.*, **13**, 171-189.

Dickinson, M. J., M. A. Bedrick, L. F., Bosart, W. E. Bracken, G. H. Hakim, D. M. Schultz, and K. Tyle, 1994: Superstorm '93: Synoptic scale precursors and NMC model performance. *Preprints, 14th Conf. on Weather Analysis and Forecasting*, Dallas, TX, Amer. Meteor. Soc., 13-15.

DiMego, G. J., L. F. Bosart, and G. W. Endersen, 1976: An examination of the frequency and mean conditions surrounding frontal incursions into the Gulf of Mexico and Caribbean Sea. *Mon. Wea. Rev.*, **104**, 2305-2324.

Dirks, R. A., J. P. Kuettner, and J. A. Moore, 1988: Genesis of Atlantic Lows Experiment (GALE) -- An overview. *Bull. Amer. Meteor. Soc.*, **69**, 148-160.

Draper, N.R., and H. Smith, 1981: *Applied Regression Analysis, 2nd ed.* New York: John Wiley.

Elsberry, R. L., and P. J. Kirchoffer, 1988: Upper-level forcing of explosive cyclogenesis over the ocean based on operationally analyzed fields. *Wea. Forecasting*, **3**, 205-216.

Emmanuel, K. A., 1984: Fronts and frontogenesis: The quasi-geostrophic model. *Dynamics of Mesoscale Weather Systems*, J. B. Klemp, Ed., NCAR Summer Colloquium Notes, 29-39.[Available from NCAR, P.O. Box 3000, Boulder, CO 80307.]

_____, 1994: Sea-air heat transfer effects on extratropical cyclones. *The Life Cycles of Extratropical Cyclones, Vol. 3*, S. Gronas and M. A. Shapiro, Eds., Bergen-Norway, 67-72.

Franceschini, G. A., 1976: A protraiture of the horizontal fluxes of dry and moist static energy around the Gulf of Mexico. *Role of the Gulf of Mexico in the Weather of the United States, a Conference on Meteorology over and Near the Gulf.* Center for Applied Geosciences, Texas A&M University, College Station, TX, pp. 17-24.

Griffiths, J. F., 1976: Climate and the Gulf of Mexico. *Role of the Gulf of Mexico in the Weather of the United States, a Conference on Meteorology over and Near the Gulf.* Center for Applied Geosciences, Texas A&M University, College Station, TX, pp. 1-15.

Grossman, R. L., and A. K. Betts, 1990: Air-sea interaction during an extreme cold air outbreak from the eastern coast of the United States. *Mon. Wea. Rev.*, **104**, 324-332.

Gulev, S. and J. Tonkacheev, 1994: On the interaction of rapidly intensifying cyclones with SST front in the north-west Atlantic. *The Life Cycles of Extratropical Cyclones, Vol. 3*, S. Gronas and M. A. Shapiro, Eds., Bergen-Norway, 96-99.

Gurka, J. J., E. P. Auciello, A. F. Gigi, J. S. Waldstreicher, K. K. Keeter, S. Businger, and L. G. Lee, 1995: Winter weather forecasting throughout the eastern United States. Part II: An operational perspective of cyclogenesis. *Wea. Forecasting.*, **10**, 21-41.

Heckman, B. E., and A. H. Thompson, 1978: Extratropical cyclogenesis over the Gulf of Mexico. *Preprints, Conference on Weather Forecasting and Analysis and Aviation Meteorology*, Silver Spring, MD, Amer. Meteor. Soc., Boston, 118-124.

Henry, W. K., 1979a: An arbitrary method of separating tropical air from "return flow" polar air. *Natl. Wea. Digest*, **4**, 22-26.

_____, 1979b: Some aspects of the fate of cold fronts in the Gulf of Mexico. *Mon. Wea. Rev.*, **107**, 1078-1082.

_____, and A. H. Thompson, 1976: An example of polar air modification over the Gulf of Mexico. *Mon. Wea. Rev.*, **104**, 1324-1327.

Hirschberg, P. A., and J. M. Fritsch, 1991: Tropopause undulations and the development of extratropical cyclones. Part I: Overview and observations from a cyclone event. *Mon. Wea. Rev.*, **119**, 496-517.

130

_____, and _____, 1991: Tropopause undulations and the development of extratropical cyclones. Part II: Diagnostic analysis and conceptual model. *Mon. Wea. Rev.*, **119**, 518-550.

_____, M. C. Parke, C. H. Wash, E. Thaler, and R. W. Spencer, 1994: The utilization of satellite-based observations of tropopause-level thermal anomalies in the nowcasting and forecating of extratropical cyclones. *Preprints, 14th Conf. on Weather Analysis and Forecasting*, Dallas, TX, Amer. Meteor. Soc., 317-322.

Holiway, C. E., and D. R. Smith, 1994: The role of tropopause undulation in the development of the "blizzard of '93" (12-15 March 1993). *Preprints, 14th Conf. on Weather Analysis and Forecasting*, Dallas, TX, Amer. Meteor. Soc., 80-84.

Holland, G. J., A. H. Lynch, and L. M. Leslie, 1987: Australian East-Coast cyclones. Part I: Synoptic overview and case study. *Mon. Wea. Rev.*, **115**, 3024-3036.

Hoskins, B. J., and M. S. Pedder, 1980: The diagnosis of middle-latitude synoptic development. *Quart. J. Roy. Meteor. Soc.*, **106**, 707-719.

Hosler, C. L., and L. A. Gamage, 1956: Cyclone frequencies in the United States for the period 1905 to 1954. *Mon. Wea. Rev.*, **84**, 388-390.

Houze, R. A. Jr., 1993: *Cloud Dynamics*. San Diego: Academic Press.

Hsu, S. A., 1970: Coastal air-circulation system: Observations and empirical model. *Mon. Wea. Rev.*, **98**, 487-509.

_____, 1988: *Coastal Meteorology*. San Diego: Academic Press.

_____, 1991: Effects of surface baroclinicity on frontal overrunning along the central Gulf coast. *J. Appl. Meteor.*, **31**, 900-907.

_____, 1993: The Gulf of Mexico -- A breeding ground for winter storms. *Mar. Wea. Log*, Spr., 1993, 4-11.

Huang, C. Y., and S. Raman, 1992: A three-dimensional numerical investigation of a Carolina coastal front and the Gulf Stream rainband. *J. Atmos. Sci.*, **49**, 560-584.

Huh, O. K., W. J. Wiseman, Jr., and L. J. Rouse, Jr., 1978: Winter cycle of sea surface thermal patterns, northeastern Gulf of Mexico. *J. Geophys. Res.*, **83**, 4523-4529.

Janish, P. R., and S. W. Lyons, 1992: NGM performance during cold-air outbreaks and periods of return flow over the Gulf of Mexico with an emphasis on moisture field evolution. *J. Appl. Meteor.*, **31**, 995-1017.

Johnson, G. A., E. A. Meindl, E. B. Mortimer, and S. J. Lynch, 1984: Features associated with repeated strong cyclogenesis in the western Gulf of Mexico during the winter of 1982-1983. *3rd Conf. on Meteorology of the Coastal Zone*, pp. 110-117.

Johnson, J. R., 1976: The origin, structure, and modification of return flow over the Gulf of Mexico. M. S. thesis, Department of Meteorology, Texas A&M Univ., 61 pp.

Karnavas, G. R., 1978: On polar air modification over the Gulf of Mexico during periods of return flow and development of low clouds. M. S. thesis, Department of Meteorology, Texas A&M Univ., 69 pp.

Keshishian, L. G., and L. F. Bosart, 1987: A case of extended east coast frontogenesis. *Mon. Wea. Rev.,* **115**, 100-117.

Keyser, D., 1986: Atmospheric Fronts: An operational perspective. *Mesoscale Meteorology and Forecasting,* P. S. Ray, Ed., Amer. Meteor. Soc., 216-258.

_____, and L. W. Uccellini, 1987: Regional models: emerging research tools for synoptic meteorologists. *Bull. Amer. Meteor. Soc.,* **68**, 306-320.

Klein, W. H., 1957: Principal tracks and mean frequencies of cyclones and anticyclones in the Northern Hemisphere. Res. Paper No. 40., U.S. Dept. of Commerce., Wea. Bur., Washington, 60 pp.

Kocin, P. J., D. A. Olson, A. C. Wick, and R. D. Harner, 1991: Surface weather analysis at the national meteorological center: Current procedures and future plans. *Wea. Forecasting,* **6**, 289-298.

Kuo, Y., R. Reed, and S. Low-Nam, 1991: Effects of surface energy fluxes in the early development and rapid intensification stages of seven explosive cyclones in the western Atlantic. *Mon. Wea. Rev.,* **119**, 457-476.

Lange, O., R. Fett, R. Landis, G. Wells, G. Rasch, E. Auciello, M. Horita, and J. Jannuzzi, 1986: Summary of a workshop/seminar on oceanic storms 9-13 September 1985, Seattle Washington. *Bull. Amer. Meteor. Soc.,* **67**, 1272-1277.

Lewis, J. K., 1992: The physics of the Gulf of Mexico. *J. Geophys. Res.,* **97**, 2141-2142.

_____, and S. A. Hsu, 1992: Mesoscale air-sea interactions related to tropical and extratropical storms in the Gulf of Mexico. *J. Geophys. Res.,* **97**, 2215-2228.

Lewis, J. M., and C. A. Crisp, 1992: Return flow in the Gulf of Mexico. Part II: Variability in return-flow thermodynamics inferred from trajectories over the Gulf. *J. Appl. Meteor.,* **31**, 882-898.

_____, C. M. Hayden, R. T. Merrill, and J. M. Schneider, 1989: GUFMEX: A study of return flow in the Gulf of Mexico. *Bull. Amer. Meteor. Soc.,* **70**, 24-29.

Liu, Q., J. M. Lewis, and J. M. Schneider, 1992: A study of cold-air modification over the Gulf of Mexico using in situ data and mixed-layer modeling. *J. Appl. Meteor.,* **31**, 909-924.

Maglaras, G. J., J. S. Waldstreicher, P. J. Kocin, A. F. Gigi, and R. A. Marine, 1995: Winter weather forecasting throughout the eastern United States. Part I: An overview. *Wea. Forecasting,* **10**, 5-20.

Mailhot, J., 1992: Numerical simulation of airmass transformation over the Gulf of Mexico. *J. Appl. Meteor.,* **31**, 946-963.

Manobianco, J., 1989: Explosive east coast cyclogenesis over the west-central North Atlantic Ocean: A composite study derived from ECMWF operational analyses. *Mon. Wea. Rev.,* **117**, 2365-2583.

132

Mansfield, D., 1994: The use of potential vorticity in forecasting cyclones: Operational aspects. *The Life Cycles of Extratropical Cyclones, Vol. 3*, S. Gronas and M. A. Shapiro, Eds., Bergen-Norway, 326-331.

Mariners Weather Log, 1960-1983: NOAA/NESDIS, U.S. Department of Commerce.

Mass, C. F., 1991: Synoptic frontal analysis: Time for a reassessment? *Bull. Amer. Meteor. Soc.*, **72**, 348-363.

Mather, J. R., H. Adams, and G. A. Yoshikoa, 1964: Coastal storms of the eastern United States. *J. Appl. Meteor.*, **3**, 693-706.

McGraw-Hill Encyclopedia of Ocean and Atmospheric Sciences, 1980 ed. New York: Mc-Graw-Hill.

Merrill, R. T., 1987: Equilibrium dewpoint temperature over the Gulf of Mexico in March. Technical paper presented at GUFMEX planning meeting, National Severe Storms Laboratory, Norman, OK, 4 pp.

_____, 1992: Synoptic analysis of the GUFMEX Return-Flow Event of 10-12 March 1988. *J. Appl. Meteor.*, **31**, 849-867.

Miller, J. E., 1946: Cyclogenesis in the Atlantic coastal region of the United States. *J. Meteor.*, **3**, 31-44.

Molinari, R. L., 1987: Air mass modification over the eastern Gulf of Mexico as a function of surface wind fields and Loop Current position. *Mon. Wea. Rev.*, **115**, 646-652.

Muller, R. A., 1977: A synoptic climatology for environmental baseline analysis: New Orleans. *J. Appl. Meteor.*, **16**, 20-34.

National Climatic Data Summary, 1960-1980: NOAA/NESDIS, U.S. Department of Commerce.

Nielsen, J. W., and P. P. Neilley, 1990: The vertical structure of New England coastal fronts. *Mon. Wea. Rev.*, **118**, 1793-1807.

Norris, D. L., 1992: *Winter cyclogenesis over the Gulf of Mexico: a climatological review.* M.S. Thesis, Department of Meteorology, Florida State University, 82 pp.

Nowlin, W. D., Jr., and H. J. McLellan, 1967: A characterization of the Gulf of Mexico waters in winter. *J. Mar. Res.*, **25**, 29-59.

_____, and C.A. Parker, 1974: Effects of a cold-air outbreak on shelf waters of the Gulf of Mexico. *J. Phys. Oceanogr.*, **4**, 467-486.

Nuss, W. A., and R. A. Anthes, 1987: A numerical investigation of low-level processes in rapid cyclogenesis. *Mon. Wea. Rev.*, **115**, 2728-2743.

_____, and D. W. Titley, 1994: Diagnosis of oceanic cyclogenesis using surface-based Q vectors. *Wea. Forecasting*, **9**, 136-155.

Orlanski, I, and J. J. Katzfev, 1987: Sensitivity of model simulations for a coastal cyclone. *Mon. Wea. Rev.*, **115**, 2792-2821.

Palmen, E., and C. W. Newton, 1969: *Atmospheric circulation systems: Their structure and interpretation.* San Diego: Academic Press, 316-326.

Petterssen, S., 1941: Cyclogenesis over southeastern United States and the Atlantic coast. *Bull. Amer. Meteor. Soc.,* **22,** 269-270.

_____, 1956: *Weather Analysis and Forecasting, Vol. I, 2nd ed.* New York : McGraw-Hill, 267-269, 320-339.

_____, and S. J. Smebye, 1971: On the development of extratropical storms. *Quart. J. Roy. Meteor. Soc.,* **97,** 457-482.

Pierrehumbert, R. T., 1986: Lee cyclogenesis. *Mesoscale Meteorology and Forecasting,* P. S. Ray, Ed., Amer. Meteor. Soc., 493-515.

Pyke, C. B., 1965: On the role of air-sea interaction in the development of cyclones. *Bull. Amer. Meteor. Soc.,* **46,** 4-15.

Reeder, M. J., 1986: the interaction of a surface cold front with a prefrontal thermodynamically well-mixed boundary layer. *Austral. Meteor. Mag.,* **34,** 137-148.

Reitan, C. H., 1974: Frequencies of cyclones and cyclogenesis for North America, 1951-1970. *Mon. Wea. Rev.,* **102,** 861-868.

_____, 1979: Trends in the frequencies of cyclone activity over North America. *Mon. Wea. Rev.,* **107,** 1684-1688.

Riordan, A. L., 1996: The coastal front: An historical perspective. *Preprints, Conf. on Coastal Oceanic and Atmospheric Prediction,* Atlanta, GA, Amer. Meteor. Soc., 212-218.

Roebber, P. J., 1993: A diagnostic case study of self-development as an antecedent conditioning process in explosive cyclogenesis. *Mon. Wea. Rev.,* **121,** 976-1006.

_____, J. R. Gyakum, and D. N. Trat, 1994: Coastal frontogenesis and precipitation during ERICA IOP 2. *Wea. Forecasting,* **9,** 21-44.

Reynolds, R. W. and T. M. Smith, 1994: Improved global sea surface temperature analyses. *J. Climate,* **7,** 929-948.

Sanders, F., 1987: A study of 500 mb vorticity maxima crossing the east coast of North America and associated surface cyclogenesis. *Wea. Forecasting,* **2,** 70-83.

_____, 1990: Surface analysis over the oceans--Searching for sea truth. *Wea. Forecasting,* **5,** 596-612.

_____, and J. R. Gyakum, 1980: Synoptic-dynamic climatology of the "bomb." *Mon. Wea. Rev.,* **108,** 1589-1606.

_____, and C. A. Doswell, III: 1995: A case for detailed surface analysis. *Bull. Amer. Meteor. Soc.,* **76,** 505-521.

Sandgathe, S. A., 1981: A numerical study of the role of air-sea fluxes in extratropical cyclogenesis, Ph.D. disserataion, Naval Postgraduate School, 134 pp.

Saucier, W. J., 1949: Texas-West Gulf cyclones. *Mon. Wea. Rev.*, 77, 219-231.

Schumann, S. A., S. A. Hsu, G. A. Johnson, J. Moser, and N. D. Walker, 1995: An overview of a strong winter low in the Gulf of Mexico 12-13 March 1993. *Natl. Wea. Dig.*, 20, 11-25.

Smilgielski, F. J., and G. P. Ellrod, 1985: Surface cyclogenesis as indicated by satellite imagery. NOAA Tech. Memo. NESDIS 9, NOAA/NESDIS, Washington, DC, 30 pp.

_____, and H. M. Mogil, 1991: Use of satellite information for improved oceanic surface analysis. *Preprints, 1st International Symposium on Winter Storms*, New Orleans, LA, Amer. Meteor., 137-144.

Spayd, L. E., 1988: Forecasting cyclogenesis using GOES water vapor satellite imagery and numerical models. *Preprints, 3rd Conf. on Satellite Meteorology and Oceanography*, Anaheim, CA, Amer. Meteor. Soc., 192-196.

Sublette, M. S., and G. S. Young, 1996: Warm-season effects of the Gulf Stream on mesoscale characteristics of the atmospheric boundary layer. *Mon. Wea. Rev.*, 124, 653-667.

Sutcliffe, R. C. 1939: Cyclonic and anticyclonic development. *Quart. J. Roy. Meteor. Soc.*, 65, 518-524.

Sweet, W., R. Fett, J. Kerling, and P. Violette, 1981: Air-sea interaction effects in the lower troposphere across the north wall of the Gulf Stream. *Mon. Wea. Rev.*, 109, 1042-1052.

Thaler, E. R., 1994: Operational forecasting of extratropical cyclones and their attendant weather in the modernized National Weather Service. *The Life Cycles of Extratropical Cyclones, Vol. 3*, S. Gronas and M. A. Shapiro, Eds., Bergen-Norway, 370-374.

Thompson, R. L., 1994: Autumnal return of tropical air to the Gulf of Mexico's coastal plain. *Wea. Forecasting*, 9, 348-360.

Tracton, M. S., 1973: The role of cumulus convection in the development of extratropical cyclones. *Mon. Wea. Rev.*, 101, 573-592.

U. S. Navy, 1985: U. S. Navy climatic study of the Caribbean Sea and Gulf of Mexico, Vol. 1-4, NAVAIR 50-1C-546, Prepared under Commander, Naval Ocean Command, NSTL, MS, 39529-5000, each volume approx. 200 pp.

Uccellini, L. W., 1990: Processes contributing to the rapid development of extratropical cyclones. *Extratropical Cyclones: The Erik Palmen Memorial Volume*, C. W., Newton and E. O. Holopanien, Eds., Amer. Meteor. Soc., 81-105.

_____, S. F. Corfidi, N. W. Junker, P. J. Kocin, and D. A. Olson, 1992: Report on the surface analysis workshop at the National Meteorological Center 25-28 March 1991. *Bull. Amer. Meteor. Soc.*, 73, 459-471.

Velden, C. S., 1992: Satellite-based microwave observations of tropopause-level thermal anomalies: Qualitative applications in extratropical cyclone events. *Wea. Forecasting*, 7, 669-682.

Warner, T. T., M. N. Lakhtakia, J. D. Doyle, and R. A. Pearson, 1990: Marine atmospheric boundary layer circulations forced by Gulf Stream sea surface temperature gradients. *Mon. Wea. Rev.*, **118**, 309-323.

Wash, C. H., R. A. Hale, P. H. Dobos, and E. J. Wright, 1992: Study of explosive and nonexplosive cyclogenesis during FGGE. *Mon. Wea. Rev.*, **120**, 40-51.

Weiss, S. J., 1992: Some aspects of forecasting severe thunderstorms during cool-season return-flow episodes. *J. Appl. Meteor.*, **31**, 964-982.

Whittaker, L. M., and L. H. Horn, 1981: Geographical and seasonal distribution of North American cyclogenesis, 1958-1977. *Mon. Wea. Rev.*, **109**, 2312-2322.

Williams, R. T., 1972: Quasi-geostrophic versus non-geostrophic frontogenesis. *J. Atmos. Sci.*, **29**, 3-10.

Zishka, K. M., and P. J. Smith, 1980: Climatology of cyclones and anticyclones over North America and surrounding ocean environs for January and July, 1950-1977. *Mon. Wea. Rev.*, **108**, 387-401.

Zubrick, S. M., and E. Thaler, 1993: Enhancements to the operational forecast process using gridded model data. *Preprints, 13th Conf. on Weather Analysis and Forecasting*, Vienna, VA, Amer. Meteor. Soc., 5-9.

Zwack, P., and B Okossi, 1986: A new method for solving the quasi-geostrophic omega equation by incorporating surface pressure tendency data. *Mon. Wea. Rev.*, **114**, 655-666.

BIOGRAPHICAL SKETCH

First Lieutenant Daniel Anthony Peters ███████████ November ████

████████ Following graduation from Red Bank Regional High School in

1988, he attended The Pennsylvania State University, and was awarded a Bachelor of

Science degree in Meteorology in 1992. He was commissioned as a Second

Lieutenant in the United States Air Force in May, 1992, and was assigned to Edwards

Air Force Base, California, as a Wing Weather Officer. Through the Air Force

Institute of Technology program, Lieutenant Peters entered the Graduate Program in

Meteorology at Florida State University in August, 1994. Upon completion of his

Master of Science degree in Meteorology in June, 1996, he will be assigned to Keesler

Air Force Base, Biloxi, Mississippi, where he will be an instructor for the Air Force

Weather School.